APSORC '97 LIST OF ABSTRACTS

POSTER SESSIONS

P300s & P400s

Wednesday afternoon, 8 October 1997

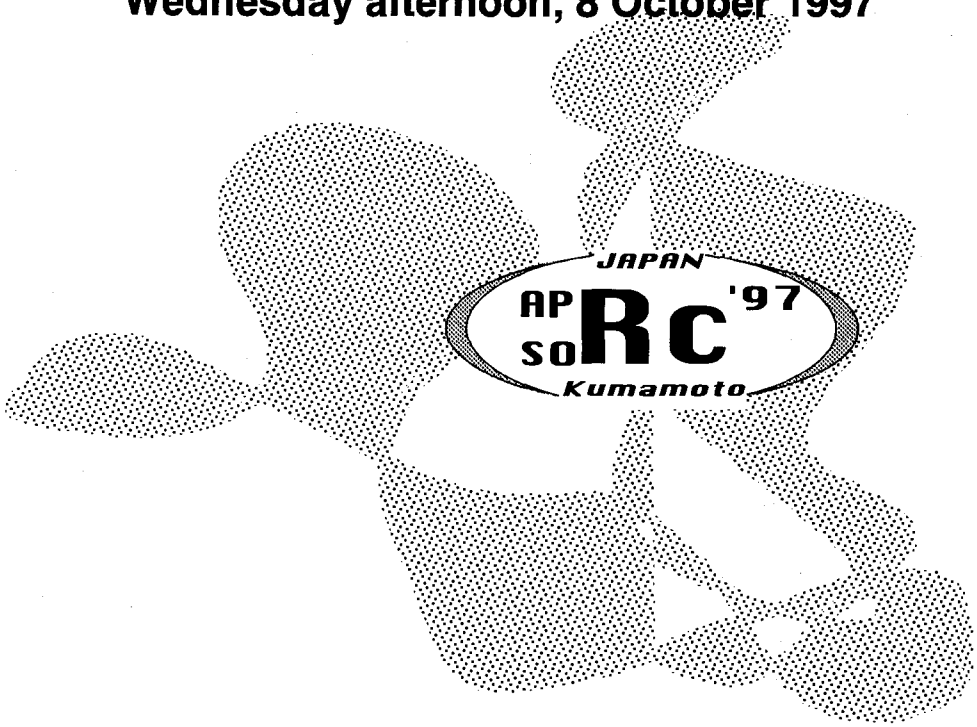

- KEYNOTE THEME -

EVER ONWARD TOWARDS THE FRONTIERS OF RADIOCHEMISTRY IN THE SECOND CENTURY OF RADIOACTIVITY DISCOVERY

P301
s.11

DNA STRAND BREAKS INDUCED BY IRON COMPLEXES IN THE PRESENCE OF (−)-EPIGALLOCATECHIN GALLATE

M. HIRASAWA[1], H. YOSHIOKA[1], T. OMORI[1] and H. YOSHIOKA[2]

[1] *Radiochemistry Research Laboratory, Faculty of Science, Shizuoka University, 836 Ohya Shizuoka-shi 422, Japan*

[2] *Institute for Environmental Health Sciences, University of Shizuoka, 52-1 Yada Shizuoka-shi 422, Japan*

Summary : DNA strand breaks were induced in the presence of iron(III) and EGCg in an SSC solution. Thus the acid dissociation constants of EGCg and stability constant of iron-EGCg complex were investigated to know behavior of iron(III) and EGCg in this solution.
Key words : DNA stand breaks, iron(III), EGCg

Tea catechins are known to be pharmacologically effective to the diseases such as carcinogenesis and mutagenesis. Epigallocatechin gallate(EGCg), which is the main component of the tea catechins, was used in the present work. We have reported that iron(III) citrate complexes coexisting with EGCg cause super coiled plasmid DNA strand breaks in an SSC buffer solution which consist of 0.15 M NaCl, 0.015 M Na-citrate(pH 7.4), while iron(III) citrate complexes rarely damage DNA. So it is a main object of our work to elucidate what kind of role EGCg plays in this solution.

First, the acid dissociation constants of EGCg were examined in an aqueous solution EGCg possessing 8 phenolic functional groups was titrated with 0.1 M NaOH, Unknown parameters were evaluated by a curve-fitting method.

Secondly, distribution behavior of iron-EGCg complexes using ^{59}Fe as a tracer was studied by means of an anion-exchange resin method. It was confirmed that the iron(III) in an aqueous solution was reduced to iron(II) by EGCg. The presence of a poly nuclear iron-EGCg complex was suggested from the analysis of the experimental results shown in Figure 1.

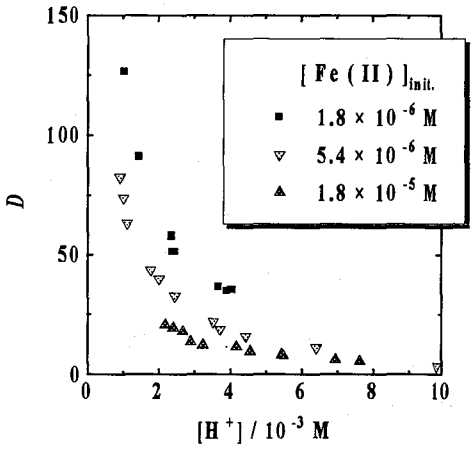

Figure 1. Dependence of partition ratio of ^{59}Fe-EGCg complexes on $[H^+]$ by means of the anion exchange method. [EGCg]= 5.0×10^{-3} M, I = 0.15 at room temperature.

Fax: 054-238-3989, e-mail: sgrmh1@sci.shizuoka.ac.jp

P302
s.12

ISOTOPIC EFFECT IN THE COURSE OF THIOPHENE HYDROGENOLYSIS UNDER HYDROGEN-^{3}H FLOW

V.M Kogan, A.A Greish. and G.V. Isagulyants.

N.D.Zelinsky Institute of Organic Chemistry, Russian Academy of Sciences, 47 Leninsky prospect, 117913 Moscow, Russian Federation.

Summary: A noticeable isotopic effect accompanied H_2S formation in the course of thiophene hydrodesulfurization under ^3H flow was detected. New forcing-out mechanism of the reaction has been proposed.

Keywords: Hydrodesulfurization, Hydrogenation, Isotopic effect, Mechanism, Thiophene, Tritium,

It was found earlier [1-3] that on the Co-Mo/Al_2O_3 sulfide catalyst surface there are stable SH groups which participate as a whole unit in formation of H_2S molecule in the course of thiophene HDS. Thus, from each catalyst SH group only one hydrogen atom comes into each H_2S molecule. There arises a problem where the second hydrogen atom which is necessary to form an H_2S molecule comes from.

The aim of the present study was to investigate into the role of gas phase hydrogen in the thiophene HDS product formation on a Co-Mo/Al_2O_3 sulfide catalyst. The research was carried out with using ^3H. It has been found that H_2 activation in the course of C_4-hydrocarbons (HC) differs from that which takes place in the course of H_2S formation. Namely, C_4-HC formation proceeds with the participation of reversibly and dissociatively adsorbed hydrogen (according to Bonhoeffer-Farcas mechanism) and H_2S formation - with the participation of molecular hydrogen (according to Rideal-Eley mechanism). The latter is accompanied with a noticeable isotopic effect, which gives us ground to consider it to be a limiting step in the thiophene HDS reaction. It is shown that thiophene molecule hydrogen does not directly take part in H_2S formation.

Generally, reaction scheme can be presented as the following steps. Onto the catalyst surface with definite numbers of vacancies and SH groups a thiophene molecule is adsorbed. Hydrogenolysis of its C-S bond takes place with participation of dissociatively adsorbed hydrogen (but not hydrogen from SH groups). The decomposition of thiophene molecule results in the formation of a new SH group and the ratio between the number of vacancies and SH groups is changed in favor of the latter. Because of that the catalyst falls into a sort of "metastable" state. It can return to its initial state by the way of forcing out any of the SH groups from its surface. Further on, SH group interacts with molecular gas phase hydrogen. H-H bond break in H_2 molecule that accompanies the interaction should limit the whole HDS reaction.

REFERENCES

1. G.V. Isagulyants, A.A. Greish, V.M. Kogan, G.M. V'yunova and G.V.Antoshin, Kinetics and Catalysis, Engl. tr., 28 (1987) 550.
2. G.V. Isagulyants, A.A. Greish, and V.M. Kogan, Kinetics and Catalysis, Engl. tr, 28 (1987) 555.
3. G.V. Isagulyants, A.A. Greish, and V.M. Kogan, in: "Proc. 9 th Int. Congr. on Catal.", (Calgary, 19878), eds. M.J. Philips and M. Ternan, 1988, Vol. 1, P.35.

Fax: + 7 095 - 135-53-28, E-mail: vmk@ioc.ac.ru

P303
s.13

WET OXIDATION OF ION-EXCHANGE RESINS IN FENTON'S REACTION SYSTEM WITH A CATHODE

D. W. KANG, H. S. YANG*

Korea Electric Power Research Institute, Taejon 305-380, Korea

** Dept. of Fine Chem. Eng. And Chemistry, Chungnam National University, Taejon 305-764, Korea*

Summary: Wet oxidation of ion-exchange resins is a high technique of volume reduction for the permanent disposal. In this study, an optimum reaction condition was determined by investigating the effect of cathode introduced to reduce Fe^{+3} and then to reuse Fe^{+2} on wet oxidation

Key wards: Fenton's reaction, Ion- exchange resins, Catalyst, Electrode, H_2O_2

ABSTRACT: Spent organic ion-exchange resins are generated in large quantities during the operation of nuclear facilities. High volume reduction is thus necessary for either on-site storage or safe transportation to a disposal site. From the viewpoint of volume reduction and safety, it is known that catalyzed oxidation by hydrogen peroxide is best among the oxidation technologies for the treatment of spent resins. In this study, excess H_2O_2 was used for complete oxidation. Reaction conditions such as flow rate of H_2O_2 , mole ratio of mixed catalyst, cathode and neutral pH in resin reaction were found to be important for efficient use of the oxidant. Catalysts such as $FeSO_4$, CuCl and $CuSO_4$ were used to activate the reaction. An optimum reaction condition was determined by investigating the effect of cathode introduced to reduce Fe^{+3} and then to reuse Fe^{+2} on wet oxidation. When a single catalyst was used, ion exchange resins decomposed at lower rate with a platinum electrodes than without the electrodes. In case of a co-catalyst, however, the resins decomposed at higher rate when used with an electrode. The total consumption of the co-catalyst used with electrodes reduced to more than one-third of that of the single catalyst used without the electrode.

Fax: 82-42-865-7604/ E-mail : dwkang@kepri.re.kr

P304
s.32

ENHANCED CELL-KILLING EFFECT OF POTASSIUM HEXACHLOROPLATINUM(IV) SOLUTION IRRADIATED BY ^{60}Co-γ-RAYS UNDER THE PRESENCE OF NH_4Cl

Y. Tanaka, T. Sumino, K. Kawai, J. Takada, K. Kawamoto and M. Akaboshi

Research Reactor Institute, Kyoto University, Kumatori-cho. Sennan-gun, Osaka, 590-04, JAPAN

Summary: Cell-killing effect of K_2PtCl_6 solutions increased when they were γ-irradiated under the presence of NH_4Cl, NaCl, $(NH_4)_2HPO_4$, ammonium acetate and did not bring about such an enhancement.

Key words: ^{60}Co-γ-ray, (K_2PtCl_6), NH_4Cl, HPLC, *cis*-diaminedichloroplatinum

The enhancement of cell-killing effect induced by ^{60}Co-γ-rays on the aqueous solutions of potassium hexachloroplatinum(IV) (K_2PtCl_6) irradiated under the presence of various concentrations of NH_4Cl was examined. HeLa S-3 cells were treated with the irradiated solutions for 60 min at 37 °C, and cell survival was measured by colony forming efficiency. The mean lethal concentration (D_0) for the cells treated with non-irradiated K_2PtCl_6 solution (1 mg/ml) was 34.5 μl/ml. However, it decreased, namely the cell-killing effect of the solution increased, with increasing radiation dose up to 2.64×10^4 Gy in the case of 0.1 M NH_4Cl solution (in this condition, the D_0 decreased to 9.6 μl/ml). (Fig.) No or only a slight enhancement was observed in the case of K_2PtCl_6 solutions irradiated under the presence of NaCl, $(NH_4)_2HPO_4$, ammonium acetate or glycine. Observation using high performance liquid chromatography (HPLC) of irradiated K_2PtCl_6 solutions revealed the formation of *cis*- and/or *trans*-diaminedichloro-platinum(IV).

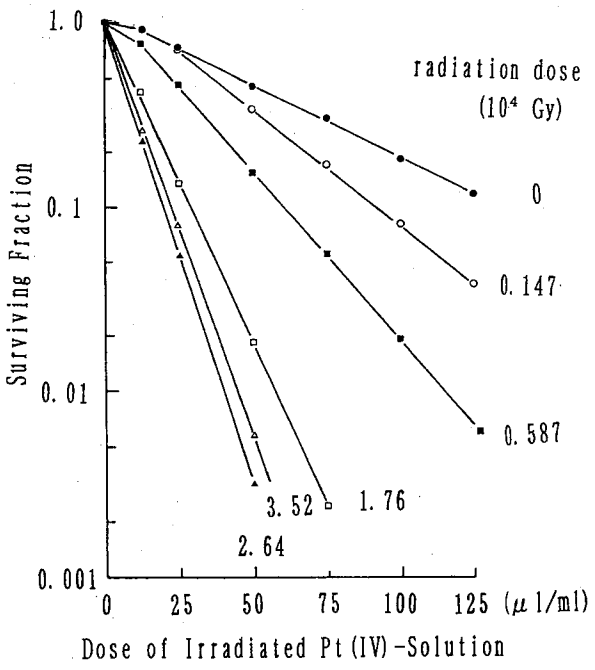

Fig. Dose-survival curves of HeLa cells treated with irradiated $K_2(PtCl_6)$ solutions for 60 min at 37 °C.

P305
s.13

DYNAMIC MOTION OF $Ce@C_{82}$ STUDIED BY PERTURBED ANGULAR CORRELATION

W. Sato[1], K. Sueki[1], K. Kikuchi[1], K. Kobayashi[1], S. Suzuki[1], Y. Achiba[1], H. Nakahara[1]*, Y. Ohkubo[2], F. Ambe[3], and K. Asai[4]

[1]*Graduate School of Science, Tokyo Metropolitan University*
1-1 Minami-Osawa, Hachioji, Tokyo 192-03, Japan
[2]*Research Reactor Institute*
Kyoto University, Noda, Kumatori, Sennan, Osaka 590-04, Japan
[3]*The Institute of Physical and Chemical Research (RIKEN)*
2-1 Hirosawa, Wako, Saitama 351-01, Japan
[4]*Department of Applied Physics and Chemistry, University of Electro-Communications, 1-5-1 Chofugaoka, Chofu, Tokyo 182, Japan*

Summary: Temperature-independent intramolecular dynamic motion of the Ce atom in $Ce@C_{82}$ was empirically observed below the freezing point of the molecular rotation, and the data analyses revealed the binding energy of the atom to the cage to be at most 2.3 eV.
Key words: $Ce@C_{82}$, TDPAC, Intramolecular motion, Binding energy, Recoil energy

Time-differential perturbed angular correlation (TDPAC) method was applied for $^{140}Ce@C_{82}$, a β^- decay product of $^{140}La@C_{82}$ produced by neutron capture reaction of $^{139}La@C_{82}$, in order to observe the temperature dependence of the reorientational correlation time of the principal axis of the the electric field gradient (EFG) at the probe nucleus of the Ce. One of the advantages of this method is that it can give direct information about the fluctuation of the principal axis of EFG. Taking the advantage of this spectroscopy, we investigated dynamic motion of the fullerenes and electronic properties of the encaged metal.

After HPLC purification of the samples, TDPAC measurements were performed on the (329-487)-keV cascade γ rays from ^{140}Ce nucleus by conventional four-counter detection system. The time-dependent attenuation of the anisotropy of angular distribution ($A_{22}G_{22}(t)$) was observed at various temperatures as partly shown in Fig. 1.

The followings were ascertained from the data analysis: 1) there are two different chemical species with different EFGs, 2) at higher temperature, $Ce@C_{82}$ molecules are rotating even in solid form and those correlation times showed temperature dependence, and 3) $A_{22}G_{22}(t)$ data at low temperatures obviously show a static perturbation causing a nuclear precession for one species, and some effect of dynamic perturbation, for the other, with little, if any, temperature dependence, which suggests the strong possibility of intramolecular dynamic motion of the encapsulated Ce atom (Fig. 2). This motion lasting for the present time scale of TDPAC measurements without the energy dissipation is considered to be enabled by the recoil effect of β^- particle emission from ^{140}La. From the energy distribution function of the recoil energy, the binding energy of the ^{140}La atom was found to be at most 2.3 eV.

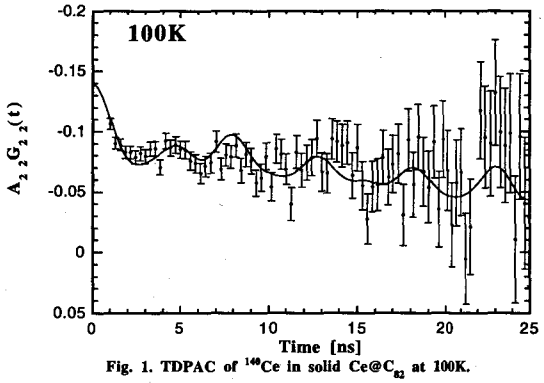

Fig. 1. TDPAC of ^{140}Ce in solid $Ce@C_{82}$ at 100K.

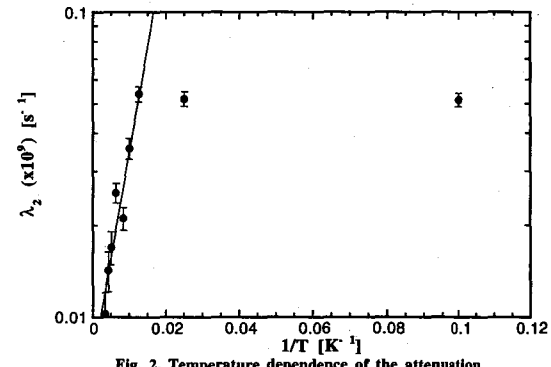

Fig. 2. Temperature dependence of the attenuation coefficients of the angular anisotropy.

Fax: +81-426-77-2525, E-mail: nakahara-hiromichi@c.metro-u.ac.jp

P306
s.13

THE CORRELATION OF SOME RECOIL FEATURES IN THE SOLID SYSTEM WITH STRUCTURAL FACTORS WATER-SOLUBLE METALLOPORPHYRIN ION ASSOCIATE

H. Shoji

Department of Chemistry, University of Tsukuba,
1-1-1 Tennodai, Tsukuba, Ibaraki 305, Japan

"Summary: the recoil feature of central metal atoms in the solid system of water-soluble metalloporphyrin ion associates showed some patterns dependent upon combinations of central metal atoms and ligands in bremsstrahlung and thermal neutron irradiation".
"Key words: water-soluble metalloporphyrin ion associate solid system, recoil of central atoms".

Abstract: The solid system of water-soluble metalloporphyrin ion associate ([M(TMPyP)][M'(TCPP)], and [M(TMPyP)][M'(TPPS)], H_2TMPyP=tetrakis(4-N-methylpyridyl)porphine, H_2TCPP=tetra(p-carboxyphenyl)-porphine, H_2TPPS=tetra(p-sulfophenyl)porphine) provides us with the microscopically homogeneous bi-component system suitable for the study of the behaviour of recoils. A number of combinations of central metal atoms and ligands have been investigated in bremsstrahlung and thermal neutron irradiation at very low temperatures. The complex yield of nuclides formed from central atoms of the complexes was measured. At present, tendencies in the complex formation in the system of different central metal atoms can be classified into the following three patterns: ① The recoil from one metal side remarkably substitutes the inactive central metal atom of the other side of the less stable complex; ② The recoil of one kind of metal shows anomalously high affinity with a certain ligand; ③ The recoil disperses rather uniformly in both component complexes. The general stability order of metalloporphyrins was proposed based on the kind of the central metal atom. If this stability order is taken into account, tendency ① can be understood. However, when a hydrophilic group was changed in the anionic complex — $-COO^-$ to $-SO_3^-$ —keeping the other conditions unchanged, the tendency of complex formation of recoils drastically changed. This is the case of [M(TMPyP)][M'(TCPP)] showing tendency ① and [M(TMPyP)][M'(TPPS)] of ③ (M,M'=Cu, Zn). Recently, very fine crystalline phase was found to be growing in these systems by X-ray powder diffraction. Moreover, their X-ray patterns were different from each other (Figs. 1,2). Although the trial for better crystallization of samples is now still going on, the correlation of the features in complex formation with the structural factors will be discussed.

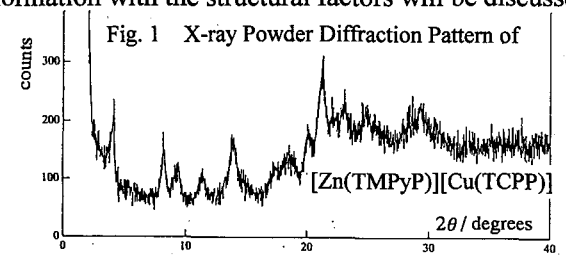

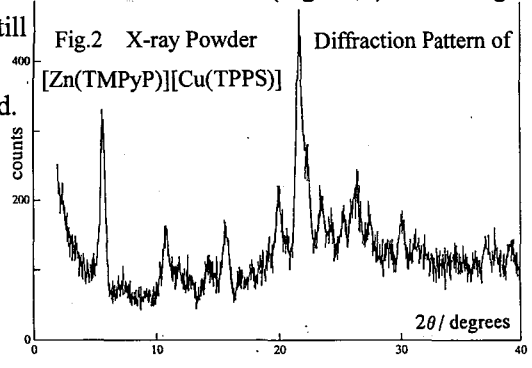

Fax: +81-298-53-6503/ E-mail: hshoji@staff.chem.tsukuba.ac.jp

P307
s.21

Study of Mixed-Valence Dinuclear Iron(II,III) Complexes $[Fe_2(bpmp)L_2](BF_4)_2$: Asymmetrically Delocalized Valence States

Teruaki Manago, Shinya Hayami, and Yonezo Maeda*

Department of Chemistry, Faculty of Science, Kyushu University, Hakozaki, Higashiku, Fukuoka 812-81

Summary: Mössbauer spectra of a mixed-valence dinuclear iron(II,III) complex show a noble temperature dependence were reported and the unusual line broadening was explained by asymmetrically delocalized valence states.
Key words: Mixed-valence complexes, intramolecular electron exchange

We report the variable temperature Mössbauer spectra of a mixed-valence dinuclear iron(II,III) complex, $[Fe_2(bpmp)(Ph(CH_2)_2COO)_2](BF_4)_2$, where Hbpmp represents 2,6-bis[bis(2-pyridylmethyl) aminoethyl]-4-methylphenol. Two quadrupole-split doublets are observed at 78 K, approach each other with increasing temperature, and remain even at 330 K. It is unique that the line widths increase with raising of temperature from 78 K to 230 K and then become narrow above 260 K. In order to interpret the temperature dependence of the spectra, the intramolecular electron exchange between two inequivalent iron atoms, one of which prefers to divalent state and the other to trivalent one, was considered. A simulation spectrum with the population of $Fe_a^{+2}Fe_b^{+3}$: $Fe_a^{+3}Fe_b^{+2}$=0.8: 0.2 is well fitted to the Mössbauer spectrum at 293 K; one of the doublets with an isomer shift of 0.86 mm s^{-1} (quadrupole splitting of 1.34 mm s^{-1}) could be assigned to $Fe^{+2.2}$, and the other with an isomer shift of 0.54 mm s^{-1} (quadrupole splitting of 0.71 mm s^{-1}) to $Fe^{+2.8}$.

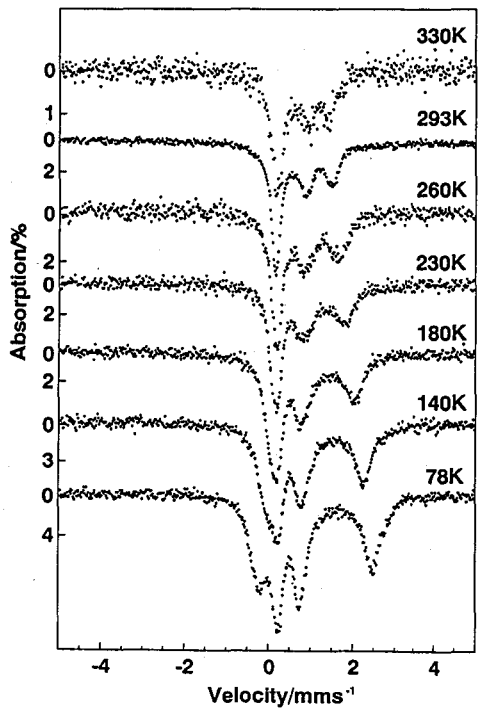

Fax: (092)642-2607, E-mail: y.maescc@mbox.nc.kyushu-u.ac.jp

P308
s.21

Syntheses and Structure of Iron(III) Complexes Containing a Quasi-Crownether Ring

S. Hayami, S. Nomiyama, S. Hirose, Y. Yano, S. Osaki[1)], and Y. Maeda*

Department of Chemistry, Faculty of Science, Kyushu University, Hakozaki, Higashiku, Fukuoka 812-81, Japan

[1)]Radioisotope Center, Kyushu University, Hakozaki, Higashiku, Fukuoka 812-81, Japan

Summary: The electronic ground states of iron(III) complexes containing a quasi-crownether ring were studied in correlation with the incorporation of alkali or alkaline-earth metal ions.

Key words: Spin-Crossover • Iron(III) Complexes • Ionophore

Schiff-base ligand H_2cr-salen which is 1:1 condensation product of 3,3'-(3,6-dioxaoctane-1,8-diyldioxy)bis(2-hydroxybenzaldehyde) and ethylenediamine was designed to incorporate alkaline or alkaline-earth metal ions. The complexes $[BaFe(cr\text{-}salen)(py)_2](ClO_4)_3$ and $[Fe(cr\text{-}salen)(py)_2]ClO_4$ were prepared and the chemical compositions were confirmed by FAB-mass spectroscopy and the electronic ground states of the complexes were determined by using ESR and ^{57}Fe Mössbauer spectroscopy. The complexes were in the high-spin state in solid state and solution. H_2cr-salen was not useful as a model compound for host-guest functional materials because $[Fe(cr\text{-}salen)(py)_2]ClO_4$ was decomposed by an addition of Ba^{2+} in acetonitrile.

Single crystals of $[BaFe(cr\text{-}salen)(MeOH)_2]_2O(ClO_4)_4 \cdot 2MeOH$ were obtained by an addition of excess Ba^{2+} into a solution of $[Fe(cr\text{-}salen)(py)_2]ClO_4$ in acetonitrile, and the X-ray structure of the complexes was determined. The complex forms a polymer chain. An iron atom is located within a square pyramidal structure composed of three oxygen and two nitrogen atoms, ten oxygen atoms being coordinated to a barium atom. The iron atom is bridged by a μ-oxo oxygen atom, the barium atom being bridged by two perchlorate ions.

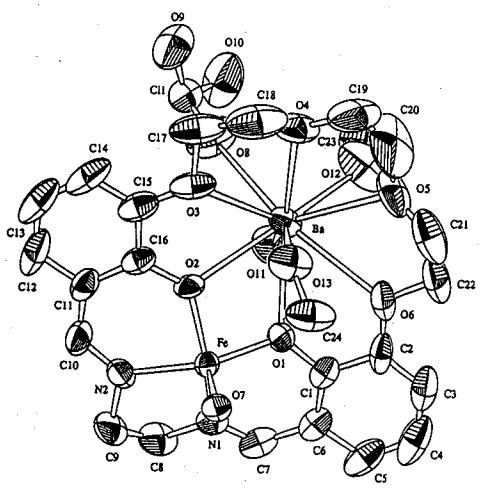

Fax: +81-92-642-2607, E-mail: y.maescc@mbox.nc.kyushu-u.ac.jp

P309 s.21 APPLICATION OF THE MÖSSBAUER SPECTROSCOPY TO THE STUDY OF THE OXIDATION STATE OF AZAFERROCENE DERIVATIVES

S. Nakashima,*, [1] T. Kitao,[2] H. Matsunaga,[2] I. Kimura,[2] H. Inamura,[2] T. Okuda,[2] and H. Sakai[3]

[1]*Radioisotope Center, Hiroshima University, Kagamiyama, Higashi-Hiroshima 739, Japan*

[2]*Department of Chemistry, Faculty of Science, Hiroshima University, Higashi-Hiroshima 739, Japan*

[3]*Department of Chemistry, Faculty of Science, Konan University, Higashi-Nada 658, Japan*

Summary: Azaferrocene has two active sites of iron and nitrogen atoms. Drastic change of the oxidation state in iodine oxidation of azaferrocene is observed by introducing the methyl substituents into the pyrrole ring, while all the N-methylates show a similar electronic state.

Key words: Azaferrocene, Oxidation state, ^{57}Fe Mössbauer spectroscopy

Two active sites of iron and nitrogen atoms in azaferrocene offer a wide range of chemistry. The two active sites have a possibility to compete to each other. In the present study we investigated the N-methylation and iodine oxidation of azaferrocene(AF), 2,5-dimethyl-(2,5-DMAF), and 2,4-dimethylazaferrocene(2,4-DMAF) by means of ^{57}Fe Mössbauer spectroscopy.

The ^{57}Fe Mössbauer parameters of AF, 2,5-DMAF, and 2,4-DMAF, which are summarized in Table, are similar to those of ferrocene, indicating the similarity of the electronic state of iron atom to ferrocene. ^{57}Fe Mössbauer spectra of the N-methylates of AF, 2,5-DMAF, and 2,4-DMAF showed the ferrocene-like doublet. The all quadrupole splittings (ΔEqs) are a little bit smaller than the original azaferrocenes, suggesting the little effect of N-methylation on the electronic state of iron. It is known that the protonation of azaferrocene only causes a change of 0.15 mm s^{-1}. The present decreases in ΔEq are similar to the value. It can be seen from Table that the iodine salt of azaferrocene shows a great decrease in the ΔEq value, while the iodine salts of 2,5-DMAF and 2,4-DMAF show the ferrocene-like doublet, in which the ΔEqs are similar to the values of N-methylates.

One of the possibility of the effect of methyl substituent is due to the less mixing of the iron d_{xy} and $d_{x^2-y^2}$ orbitals and p orbital in the ligand. This might be the reason why the donation ability of the methyl substituent makes the oxidation of nitrogen in pyrrole ring easier. It can be concluded that the oxidation of azaferrocenes is competitive at the two sites; iron and nitrogen. The oxidation site of nitrogen is promoted by the introduction of methyl substituent in the pyrrole ring.

Table ^{57}Fe Mössbauer parameters

		AF		2,5-DMAF		2,4-DMAF	
	T/ K	δ[a]/ mm s^{-1}	ΔEq/ mm s^{-1}	δ[a]/ mm s^{-1}	ΔEq/ mm s^{-1}	δ[a]/ mm s^{-1}	ΔEq/ mm s^{-1}
Before	298	0.47	2.42	0.47[b]	2.49[b]	0.51[b]	2.46[b]
oxidation	80	0.56	2.49	0.53	2.47	0.54	2.47
N-	298	0.44	2.32	0.45	2.40	0.46	2.41
methylate	80	0.50	2.34	0.52	2.42	0.54	2.44
Iodine	298	0.36	0.81	0.47	2.37	0.46	2.35
salt	80	0.43	0.75	0.52	2.39	0.53	2.34

[a]Relative to metallic iron foil. [b]Measured at 250 K.

Fax: +81-824-24-0700 E-mail: snaka@ue.ipc.hiroshima-u.ac.jp

P310
s.21

^{57}Fe MÖSSBAUER SPECTROSCOPIC AND MAGNETIC STUDY FOR SPIN-CROSSOVER POLYMER COMPLEX, Fe(3-Chloropyridine)$_2$Ni(CN)$_4$

T. Kitazawa[1]*, Mi.Takahashi[1], Ma. Takahashi[1], M. Enomoto [2], A. Miyazaki [2], T. Enoki [2], M. Takeda [1],

1) Department of Chemistry, Faculty of Science, Toho University, Miyama, Funabashi, Chiba 274, Japan

2) Department of Chemistry, Tokyo Institute of Technology, Ookayama, Meguro- ku, Tokyo 152, Japan.

Summary: The spin-crossover of Fe(3-chloropyridine)$_2$Ni(CN)$_4$ **2** occurs between 120 K and 80 K. An high spin iron(II) residual is observed at low temperatures.

Key Words: ^{57}Fe Mössbauer spectroscopy, spin-croossover, coordination polymer, SQUID

The Hofmann pyridine complex Fe(py)$_2$Ni(CN)$_4$ **1** shows iron(II) spin-crossover behavior, revealed by using ^{57}Fe Mössbauer spectroscopy and SQUID technique[1]. The spin-transition of octahedral iron(II) site in **1** occurs between 210 K and 170 K with hysteresis. So far thermally induced changes of the spin multiplicity of iron(II) and iron(III) have been known for discrete iron complex molecules. Molecular interactions between the spin-changing molecules may be different between the discrete molecular systems and our new coordination polymer system, thus causing potential differences in spin transition mechanisms. So we have been interested in the two dimensional coordination polymer compounds based on iron(II) tetracyanonickelate (II), whose sheet has pyridine derivatives protruding up and down at each octahedral iron(II) atom. We report here ^{57}Fe Mössbauer spectra and magnetic susceptibility data obtained by SQUID technique for newly synthesized polymer complex Fe(3-chloropyridine)$_2$Ni(CN)$_4$ **2.** The spin crossover behavior of **2** happens between 120 K and 80 K, being lower than those of **1**.

As shown in Fig, ^{57}Fe Mössbauer spectra of **2** show that spin state of iron(II) at RT is in the high spin (IS = 1.07 mm/s, QS = 1.32 mm/s) and that low spin and high spin sites coexist in a ratio of 2:3 at 80 K (LS site: IS = 0.52 mm/s, QS = 0 mm/s; HS site:IS = 1.18 mm/s, QS = 1.91 mm/s). Being different from no high spin iron(II) residual in **1**, an high spin residual in **2** is observed under low temperature ranges. SQUID data for **2** agree with the residual of high spin iron(II) site. The substitution effect of pyridine ring may be associated with the residual of high spin iron(II) ions.

[1] T. Kitazawa *et al.*, *J. Mater.Chem*, 1996,6,119

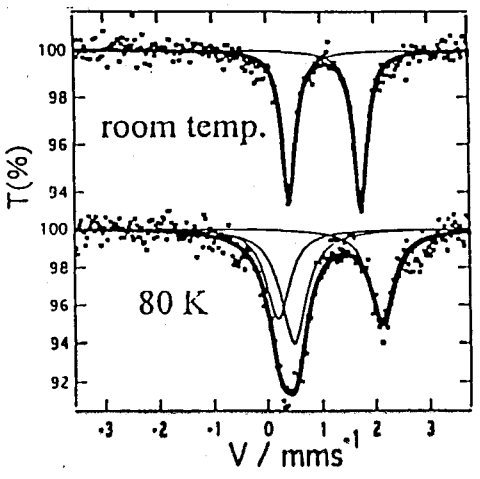

Fig. ^{57}Fe Mössbauer spectra of **2**

+81-474-75-1855, kitazawa@toho-u.ac.jp

P311
s.21

THE MICROENVIRONMENT OF IRON IN (Ba, Ca) (Fe, Co)$O_{3-\delta}$ CATALYST SYSTEM : MÖSSBAUER STUDY

Z. Homonnay[2], K. Nomura[1], G. Juhasz[2], A. Vertes[2], Y. Ujihira[3]

1 Graduate School of Engineering, The University of Tokyo, Hongo 7-3-1, Bunkyo-ku, Tokyo 113, Japan,
2 Department of Nuclear Chemistry, Eotvos University, P.O. Box 32, H-1518, Budapest 112, Hungary,
3Research Center for Advanced Science and Technology, The University of Tokyo,

The microenvironment of iron in prominent perovskite oxides for reduction of greenhouse gases from industrial effluents has been characterized by Mössbauer spectrometry, and the effect of Ca-doping will be presented.

Perovskite oxides, catalysis, greenhouse gas, CO_2, CH_4, Moessbauer spectrometry,

Perovskite oxides, (Ba, Ca) (Co, Fe) $O_{3-\delta}$, are prominent materials for CH_4 coupling and CO_2 absorption. In CH_4 atmosphere, the perovskite oxides played a role of deep oxidation between 300 and 550 °C and the Co rich perovskite oxides provided the nearly 100% selectivity to C2 hydrocarbons in the temperature of 550 to 750 °C [1]. In CO_2 and CO_2 + air atmospheres, the perovskite oxides absorbed CO_2 rapidly at temperatures between 600 and 900 °C [2]. These remarkable properties may permit application of these oxides to the reduction of greenhouse gases from industrial effluents. It has been considered that the incorporation of Ca^{2+} into Ba^{2+} sites and the mixed valence states of Co and Fe ions make it more effective for the absorption of CO_2 at high temperatures. Some of these oxides have been analyzed by Transmission Mössbauer spectrometry [3] and Emission Mössbauer spectrometry [4]. With the increase of Co content ($\geqq 0.8$), the cubic phase became the orthorhombic structures, but all these compounds showed the cubic phase at higher than 750 °C. The ordering of the oxygen deficiencies is considered to be important for CH_4 coupling and CO_2 absorption. At room temperature, the magnetically inhomogeneous broad peaks and the special magnetic sextet with 47 T have sometimes appeared in addition to paramagnetic peaks of Fe(III) and Fe(IV) by mixing Ba and Ca ions in these perovskite oxides. In order to clarify the production of inhomogeneous peaks and the specific magnetic sextet, the perovskite oxides with different Ba/Ca ratio were treated in various atmospheres and heating conditions. The effect of Ca doping in these oxides were mainly characterized by Mössbauer spectra, and the results will be presented here.

[1] K. Nomura, T. Hayakawa, K. Takehira, Y. Ujihira, Applied Catalysis A: General, 101(1993) 63.
[2] K. Nomura, Y. Ujihira, T. Hayakawa, K. Takehira, Applied Catalysis A: General, 137 (1996) 25.
[3] K. Nomura, Z. Homonnay, A. Vertes, V. Chechersky, A. Nath, Y. Ujihira, T. Hayakawa, K. Takehira, Czechoslovak J. of Physics, 47 (1997) in press.
[4] K. Nomura, Z. Homonnay, G. Vanko, A. Vertes, L. Poppl, A. Nath, T. Hayakawa, and K. Takehira, the proceedings of ISIAME'97, (ed. by H. Pollak and U. Karfunkel) in press.

1 E-mail: kiyoshin@sophie.gen.u-tokyo.ac.jp
2 E-mail: homonnay@szerves.chem.elte.hu

P312
s.21

SUPERPARAMAGNETIC BEHAVIOR OF IRON OXIDES SUPPORTED ON POROUS SILICA GELS

S. Iijima[1], A. Nomura[2], F. Mizukami[2], S. Shin[2] and F. Mizutani[1]

[1] *National Institute of Bioscience and Human-Technology, Higashi 1-1, Tsukuba, Ibaraki 305, Japan*
[2] *National Institute of Materials and Chemical Research, Higashi 1-1, Tsukuba, Ibaraki 305, Japan*

Summary: Fine particles of γ-Fe_2O_3 were supported on microbeads of silica gel. ^{57}Fe Mössbauer studies showed that the particle size of the γ-Fe_2O_3 was regulated by the mean pore diameter of the silica gel support employed.
Key words: Mössbauer spectroscopy, superparamagnetism, maghemite, hematite, silica gel

Recently, ultrafine particles have received increased attention. Among the transition metal oxides, α-Fe_2O_3 (hematite) nanocrystals have been most extensively investigated in connection with the understanding of their superparamagnetic behavior, and a number of papers have reported on the α-Fe_2O_3 nanocrystals on support materials such as silica gel, Al_2O_3 and zeolite. In contrast, γ-Fe_2O_3 (maghemite) have not been supported on such materials to our knowledge. In the present study, we have prepared silica gel supported γ-Fe_2O_3 nanocrystals, and have investigated their characteristics mainly by using ^{57}Fe Mössbauer spectroscopy.

Silica gel microbeads with the mean pore diameter (D) of 4 - 82 nm were pretreated with citric acid and then immersed in an $Fe(NO_3)_3$ solution. After being dried, the substrates were calcinated at 400 °C for 1 h. X-Ray diffraction patterns, magnetization measurements and Mössbauer spectra showed that γ-Fe_2O_3 was formed on the substrates.

The Mössbauer spectral shape at room temperature of the supported γ-Fe_2O_3 showed a variation with the D value of the silica gel base employed (Fig. 1). The samples with $D \leq 16$ nm virtually showed only a single quadrupole doublet. When D incresed upto 34 nm, wings on the both sides of the central doublet became apparent. At D = 82 nm, a magnetically-split sextet was clearly observed in the spectrum. These results suggest that the pore size of the silica gel base controls the particle size of the γ-Fe_2O_3 formed; larger particles give more distinct magnetic relaxation or magnetic splitting in the Mössbauer spectra. The particle sizes were estimated from X-ray powder patterns to be 4.2 and 9.5 nm for the samples with D = 13 and 82 nm, respectively. Each sample showed a temperature-dependent Mössbauer spectrum, which is characteristic of superparamagnets. In the case of α-Fe_2O_3 particles prepared by using the same silica gel beads, it was indicated by the Mössbauer spectra and the electron micrographs that there are relatively large particles of the oxide on the surface of the beads, in addition to the particles in the silica gel micropores.

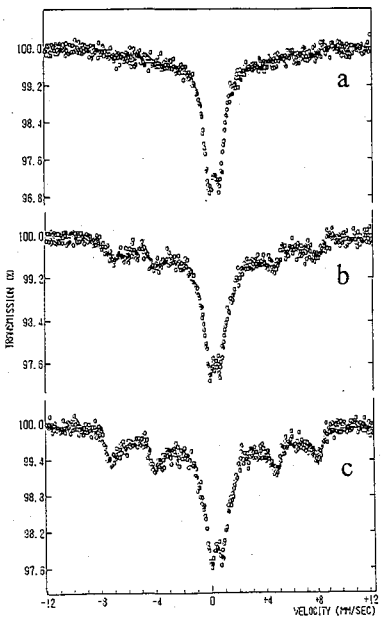

Fig. 1. Mössbauer spectra of γ-Fe_2O_3 particles supported on the silica gels of D = (a) 34, (b) 48 and (c) 82 nm.

P313
s.21

MÖSSBAUER STUDY ON THE CRYSTALLIZATION OF IR-TRANSMITTING ALUMINATE GLASSES

T. NISHIDA, S. KUBUKI, and Y. MAEDA
Department of Chemistry, Faculty of Science, Kyushu University
Hakozaki, Higashiku, Fukuoka 812-81, Japan

Summary: Mössbauer spectra of $60CaO \cdot 27Al_2O_3 \cdot 13Fe_2O_3$ glass-ceramics show two sextets due to antiferromagnetic $Ca_2Fe_2O_5$ and the doublet due to $12CaO \cdot 7Al_2O_3$ phase. The Al(III) preferentially substitutes the tetrahedral Fe(III) in the $Ca_2Fe_2O_5$ phase.
Key words: aluminate glass, crystallization mechanism, Mössbauer, FT-IR, DTA, XRD

The Mössbauer effect is an effective tool for investigating the local structure of inorganic glasses. The Mössbauer ions play a role of 'probe', from which we can know the nature of the chemical bond and the symmetry of the structural units. As for the site occupation of Mössbauer ions, Nishida proposed three **general rules** [1,2] using the Debye temperature, γ-ray irradiation effect, and the linear relationship between the quadrupole splitting (Δ) of Fe(III) and the glass transition temperature (*Tg*).

The Mössbauer spectra of IR-transmitting $60CaO \cdot 35Al_2O_3 \cdot 5Fe_2O_3$ glass-ceramics prepared by the heat treatment at the crystallization temperature (*Tc*) consist of two quadrupole doublets due to the tetrahedral Fe(III) ions; one substituting the Al(III) of mayenite ($12CaO \cdot 7Al_2O_3$) phase and the other remaining in the glassy phase. A heat treatment of $60CaO \cdot 27Al_2O_3 \cdot 13Fe_2O_3$ glass at the *Tc* resulted in the formation of antiferromagnetic dicalcium ferrite ($Ca_2Fe_2O_5$) and mayenite. The Mössbauer spectra showed two sextets, as shown in Fig. 1. The outer sextet was ascribed to the octahedral Fe(III) with an internal magnetic field (*H*int) of 45 T. The inner doublet was ascribed to the tetrahedral Fe(III) with the *H*int of 39 T, and the smaller absorption area indicated the preferential substitution of Al(III) for tetrahedral Fe(III).

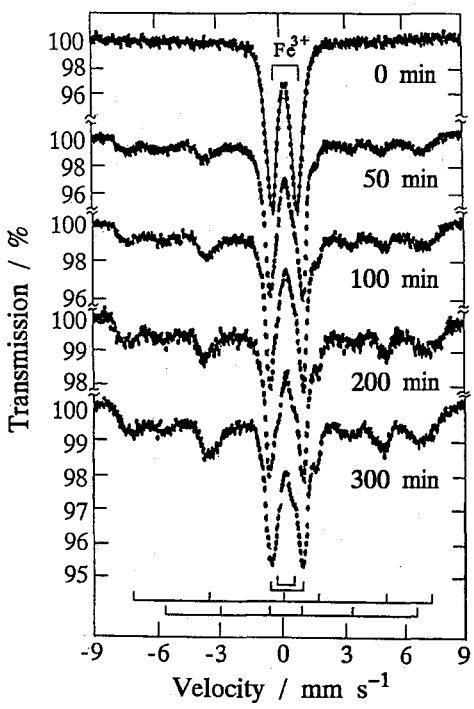

Fig. 1. Mössbauer spectra of $60CaO \cdot 27Al_2O_3 \cdot 13Fe_2O_3$ glass-ceramics heat treated at 750 °C for 0~300 min.

The 'IR-transmission' method and the DTA method yielded the activation energy of 4.2~4.9 ±0.4 eV, which are equal to the Al−O bond energy of 4.4 eV. This result indicates that the cleavage of Al−O bond triggers the crystallization and the mayenite phase is formed at the early stage. The same conclusion was obtained for $60CaO \cdot 10BaO \cdot 17Al_2O_3 \cdot 13Fe_2O_3$ glass.

References:

1) T. Nishida, *J. Non-Cryst. Solids*, 177, 257 (1994). 2) T. Nishida, in *Mössbauer Spectroscopy of Sophisticated Oxides*, Akadémiai Kiadó, Budapest, 1997, Ch. 2 (pp. 27-87).

Tel/Fax: +81-92-642-2591. E-mail: glassscc@mbox.nc.kyushu-u.ac.jp

P314
s.21

MÖSSBAUER STUDY OF JAPANESE ANCIENT IRON SLAG

A. Nakanishi, T. Kobayashi and S. Miono[1]

Department of Physics, Shiga University of Medical Science, Seta, Otsu ,Shiga 520-21, JAPAN

[1] *Department of Physics, Osaka City University, Sumiyoshi, Osaka 558, JAPAN*

Summary: Mössbauer spectroscopy was applied to ancient iron slags excavated at the ancient ruins of iron manufacturing in order to investigate the raw material and the operative conditions of the furnace.

Key Words: Mössbauer spectroscopy, ancient iron slag.

At the ancient ruins of iron manufacturing, a large amount of iron slag was found. The formation of the slag is affected by the raw material and the operative conditions of the furnace, where iron ore and iron sand had been used as the raw material. The iron slag can be divided into two categories. One is a smelting slag produced in the smelting process of the raw material. Another is a smith forging slag produced in the process of removing the impurity from the metallic iron obtained by the smelting process. In this study in order to investigate the raw material and the operative conditions of the furnace, Mössbauer measurements of the iron slags excavated at the ancient ruins, later than 7 A.D., were carried out. A typical spectrum is shown in Fig. 1.

From Mössbauer spectra, it is found that the iron slag consists of fayalite(Fe_2SiO_4), wüstite (Fe_xO, $x<1$), magnetite (Fe_3O_4) and ulvöspinel (Fe_2TiO_4). Since iron sand obtained in Japan consists magnetite- ulvöspinel (Fe_3O_4- Fe_2TiO_4) solid solution, it is necessary to remove the titanium from the iron sand during the smelting process. Thus, slag having ulvöspinel is a smelting slag, where iron sand was used as raw material. The slag which mainly consists of fayalite was produced during the smelting process of the iron ore because the iron ore contains few amount of titanium. The slag which consists of a large amount of wüstite is considered to be a smith forging slag.

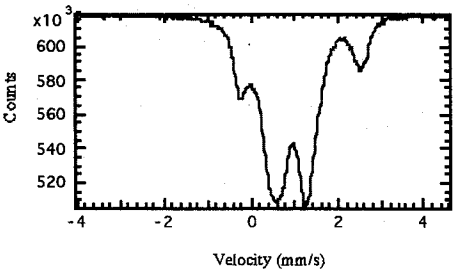

Fig. 1 A typical spectrum of the slag. The inner doublet is due to wüstite and the outer one is due to fayalite.

Fax: +81-775-48-2415, E-mail: nakanisi@belle.shiga-med.ac.jp

P315
s.21

FORMATION OF IRON FINE-PARTICLES IN A CRYSTAL LATTICE BY THE COMPUTER SIMULATION

T. Kobayashi, A. Nakanishi and K. Fukumura

Department of Physics, Shiga University of Medical Science, Seta Otsu, 520-21 Shiga, Japan

Summary : The Mössbauer spectrum was simulated with the arrangement of atoms obtained by a computer and compared with that observed with fine-particles formed in a sapphire crystal by the implantation technique.

Key words : fine-particle, computer simulation, Mössbauer spectroscopy

The growing up of iron fine-particles was simulated with a computer and the expected Mössbauer spectra were calculated from the arrangement of atoms which were compared with the observed spectra of fine particles of ^{57}Fe formed in a sapphire crystal by the implantation technique at the dose from 4×10^{16} to 1×10^{17} Fe/cm^2.

In the simulation, a primitive lattice of α-iron was assumed in the sapphire crystal. An implanted iron atom is scattered in the sapphire crystal, and arrive at some position in the primitive lattice with very low kinetic energy and without bonding with other ions. After that, the atom approaches a room where the density of iron atoms is locally the greatest, and rests somewhere in the room. After repeating this procedure again and again, the arrangement of iron atoms was simulated and many fine particles were formed in the lattice. The magnetic hyperfine field of an iron atom is supposed to be influenced by the nearest (nn) and next nearest (nnn) neighbors[1] as

$$H(n,m) \propto H_{Fe} \cdot n_r \qquad (1)$$

when the iron atom has n nearest neighbors and m next nearest neighbors around it, where H_{Fe} is the hyperfine field of bulk α-iron,

$$r_{12} = c_2/c_1, \qquad n_r = n + r_{12}m \qquad (2)$$

and c_1 and c_2 are the constants describing the influence of nn and nnn. From the simulated arrangement of iron atoms, the Mössbauer spectrum was calculated with the use of Eq. (1) and the agreement between the observed and calculated spectra is satisfactory on the whole.

REFERENCE

1. G. K. Wertheim, V. Jaccarino, J. H. Wernick and N. E. Buchanan, Phys. Rev. Lett., **12**, 24 (1964).

Fax: +81-775-48-2415, E-mail: kobayas@sums.shiga-med.ac.jp

P316
s.22

POSITRON AND POSITRONIUM LIFETIME STUDY OF SOME AQUEOUS SOLUTIONS OF CHIRAL MATERIALS

K. SÜVEGH, A. DOMJÁN, A. VÉRTES

Department of Nuclear Chemistry, Eötvös Loránd University, H-1518 Budapest 112, P. O. Box 32, Hungary

Summary:
Key words:

We studied the aqueous solutions of tartaric acid, alanine, and cysteine in the function of temperature by positron lifetime spectroscopy. The results were compared with those obtained in pure water under similar conditions. We always observed a sharp minimum of the positron lifetime at around 41 ℃ in water and in the solutions of the stereo-isomers. It has been found that the lifetime minima were different for the natural stereo-isomers and for the isomers which can not be found in the nature.

Fax: 36-1 209-0602, E-mail: vertesa@ludens.elte.hu

P317
s.22

POSITRONIUM IN A LAYERED-STRUCTURE MATERIAL: MONTMORILLONITE

M. Sano[1], H. Murakami[2] and K. Ichimura[*3]

1 *Department of Chemistry, Division of Natural Sciences, International Christian University, Mitaka, Tokyo 181, Japan*
2 *Department of Physics, Faculty of Education, Tokyo Gakugei University, Koganei, Tokyo 184, Japan*
3 *Department of Chemistry, Faculty of Science, Kumamoto University, Kumamoto 860, Japan*

Summary : The line-shape parameters of the Doppler-broadened spectra for ion-exchanged (Na, Zn, Al, Cu and alkylammonium) montmorillonites (mont) demonstrate that Ps atoms are predominantly distributed in the interlayer spaces of mont, rather than in the aluminosilicate layers.
Key words : Positron annihilation, positronium, montmorillonite, alkylammonium intercalation.

We have studied annihilation of positrons in montmorillonite (abbreviated to mont hereafter), of which interlayer space can be modified by being filled with various kinds of intercalants, in order to know the region where Ps atoms are distributed in layered-structure materials.

Homo-ionic Na-mont (1) prepared from montmorillonite (Kunipia F, Kunimine Industries Co., Ltd, Tokyo) was converted into Zn-mont (2), Al-mont (3), Cu-mont (4), tetramethylammonium-mont (5), *n*-hexylammonium-mont (6), octadecyltrimethylammonium-mont (7) and dimethyl-dioctadecylammonium-mont (8) by being stirred in water with the corresponding chloride or bromide. The basal spacings of intercalated-monts are (1):1.25, (2):1.53, (3):1.54, (4):1.24, (5):1.40, (6):1.33, (7):2.24 and (8):3.94 nm, respectively. A small piece of positron source, ^{22}NaCl of *ca.* 0.6 MBq sealed between two thin Mylar films, was buried in a powder sample contained in a Pyrex-glass tube. Positron-electron annihilation spectra were obtained from Doppler broadening of 511 keV radiation with the energy resolution of 1.01 keV (FWHM), and positron-lifetime spectra were obtained by means of a fast-fast coincidence system with the time resolution of 0.260 ns.

The observed positron-lifetime spectra were analyzed by three exponentials ; the shortest-lived component τ_1 due to *para*-Ps (*p*-Ps) being fixed at 0.125 ns and the ratio of the intensity I_1 due to *p*-Ps to that of the longest-lived component I_3 due to the pick-off annihilation of *ortho*-Ps at 1/3. When Na cations in Na-mont (τ_3=1.38 ns) are exchanged for paramagnetic Cu^{2+} ions, the component τ_3 was extremely shortened to 0.62±0.01 ns (I_3=9.7±0.1%). Line-shape parameters of Doppler-broadened spectra S for alkylammonium-intercalated monts range from 0.551±0.003 to 0.580±0.003, and are greatly different from the S value for the original Na-mont, 0.525±0.003. They are found to be almost equal to the S values observed for the corresponding pristine alkylammonium salts used for the intercalation, as shown in Fig. 1, which demonstrates that Ps atoms are predominantly distributed in the interlayer spaces of montmorillionite.

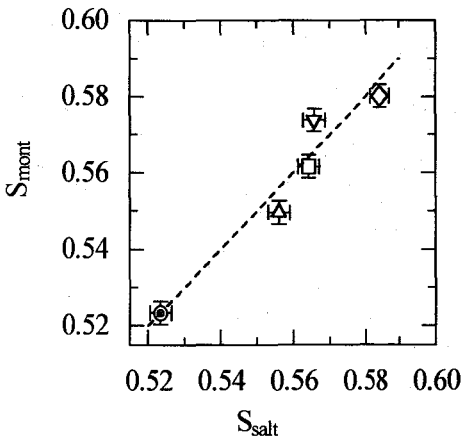

Fig. 1. S_{mont} values for alkylammonium-intercalated monts against S_{salt} values for the corresponding alkylammonium salts, ◎:1, △:5, □:6, ▽:7 and ◇:8.

FAX:+81-96-342-3376, E-mail:ichimura@gpo.kumamoto-u.ac.jp

P318
s.22

APPLICATION OF A PULSED SLOW POSITRON BEAM TO POLYMER

N.Oshima [1], E.Hamada [1], T.Suzuki [2], K.Kondo [2], I.Kanazawa [3] and Y.Ito [4]

[1] *Department of Accelerator Science, The Graduate University for Advanced Studies, 1-1 Oho, Tsukuba, Ibaraki 305, Japan*
[2] *Radiation Science Center, High Energy Accelerator Research Organization(KEK), 1-1 Oho, Tsukuba, Ibaraki 305, Japan*
[3] *Department of Physics, Tokyo Gakugei University, 4-1-1, Nukuikitamachi, Koganei, Tokyo 184, Japan*
[4] *Research Center for Nuclear Science and Technology, The University of Tokyo, Tokai, Ibaraki 319-11, Japan*

Summary: The positron lifetime spectra of polymers (teflon and polyethylene) were measured using a newly developed pulsed slow positron beam system in order to evaluate the possibility of its application to the study of near-surface stracture of polymers.

Key word: pulsed positron beam, positron annihilation, positron lifetime, polymer

Pulsed slow positron beam is a unique probe to evaluate characteristics of condensed matter. A feature of the pulsed positron beam is that a positron lifetime spectrum can be measured at an arbitrary depth (10nm to 4μm) of specimens using the variable beam energy (0.2 to 30keV), while an ordinary method using positrons from ^{22}Na is only applicable to a bulk study (100μm).

A pulsing system for slow positrons is under development. Slow positrons are derived by moderating fast positrons from 30mCi ^{22}Na through a tungsten single crystal film (1μm). The slow positrons are guided about 1.9m to a target chamber by magnetic field (70G) of solenoidal and Helmholtz coils. The pulsing is done by using time varying moderator bias which is produced by an arbitrary waveform generator and a post amplifier. Slow positrons are accelerated for pulsing and are focused on the target at 25 to 40MHz repetition. Positron lifetimes are defined by the time difference between the detection time of positron annihilation gamma rays (start signal) and pulsing trigger signals from the waveform generator (stop signal).

The time resolution achieved so far is about 1.5ns, which is much larger than that of an ordinary method using direct positrons from ^{22}Na (250ps). However the 1.5ns time resolution would be applicable to some samples like polymer, where the ortho-positronium lifetime is longer than about 2ns.

The positron lifetime spectrum for aluminum and teflon measured by the system are shown in the figure. It is clear that the positron lifetime of teflon (~ 4ns) is longer than that of aluminum (~ 1ns).

The possibility of the application of the system to polymer study will be discussed in more detail.

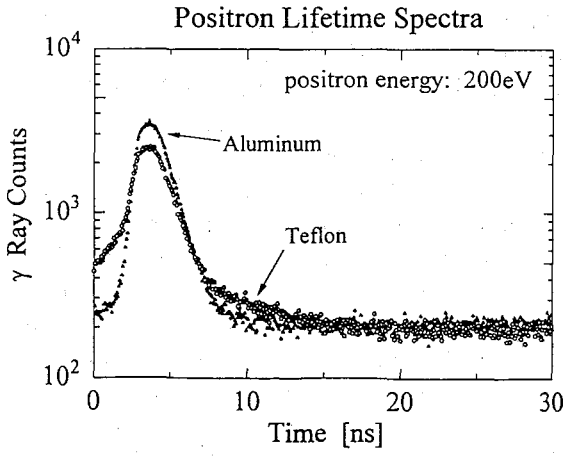

Fax: +81-298-64-1993, E-mail: takenori.suzuki@kek.jp

P319
s.23

LASER-INDUCED FLUORESCENCE STUDY ON THE INTERACTION OF EU(III) WITH POLYCARBOXYLATES

Y. Takahashi[1,5], T. Kimura[2], Y. Kato[2], Y. Minai[3], Y. Makide[1], and T. Tominaga[4]

[1]Radioisotope Center, University of Tokyo, Yayoi, Bunkyo-ku, Tokyo 113, JAPAN
[2]Japan Atomic Energy Research Institute, Tokai-mura, Ibaraki 319-11, JAPAN
[3]Faculty of Humanities, Musashi University, Toyotama-kami, Nerima-ku, Tokyo 176, JAPAN
[4]Professor Emeritus, University of Tokyo, Hongo, Bunkyo-ku, Tokyo 113, JAPAN
[5]Research Fellow of the Japan Society for the Promotion of Science

Summary: Laser-induced fluorescence spectroscopy was applied to the study of pH and salt concenctration effects on the number of water molecules in the primary hydration sphere of Eu(III) in polyacrylate, polymaleate, polymethacrylate, and poly-α-hydroxyacrylate complexes.
Key words: Laser-induced fluorescence spectroscopy, Eu(III), Polycarboxylate complexes

Formation of humate complexes has been recognized as an important factor controlling environmental behavior of actinides and lanthanides. In order to clarify characteristics of humic acid as polyelectrolyte, synthetic polycarboxylate ligands have been often employed as model substances. We applied laser-induced fluorescence spectroscopy (LIFS) to polyacrylate (PAA), polymaleate (PMA), polymethacrylate (PMAA), and poly-α-hydroxyacrylate (PHAA) complexes so as to obtain the structural information of metal-polyelectrolyte complexes. By using LIFS for Eu(III), fluorescence lifetime reflecting the number of water molecules in the primary hydration sphere of Eu(III) (N_{H_2O}) can be obtained.

Formation of polycarboxylate complexes with Eu(III) in the conditions employed for LIFS experiments was confirmed by two methods, speciation calculation based on stability constants determined by solvent extraction and direct measurement by dialysis using Eu-152 tracer. The polyelectrolyte complexes are found as dominant species above pH ca. 4 in the following condition: total concentration of Eu(III) and carboxylate, 0.15 mM and 0.030 eq/l, respectively; the concentration of supporting electrolyte, C_S, 0.010 M ($NaClO_4$).

The N_{H_2O} in the $EuCl_3$ solution was ca. 9 below pH 6 (aqua complex), which decreased above pH 6 showing the formation of carbonate complexes in the solution. Figure 1 shows the pH dependence of N_{H_2O} in polycarboxylate complexes. The N_{H_2O} of PAA complex decreased sharply around pH 2.5 showing the complex formation and it decreased gradually from 4 to 2.5 between pH 3.5 and 9, indicating that larger number of carboxylate ligands were bound at higher pH. The N_{H_2O} of PAA complex implies that more than three carboxylate ligands are bound to Eu(III), since N_{H_2O} of 1:3 complex of Eu(III)-propionate was ca. 4.2, larger than PAA. In PHAA complex, N_{H_2O} was smaller than that of PAA complex, while N_{H_2O} in PMA was larger than that in PAA. Stability constants of these polycarboxylate complexes determined were in the order of PHAA > PAA > PMA. This shows that, the more dehydrated in the polymolecule, Eu(III) forms more stable complex with these ligands. The N_{H_2O} in PMAA behaved differently: it is almost identical to that of PAA complex between pH 3 and 5, whereas it has a maximum between pH 5 and 8. This may be due to the abrupt transition of PMAA conformation, as has been reported in many works based on pH titration and viscosity measurements.

As C_S increases, N_{H_2O} of polycarboxylate complexes generally decreased when the degree of ionization of polycarboxylate was 0.6, due to the reduced repulsion between dissociated carboxylate ligands by the shielding effect of added Na^+ ion. In particular, the decreasing rate of N_{H_2O} vs. C_S was larger for PMA and PMAA complexes than others. These results suggest that the repulsion between ligands is important for the conformation of polycarboxylate in the solution.

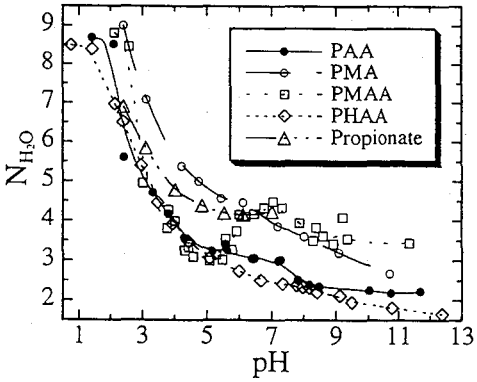

Fig. 1. The pH dependence of N_{H_2O} in polycarboxylate and propionate complexes. Eu: 0.15 mM; total carboxylate: 0.030 eq/l; C_s: 0.010 M.

P320
s.20

SOLVENT EXTRACTION OF TECHNETIUM(VII) BY CYCLIC AMIDES

Shinichi SUZUKI*, Masakazu TAMURA, Shoichi TACHIMORI
Yoshiharu USUI[1]

Department of Chemistry and Fuel Research, Japan Atomic Energy Research Institute
Tokai-mura Naka-gun Ibaraki 319-11 Japan
[1]The Graduate School of Science and Engineering, Ibaraki University
Bunkyou Mito-shi Ibaraki 310 Japan

Summary: Cyclic amides are noted as one of the alternative extractants of tributylphosphate (TBP) in the field of nuclear fuel reprocessing. Eight substituted cyclic amides have been synthesized and the extraction of Tc (VII) by the substituted cyclic amides was investigated under various conditions.
Key words: Technetium, cyclic amide, distribution coefficient, steric effect

ABSTRACT

In this study, eight substituted cyclic amides have been synthesized and the extraction of Tc (VII) by the substituted cyclic amides was investigated under various conditions. The amides investigated are N-(2-ethyl)hexylbutyrolactam (EHBLA), N-(2-ethyl)hexylvalerolactam (EHVLA), N-(2-ethyl)hexylcaprolactam (EHCLA), N-octylcaprolactam (OCLA), and substituted ε -caprolactam; 2-octyl-N-(2-ethyl)hexylcaprolactam (2OEHCLA), 3-octyl-N-(2-ethyl)hexylcaprolactam (3OEHCLA) and 5-octyl-N-(2-ethyl)hexylcaprolactam (5OEHCLA). Distribution ratio of ^{99}Tc(VII) : D_{Tc} between nitric acid solution and cyclic amides in dodecane was determined from measurement of ^{99}Tc radioactivity by using liquid scintillation counter. Fig.1 shows that D_{Tc} by EHBLA, EHVLA and EHCLA of a respective concentration of 1 M in dodecane increased with an increase in acid concentration and the third phase has been appeared in aqueous conditions of 0.1 N HNO_3 for EHBLA, 0.3 N HNO_3 for EHVLA, and of 1 N HNO_3 for EHCLA. D_{Tc} by EHCLA is less than that of EHBLA and EHVLA in nitric acid concentration area, this result was caused by difference of cyclic amides structure. A nitric acid dependency of the D_{Tc} with 0.1 M substituted cyclic amides was similar to that with TBP in high acid concentration range. D_{Tc} with 2OEHCLA was less than that of mixture of 3OEHCLA and 5OEHCLA because of steric hindrance with neighboring n-octyl group. In the presentation, we will discuss the relationship between the D_{Tc} and ring structure, especially steric effect around oxygen donor atom of the employed amides as well as the extraction behavior of nitric acid with the amides.

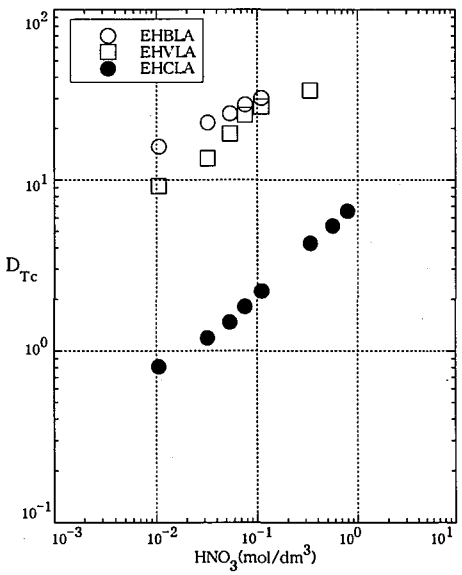

Fig.1 Nitric acid concentration dependancy of D_{Tc} by 1 M cyclic amides-dodecane. (25℃)

E-mail: suzuki@mummy.tokai.jaeri.go.jp

P321
s.20

STUDY ON THE EXTRACTION OF TRIVALENT LANTHANIDE IONS WITH N,N'-DIMETHYL-N,N'-DIPHENYL-MALONAMIDE AND -DIGLYCOLAMIDE

H. Narita[1,2], T. Yaita[1], K. Tamura[1] and S. Tachimori[1,2]

[1]*Department of Chemistry and Fuel Research, Japan Atomic Energy Research Institute Tokai-mura Naka-gun Ibaraki 319-11 Japan*

[2]*The Graduate school of Science and Engineering, Ibaraki University Bunkyo Mito-shi Ibaraki 310 Japan*

Summary: The extraction behavior of trivalent lanthanide ions with the two types of diamides, N,N'-dimethyl-N,N'-diphenyl-malonamide and -diglycolamide, was investigated by distribution ratios and spectroscopic methods.

Key words: lanthanide, extraction, malonamide, diglycolamide, FT-IR

Diamide compounds have been extensively investigated as useful extractants of actinides and lanthanides in the nuclear fuel cycle. However any detailed extraction properties of diamides for the whole series of trivalent lanthanide ions (Ln(III)) has not been found yet. In the present study, the extractions of all Ln(III), except Pm, from nitric acid solutions were carried out by using two diamides; 1) N,N'-dimethyl-N,N'-diphenyl-malonamide (MA) which has two carbonyl amide groups, 2) N,N'-dimethyl-N,N'-diphenyl-diglycolamide (DGA) consisting of an ether and two carbonyl amide groups (Fig.1), and the structural properties of diamide-Ln complexes were investigated by spectroscopic method.

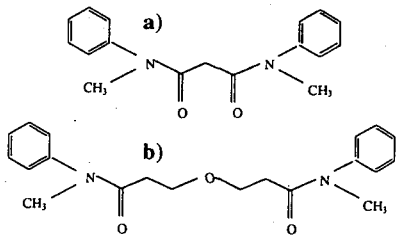

Figure 1. Structure of N,N'-dimethyl-N,N'-diphenyl a)-malonamide, b)-diglycolamide

The relations between atomic number and the distribution ratio (D) of Ln(III) from 4 mol dm^{-3} of nitric acid with 0.2 mol dm^{-3} of each extractant are shown in Fig.2. The D's in the DGA system are much higher than those in the MA system; about 10^3 for lighter Ln, about 10^6 for heavier Ln. The lanthanide patterns show a difference between the MA and the DGA system. In the MA system, the D's decrease with an increase in atomc numer. On the other hand, in the DGA system, the D's increase with an increase in atomic number.

On the FT-IR spectra of the extracted species in the both systems, the peak based on the carbonyl stretching shifted to low wave number. The magnitude of the shifts in the DGA system was larger than that in the MA system, suggesting that the interactions between Ln(III) and the carbonyl oygens in the Ln-DGA complexes are stronger than those in the Ln-MA complexes. Further datailed structual information by UV-vis is currently under intensive investigation.

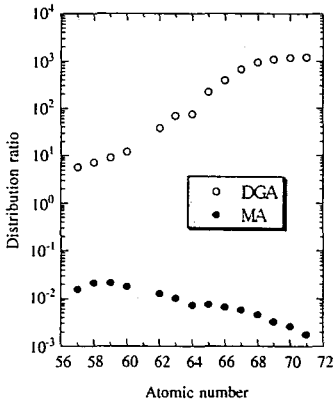

Figure 2. Lanthanide patterns for distribution ratios of Ln. Each extractant concentration is 0.2 mol dm^{-3} in chloroform. Nitric acid concentration is 4 mol dm^{-3}.

Fax: +81-29-282-6723, E-mail: narita@mummy.tokai.jaeri.go.jp

P323
s.24

Observation of Radioactive Hetero-Fullerenes Using Radiochemical Techniques

K. Sueki[1], K. Shikano[2], T. Shigematsu[2],K. Masumoto[3], T. Ohtsuki[4]

[1]*Department of Chemistry, Tokyo Metropolitan University*
[2]*NTT Opto-Electronics Laboratory*
[3]*KEK, Radiation Science Center, Tanashi Branch*
[4]*Laboratory of Nuclear Science, Tohoku University*

Summary: Fullerenes; C_{60} and C_{70}, were irradiated by 10 MeV deuteron beam. The irradiated samples were dissolved in CS_2 and filtrated to remove insoluble by-products. Finally, radioactive $^{13}NC_{59}$ and $^{13}NC_{69}$ fullerenes and products, such as fullerene dimers, trimers labeled with ^{13}N, were isolated and detected in a liquid phase by radiochromatopraphy.
Key word: Radiochromatography, ^{13}N hetero-fullerene

Fullerenes and fullerene derivatives have attracted the attention of many workers because of their interesting physical and chemical properties. Recently, it has become noteworthy and important to study the properties or the behavior of fullerenes by applying radiochemical techniques. In our previous study[1], Radioactive fullerenes such as $^{11}CC_{59}$, $^{11}CC_{69}$ and dimers were produced by nuclear reactions though the initial recoil energy was much higher than the intramolecular bonding energy level. In this conference, we also demonstrate the production of radioactive Hetero-fullerenes labeled with ^{13}N by the recoil process following nuclear reactions.

Samples of 99.5 % purified C_{60} or C_{70} fullerenes were wrapped in thin aluminum foil and irradiated with 8 or 10 MeV deuterons at the Cyclotron Radio Isotope Center(CYRIC), Tohoku University and the NTT Opto-Electronics Laboratory. The beam current was typically 2 μA and the irradiation time was set to 10 min. The irradiated samples were dissolved in CS_2, and then filtrated with a millipore filter to remove insoluble by-products. The soluble fraction was injected into a HPLCequipped with Buckyprep or 5PBB column at the flow rate of 1 ml/min. The elution behavior was monitored by a UV detector and two on-line BGO scintillation detectors to count 511 keV γ-rays emitting from ^{13}N in coincidence. Data from the radiochromatogram were accumulated by means of a multi-channel scaler system(MCS), using a personal computer.

Several peaks were detected in the radiochromatogram of C_{60} and C_{70} fullerenes. The first peak of each elution curve can be assigned to $^{13}NC_{59}$ and $^{13}NC_{69}$ since the each peak corresponds to the C_{60} and C_{70} absorption peak of UV monitor, respectively. The second peak were also observed for the C_{60} and C_{70} samples, respectively, though they could not be observed clearly in the UV-chromatogram at the same retention. As we showed the evidence of dimer fullerenes in ref.[1]; $^{11}CC_{59}$+C_{60}, $^{11}CC_{69}$+C_{70}, this result may also indicate the possibility of dimer of hetero-fullerenes including ^{13}N in the cage.

[1] T. Ohtsuki, K. Masumoto, K. Sueki, K. Kobayashi, K. Kikuchi, J. Am. Chem. Soc., **117**, 12869(1995).

---

1)Minami-Osawa, Hachioji, Tokyo 192-03, Japan, E-mail:sueki-keisuke@c.metro-u.ac.jp
2)Shirakata, Tokai, Ibaraki 319-11, Japan, E-mail: shikano@iba.iecl.ntt.co.jp, shigematsu@
3)Midori-cho, Tanashi, Tokyo, Japan, E-mail: masumoto@tanashi.kek.jp
4) Mikamine, Taihaku, Sendai 982, Japan, E-mail: Ohtsuki@LNS.tohoku.ac.jp

P324
s.41

MODEL EXPERIMENT OF GAS-PHASE RAPID CHEMISTRY FOR ACTINIDES AND TRANSACTINIDES

T.Kaneko, K.Tamura, S.Kimura and H.Kudo*

Department of Chemistry, Faculty of Science, Niigata University,
8050 Ikarashi 2-no-Cho, Niigata, 950-21, Japan

Summary : The gas phase reaction of lanthanum chloride and dipivaloylmethane(dpm) was investigated. $LaCl_2$(dpm) was found to be a main product. We have also studied temperature dependence of this reaction in detail.
Key words : lanthanum, dpm, gas phase reaction

The thermochromatography is has been used for the investigation of chemical properties of short-lived heavy elements. In the thermochromatography nuclides of interest are converted to volatile compound in a gas phase. As dpm complexes are known to be volatile, we have examined the applicability for thermochromatography.

As a model experiment of complexing properties of heavy elements in a gas phase, we have studied the reactivity of lanthanide and dpm in a gas phase. Lanthanum chloride was used in this work.

The experimental apparatus consists of a dpm vapor generator, a reaction chamber and the mass spectrometer. Reaction products of $LaCl_3$ and dpm were carried from reaction chamber to the mass spectrometer continuously by helium carrier gas. The temperature of the reaction chamber was controlled and the heating rate was also varied.

As shown in fig.1, substitution products of $LaCl_2$(dpm), $LaCl(dpm)_2$ and $La(dpm)_3$ have been ascertained. Among them $LaCl_2$(dpm) was a main product which has not been synthesized so far. The heating rate dependence of the peak temperature of its chromatogram was also measured.

The detailed discussion will be present.

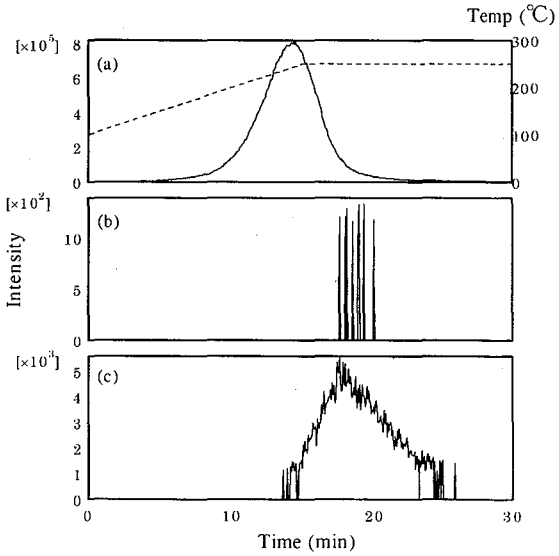

Fig.1 Chromatogram of (a) $LaCl_2$(dpm) (m/z=391), (b) $LaCl(dpm)_2$ (m/z=540) and (c) $La(dpm)_3$ (m/z =691). The temperature of the reaction chamber was elevated from 100℃ to 250℃ at 10℃/min.

Fax : +81-25-262-6116, E-mail : hkudo@sc.niigata-u.ac.jp

P325
S.41

Anisotropy in the Physical Properties of UNiGa under High Pressure

F.Honda, G.Oomi*, A.V.Andreev**, K.Prokeš**, L.Havela** and V.Sechovský**

Department of Physics, Kumamoto University, Kurokami 2-39-1, Kumamoto 860, Japan
**Department of Mechanical Engineering and Materials science, Kumamoto University, Kurokami 2-39-1, Kumamoto 860, Japan*
***Department of Metal Physics, Charles University, 12116 Prague, The Czech Republic*

Summary: The linear thermal expansion, compressibility and electrical resistivity of UNiGa have been measured under high pressure. The huge anisotropic behaviors are observed in each physical properties. The data was analyzed in terms of chemical bonding.
Key words: Uranium compounds, High pressure, Magnetic anisotropy

UNiGa belongs to the large group of isostructual *UTX* (*T* :transition metal, *X* :*p*-metal) compounds which crystallizes ZrNiAl-type hexagonal structure consisting of a sequence of U-Ni and Ni-Ga basal plane layers. In this compounds U has a magnetic moment, ~1.3 μ_B. The *c*-axis is easy magnetization axis. UNiGa orders antiferromagnetically at 40 K and indicates 3 order-order transitions at lower temperature. Magnetic structure of UNiGa is collinear and reveals a huge uniaxial magnetic anisotropy because the magnetic moment of U arranges parallel to the *c*-axis in all magnetic phases. All antiferromagnetic (AF) phases consist of ferromagnetic basal plane sheets which are coupled antiferromagnetically along *c*-axis. It is reported that this enormous magnetic anisotropy is strongly reflected in the physical properties of UNiGa.

In the present work, the linear thermal expansion, the linear compressibility and electrical resistivity of single crystalline UNiGa has been measured under high pressure up to 2.2 GPa. It is found that there are large anisotropic behaviors in these quantities. For instance, the thermal expansion coefficient of *a*-axis ($\alpha_a \sim 16\times10^{-6}$) is about three times larger than that of *c*-axis ($\alpha_c \sim 5\times10^{-6}$) at room temperature. The linear compressibility (κ) is also anisotropic, which correlates the linear thermal expansion coefficients of the crystal axis. We can estimate the temperature dependence of the linear compressibility from this measurement. κ_a decreases and κ_c increases with decreasing temperature . It suggests that this phenomena is related to the uniaxial magnetic structure.

Fax: +81-96-342-2749, e-mail: c3170@gpo.kumamoto-u.ac.jp

P326
s.42/24

TRANSPORT MECHANISM OF HYDROGEN THROUGH OXIDE FILM FORMED ON ZIRCALOY-4

Y.Hatano[1], R.Hitaka[1], M.Sugisaki[1] and M.Hayashi[2]
[1]*Department of Nuclear Engineering, Faculty of Engineering, Kyushu University, Fukuoka 812-81, Japan*
[2]*Technical Development Department, Nuclear Fuel Industries, Ltd., 950 Ohaza-noda Kumatori-cho, Sennan-gun, Osaka 590-04, Japan*

Summary: The depth profile of deuterium in the oxide film of Zircaloy-4 was measured with secondary ion mass spectroscopy to examine the diffusive motion of hydrogen in the oxide. The distribution of deuterium was dependent upon the size distribution of $Zr(Fe,Cr)_2$ precipitates.
Key words: Zircaloy, Hydrogen, Oxide Film, Transport, SIMS

The hydrogen uptake behavior of Zircaloy is an important problem to evaluate the performance of fuel claddings of water-cooled reactors. The transport mechanism of hydrogen through zirconium oxide layer formed on Zircaloy, however, has not been fully clarified in spite of the common understanding that the hydrogen uptake behavior of Zircaloy is strongly dependent upon its alloy composition and heat-treatments during fabrication. Then, an aim of the present study is to clarify the diffusive motion of hydrogen in the zirconium oxide layer formed on Zircaloy-4. In order to examine the diffusion process of hydrogen in the zirconium oxide layer, some special experimental techniques were devised: The specimens were first oxidized in 0.1 MPa H_2O steam at 673 K to form the oxide layer of about 1.3 μm. Next, they were again oxidized in D_2O steam under the same condition, in which the thickness of the oxide layer increased by about 0.2 μm and deuterium diffused into the oxide layer. The depth profile of deuterium was measured with secondary ion mass spectroscopy(SIMS), in which the secondary ion yield of deuterium was calibrated by making use of radioactivity of tritium as follows: The specimen once oxidized in H_2O steam under the above condition was oxidized in HTO steam in stead of in D_2O steam. Then, the radioactivity of tritium present in the oxide layer was measured with a liquid scintillation counter, in which the specimen was directly immersed in the cocktail. The depth profile given by SIMS was calibrated with the obtained radioactivity by taking into consideration the escape probability of β-ray of tritium through the oxide layer.

The depth profiles of deuterium in the oxide films of the specimens having different size distributions of $Zr(Fe,Cr)_2$ precipitate are shown in Fig.1. In the case of specimen having the fine precipitate, the diffusion profile of deuterium was successfully explained by a diffusion equation. In the case of specimen having the coarse ones, however, the depth profile was not represented by the diffusion equation. These results were interpreted as follows: In the former case, the fine precipitates in the oxide layer were completely oxidized and hydrogen diffused homogeneously through the zirconium oxide. In the latter case, however, the coarse precipitates in the oxide layer were not completely oxidized and their core region remained in a metallic state, in which a large amount of hydrogen was retained. On the basis of these experimental results, the relation between the hydrogen uptake behavior and the heat-treatment was discussed.

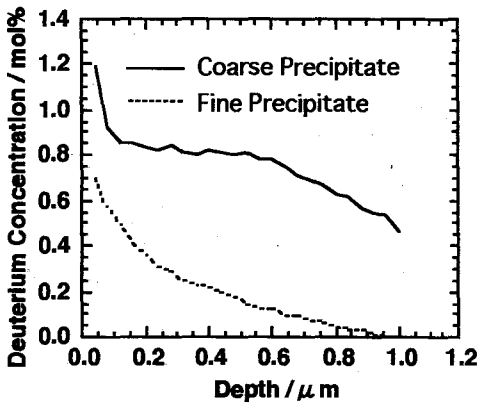

Fig.1 Depth profiles of deuterium in oxide films of Zircaloy-4

FAX:+81-92-642-3800, E-mail: yhata@nucl.kyushu-u.ac.jp

P327
s.43

ION EXCHANGERS IN RADIOACTIVE WASTE MANAGEMENT INFLUENCE OF BENTONITE IN REMOVAL OF Zn(II) & Cd(II)

S.P. Mishra, D. Tiwari, V.K. Singh

Nuclear and Radiochemistry Laboratory, Department of Chemistry, Faculty of Science, Banaras Hindu University, Varanasi-221 005, INDIA.

Summary : Bentonite is effective for the removal of Zn(II) ions as compare to Cd(II) ions and quite stable towards ionizing radiations, at least, for the removal of these ions.
Key words : Zn(II), Cd(II), Radiotracer, Freundlich isotherm, Radiation stability, Desorption.

The uptake of radioactive species on clay minerals may provide an important geochemical barrier to radionuclides released from nuclear wastes geological repositories to the accessible environment or biosphere. An attempt has been made to assess the suitability of bentonite in the removal process for Zn(II) & Cd(II) ions, as fission fragments occurring in low yields, present in aqueous solution under simulated conditions. These ions have a significant role in biological systems as zinc is an essential ion present as micronutrient, whereas cadmium is a non-essential ion which often occurs along with zinc in nature.

The present paper reports the influence of naturally obtained bentonite towards removal of the two ions from aqueous solutions at micro to tracer concentrations using 'radiotracer technique'. Various physico-chemical data enable us to propose the mechanism involved at the solid/solution interface. It was observed that with the increase of adsorptive concentration (10^{-8} to 10^{-2} mol dm^{-3}; *cf.* Table), temperature (303 to 333 K) and pH *ca.* (3 to 10), the amounts removed from aqueous solution increase. The first order rate of uptake follows Freundlich adsorption isotherm and the deductions of thermodynamic parameters infer about the endothermic nature with exchange type of mechanism. Furthermore, as no significant desorption could take place into the bulk concentration suggests the irreversibility of the uptake process. The influence of several added cations/anions was also assessed in the uptake process as these are often present as co-ions in aqueous wastes. It was observed that these added ions cause for low or high inhibition for the removal process.

To assess the influence of ionizing radiations on the surface property and hence the uptake behaviours of sorbent, bentonite was irradiated with a (Ra-Be) neutron source having an integral neutron flux *ca.* 3.85×10^{6} n/sec. and associated with a nominal γ-dose of 1.78 Gy/h. The solid was also irradiated with a high dose γ-cell (Co-60 source) having an activity of *ca.* 2250 Ci (mean dose rate *ca.* 4.66 KGy/h). The results indicate that irradiations could not affect significantly in the uptake of Zn(II) and Cd(II) ions on the surface of bentonite. The results indicate the applicability of bentonite in its potential use in radioactive waste management.

Table : *Change in adsorption of Zn(II) & Cd(II) on the surface of bentonite at different adsorptive concentrations (Temperature : 303K; pH ~ 6.8).*

	Amount adsorbed (mol g^{-1})						
Zn(II)	0.54×10^{-3}	0.56×10^{-4}	0.59×10^{-5}	0.65×10^{-6}	0.72×10^{-7}	0.80×10^{-8}	0.89×10^{-9}
Cd(II)	0.26×10^{-3}	0.28×10^{-4}	0.30×10^{-5}	0.34×10^{-6}	0.39×10^{-7}	0.45×10^{-8}	0.54×10^{-9}
Initial adsorptive conc.(mol dm^{-3})	10^{-2}	10^{-3}	10^{-4}	10^{-5}	10^{-6}	10^{-7}	10^{-8}

Fax : +91-542-317074

P328
s.43

ADSORPTION CHARACTERISTICS OF CARBON-14 ON ION EXCHANGE RESIN IN NUCLEAR POWER PLANT

K. P. LEE, H. J. KIM, K. S. PARK[1], D. W. KANG, C. HUH[2]

[1] *Kyungpook Natioanal University, Department of Chemistry, Taegu 702-701, Korea*

[2] *Korea Electric Power Research Institute , Material and Corrosion Research Laboratory, Taejon 305-308, Korea*

Summary: C-14 is produced in Nuclear Power Plants through the neutron activation process. Almost all C-14 in moderator is adsorbed by ion exchange resin. In this study, the adsorption characteristics of C-14 on the ion exchange resin were investigated at various condition.

Key words: C-14, ion exchange resin.

Wolsung nuclear power plants is a heavy water moderated and cooled, natural uranium fuelled, pressurized water reactor. 95 % of C-14 produced in moderator of heavy water reactor and almost all C-14 in moderator is adsorbed by ion exchange resin.

In this study, the adsorption characteristics of carbonates form compounds on an anion and cation exchange resin were investigated at vatious temperature, pH and concentration of C-14 to determine the release rate of C-14 in Wolsung power plants.

Furthermore, production and release rate of C-14 were measured directly from the moderator in Wolsung power plants to determine the storage capacity of C-14 on the ion exchange resin.

Fax: +82-53-950-5899, E-mail: Chejuman@mail.taegu.net

P329
s.43

SORPTION BEHAVIOR OF Am(III) ONTO GRANITE

A. Kitamura[1], T. Yamamoto[1], H. Moriyama[2] and S. Nishikawa[2]

[1] *Department of Nuclear Engineering, Faculty of Engineering, Osaka University, 2-1, Yamadaoka, Suita, Osaka, 565, Japan*

[2] *Research Reactor Institute, Kyoto University, Noda, Kumatori-cho, Sennan-gun, Osaka, 590-04, Japan*

Summary: Distribution coefficient (K_d) of Am(III) onto granite was determined. The obtained K_d values were successfully analyzed by using an electrical double layer model and the sorption mechanism was discussed on the basis of the present analysis.

Key words: radioactive nuclide migration, Am(III), granite, sorption, electrical double layer model

The migration behavior of radionuclides in geologic media is important for the safety assessment of radioactive waste disposal and is being investigated extensively in many institutions. However, the mechanism is not clearly understood, even for the sorption itself, and it is still hard to predict the migration behavior of the radionuclides with sufficient reliability. Much more efforts are needed for a complete understanding of the processes involved. The present study deals with the sorption behavior of Am(III) onto one of the geologic formations, that is granite. The distribution coefficient (K_d) was measured as a function of pH and ionic strength, and was analyzed by an electrical double layer model in order to get some insights of the sorption mechanism.

A batch method was applied to the measurement of the K_d of Am(III) onto the granite sample which was obtained from Inada, Ibaraki, Japan, and was crushed to the mesh size of 32-60. The Inada granite of 0.1 g was added into a $NaClO_4$ solution containing Am(III). The distribution coefficient of Am(III) onto the granite was determined in the solution of which pH ranged from 2.5 to 11.5 and ionic strength was set at 10^{-2} mol dm^{-3} and 10^{-1} mol dm^{-3}. After the equilibration of 1 week, the radioactivity of ^{241}Am in the liquid phase was measured. In this study, the colloid species in the solution was removed with using 0.45 μm membrane filter, and the K_d value was calculated as the ratio between the amount of Am sorbed onto granite and the amount of Am remained in the solution. The obtained K_d values were found to increase with increasing pH and with decreasing ionic strength. The obtained data were successfully analyzed by an electrical double layer model and the optimum parameter values of the double layer electrostatics and sorption reactions were obtained. The sorption mechanisms of Am(III) was discussed on the basis of the present analysis.

Fax +81-6-875-5696, E-mail: akitam@nucl.eng.osaka-u.ac.jp

P330
s.43

THERMAL NEUTRON CROSS SECTION AND RESONANCE INTEGRAL OF THE REACTION $^{135}Cs(n, \gamma)^{136}Cs$

Y. Hatsukawa[a], N. Shinohara[a], K. Hata[a], K. Kobayashi[a], S. Motoishi[a], M. Tanase[a]
T. Kato[b,c], S. Nakamura[b] and H. Harada[b]

[a]*Japan Atomic Energy Research Institute, Tokai, Ibaraki 319-11 Japan*
[b]*Power Reactor and Nuclear Fuel Development Corp., Tokai, Ibaraki 319-11 Japan*
[c]*Gifu College of Medical Technology, Seki, Gifu 501-32 Japan*

Summary:The thermal neutron capture cross section(σ_0) and the resonance integral(I_0) of the reaction $^{135}Cs(n,\gamma)^{136}Cs$ were measured by means of an activation method to obtain fundamental data for research on the transmutation of nuclear waste.
Key words: nuclear waste, transmutation, thermal neutron cross section, resonance integral, ^{135}Cs, quadrupole mass spectrometer, JRR-3

For the management of radioactive nuclear waste, feasibility of the use of high flux fission reactors and high intensity accelerators as intense neutron sources has been investigated for the nuclear transmutation of the waste. Precise thermal neutron cross section(σ_0) and the resonance integral(I_0) are necessary to determine the transmutation rate of the waste nuclides in the neutron sources. The present study was designed to obtain reliable values of the cross section and the resonance integral of the $^{135}Cs(n,\gamma)^{136}Cs$ reaction. ^{135}Cs included in a "standardized solution" of ^{137}Cs were use as a target in this experiment, since it is hard to obtain isotopically-pure material of ^{135}Cs. The ratio of the atom number of ^{135}Cs to that of ^{137}Cs was determined to be 0.89 ± 0.03 with a quadrupole mass spectrometer(1). Two sets of ^{135}Cs-^{137}Cs targets were prepared. Each target contained about 0.37 MBq of ^{137}Cs. One set of the caesium solution target with neutron flux monitor wires was housed in an aluminum capsules, and another set was put in a Cd shield case to determine the epithermal fraction of the neutron flux at the target position. Both targets were irradiated with neutrons in the JRR-3 Reactor of JAERI. After the neutron irradiation, γ-ray spectra of the ^{135}Cs-^{137}Cs targets were measured with high purity Ge detector. Gamma rays with the energies of 819, 1048 and 1235 keV from ^{136}Cs were observed at together with γ-rays from ^{134}Cs and ^{137}Cs. Weighted average of the half-life of ^{136}Cs obtained from the decay analysis of the three γ-rays is 12.63 ± 0.04 days which is close to the value previously reported(13.16 d). The cross section(σ_0) and the resonance integral(I_0) of the reaction $^{135}Cs(n,\gamma)^{136}Cs$ were determined to be 8.3 ± 0.3 barn and 38.1 ± 2.6 barn, respectively. The σ_0 is agreement with the value reported by Baerg et al.(2) within the limit of error, while the I_0 of is 2/3 smaller than reported by Baerg et al.(2)

(1)H. Harada et al., J. Nucl. Sci. Technol., 34, 498-502(1997)
(2)Baerg, et al., Can. J. Phys., 36, 863(1958)

P332
S.41

POSSIBILITIES OF SEPARATION AND PURIFICATION OF ACTINIDE AND TRANSACTINIDE ELEMENTS BY COMBINED ION EXCHANGE - SOLVENT EXTRACTION METHOD

L. I. GUSEVA, G. S. TIKHOMIROVA[1], N. SHINOHARA[2]

[1] *Vernadsky Institute of Geochemistry and Analytical Chemistry, Russian Academy of Sciences, Kosygin str. 19, Moscow 117975 Russia*
[2] *Department of Radioisotopes, Japan Atomic Energy Institute, Takai-mura, Ibaraki 319-11, Japan*

Summary:
Key words:

First "Combined Ion Exchange - Solvent Extraction" (CIESE) method was proposed by Korkisch for separation of U, Th, Zr and Hf from accompanying elements [1-3]. In this technique ion exchange resins are used as stationary phase while mixed aqueous-organic solutions containing various extractions (ethers, ketons, organophosphorous compounds) are employed as eluents. Therefore both ion exchange and solvent extraction processes are effective simultaneously.

In this report the possibility of such systems using for separation and purification of actinide and transactinide elements has been investigated. The cation-exchange behaviour of Th, Pa, U, Np, Pu, Am, Cm, Bk, Cf, and Hf, Zr as the lighter homologs of element 104 in mixed aqueous-organic HNO_3 solutions containing trioctylphosphine oxide (TOPO) has been studied in detail. The dependence of distribution coefficients of investigated elements upon the nature of solvents, composition of the solution HNO_3 and TOPO concentration, as well as the presence of oxidant (PbO_2) in the resin phase have been determined. The column experiments have been carried out. It was shown that in studied systems trivalent transplutonium elements (TPE), REE's, and numerous other elements are strongly adsorbed on cation-exchange column while light actinides (Th, Pa, U, Np and Pu) and d-transition elements (Hf, Zr) pass through the column making possible their quantitative separation. In the presence of oxidant (PbO_2) in the resin phase Bk(Ⅲ) was oxidized to Bk(Ⅳ) and was separated from other sorbed elements with acetonitrile-HNO_3-TOPO solutions. By passing the solution containing Bk(Ⅳ) through another cation-exchange column without oxidant Bk(Ⅳ) was reduced to Bk(Ⅲ) which strongly ratained by cation-exchanger and separated from nosorbed elements. Optimum conditions for separation and purification of actinide elements have been chosen. As results highly effective and selective methods of TPE separation from light actinides and some fission elements on cation-exchange column with organic solvent-HNO_3-TOPO solutions have been developed. A new method of berkelium separation from all actinides and numerous other elements with high factor of purification ($>10^4$) have been elaborated. The possibilities of investigated systems for separation of transactinide elements have been shown.

Fax: (7-095)938-20-54, E-mail: elkoz@geokhi.msk.su

P333
s.31

SYNTHESIS OF ^{186}Re-DMSA AND ITS BIODISTRIBUTIONS IN MICE

N. NOGAWA, S. MOMOSE[1], K. MIYAZAWA[1], Y. MAKIDE, K. OOHASHI[1], K. HASHIMOTO[2] AND N. MORIKAWA

Radioisotope Center, The University of Tokyo, 2-11-16, Yayoi, Bunkyo-ku, Tokyo 113, Japan
[1]Faculty of Pharmaceutical Sciences, Chiba University
[2]Department of Radioisotopes, Japan Atomic Energy Research Institute

Summary: A ^{186}Re-DMSA was prepared in more than 95% yield under the conditions of mole ratio of Re:DMSA:Sn = 1:20:20 - 1:20:30, pH; 0.8 - 1.5, reaction time; 30 - 50 min.. The skeletal uptake of 15 % was obtained by biodistribution test of mice.
Key words: rhenium-186, DMSA, bone pain, skeletal uptake

Both ^{186}Re and ^{188}Re emit β^- rays which are effective for therapeutic application to special cancers involving labeled complexes or monoclonal antibodies and for palliative treatment of metastatic bone pain. ^{99m}Tc complex of meso-2,3-dimercaptosuccinic acid (DMSA) is widely used as a renal imaging agent. Recently a ^{99m}Tc-DMSA has been reported as tumor-seeking agent. The situations encouraged us to try the synthesis of ^{186}Re-DMSA and the clarification of its biodistribution.

Rhenium-186 was supplied from the JAERI as ReO_4^- in an aqueous solution. The radioactivity was 16 - 23 GBq/g Re, 0.37 - 0.25 GBq/ml. A aqueous mixture of NaOH, ^{186}Re-ReO_4^-, $SnCl_2$, and L-ascorbic acid was heated on a water bath after adjustment of pH with 3M HCl. The ^{186}Re-DMSA complex in the solution was analyzed by silica gel TLC, PC, and EP (electrophoresis). The radiochemical yield of more than 95% was obtained under the following conditions: mole ratio of Re:DMSA:Sn = 1:20:20 - 1:20:30, pH of the reaction mixture; 0.8 - 1.5, reaction time; 30 - 50 min. The yield depends on the concentration of L-ascorbic acid to a lesser extent. The complex in a acetate buffer solution was kept stable for 1 h without any detectable decomposition. More than 90% of ^{186}Re-DMSA survived after 24 hours in the buffer solution and in the normal mouse serum at 37 ℃. An EP analysis suggested that the complex was not bound to the calcium(II) ions but bound to the proteins in the serum.

Biodistribution was assayed after i.v. injection of ^{186}Re-DMSA (10 - 20 kBq) in the 100 μl buffer solution to DDY male mice 25 - 27 g weight, five weeks aged. Organs of interest were excised after 10 min., 1h, 3h, 6h, or 24h. ^{186}Re radioactivity in the organs was counted. The uptake to skeletal, kidney and stomach were 15 %(in % injection dose/g organ), 10 % and less than 1 % respectively. The distribution was very similar to that of bone-localizing ^{99m}Tc(V)-DMSA. The urinary excretion reached to 50 % of the injection dose within 3 h and to its about 70 % for 24 h post-injection. ReO_4^- was not detected in the urine.

Fax: +81-3-3816-0422, E-mail: nogawa@ric.u-tokyo.ac.jp

P335 RESIDUAL NEUTRON-INDUCED RADIOACTIVITIES OF ^{60}Co AND ^{152}Eu IN ROCKS EXPOSED TO NAGASAKI ATOMIC BOMBING.

T. Shimasaki, M. Yoshida, T. Takatsuji, Y. Okumura*

Department of Radiation Biophysics, Atomic Disease Institute, Nagasaki University School of Medicine, 14-2 Sakamoto 1-Chome, Nagasaki, 852
**Present affiliation: Research Center for Isotope Science, Kumamoto University, 2-2 Honjo 2-Chome, Kumamoto, 860*

Summary: In order to confirm whether or not these are a systematic discrepancy in DS86, we have measured the residual radioactivities of ^{60}Co and ^{152}Eu in rocks exposed to Nagasaki atomic bombing. The results indicate that there might exist a systematic discrepancy similar to that Hiroshima.
Key word: ^{60}Co/Co, ^{152}Eu/Eu, Residual neutron-induced radioactivity, Atomic bomb

In the evaluation of low-energy neutrons, as given in the final report, a systematic discrepancy between the ^{60}Co data collected by Hashizume et al. and activation calculation based on DS86 neutrons was found both in Nagasaki and Hiroshima. This problem was not clarified at the time. The ^{152}Eu data were unable to confirm the ^{60}Co discrepancy. Thereafter, additional ^{60}Co, ^{152}Eu and ^{36}Cl data were accumulated, and the discrepancy was confirmed at least in Hiroshima.

We have been measuring the residual ^{60}Co and ^{152}Eu in Nagasaki. Although the half life of ^{60}Co($T_{1/2}$=5.27 y) is much shorter than that of ^{152}Eu($T_{1/2}$=13.5 y), the former radioactivity is still measurable with a low-background γ-ray spectrometer in rocks samples.

Residual radioactivity measurement of ^{152}Eu for mineral samples in Nagasaki were performed by Nakanishi et al.. Large deviation of the data were not enough to ensure the ^{60}Co discrepancy. Recently, Straume et al. have measured ^{36}Cl at three locations up to 1250m slant range in Nagasaki. They concluded that a good agreement was observed between the measurements and calculation based on DS86 neutrons and the large discrepancy observed in Hiroshima appears not to be due to uncertainties in air-transport calculations.

We have obtained 51 rock samples. These samples are measured with a pure germanium semiconductor detector. Specific activities of ^{152}Eu/Eu and ^{60}Co/Co against ground distance is shown in Fig. 1. The calculation/measured ratio both for ^{60}Co and ^{152}Eu are shown in Fig. 2. These results indicate that there might exist a systematic discrepancy similar to that Hiroshima.

Fig.1

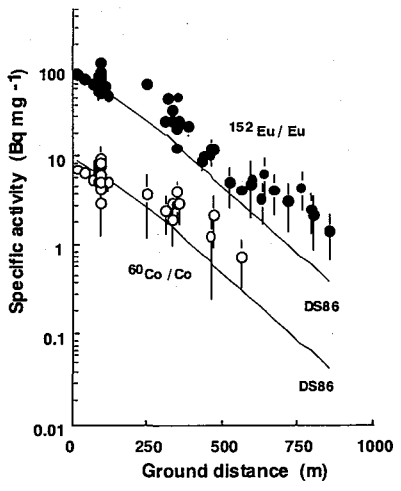

Fig.2

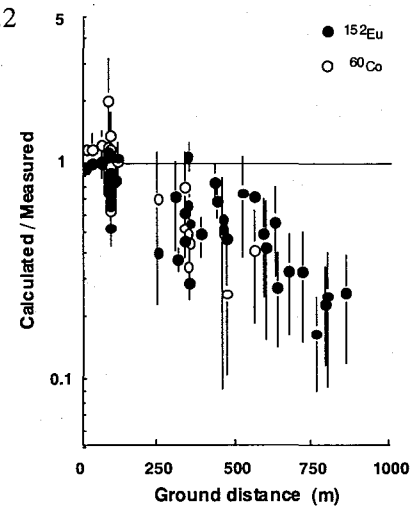

Fax: +81-96-373-5718, E-mail: tshima@kaiju.medic.kumamoto-u.ac.jp

P338 QUALITATIVE MONITORING OF THE QUALITY BY NUCLEAR TECHNIQUES

P. A. de SOUZA Jr.[1], A. D. CHEQUER[2], T. MORIMOTO[3], K. NOMURA[4]

[1] *Departomento de Física, Centro de Ciências Exatas, Universidade Federal do Espírito Santo, 29060-900 Vitória, E. S., Brazil*

[2] *Enfermaria "São Francisco" de Pneumalogia, Escola de Medicina da Santa Case de Misericórdia 29000-000 Vitória, E. S., Brazil*

[3] *IDC, Companhia Siderúrgica de Tubarão, 29164-280 Serra, E. S., Brazil*

[4] *Graduate School of Engineering, The University of Tokyo, Hongo 7-3-1, Bunkyo-ku, Tokyo 113*

Summary:

Key words:

The present investigation consists of the application of several techniques such as Mössbauer spectroscopy, X-ray diffraction, atomic absorption, electron probe micro analysis (EPMA), and thermo-gravimetric analysis, mass spectrometer, to the identification of the particulate matter in atmospheric aerosols monitoring. The main sources of particulate matter and its emission characteristics within the industries have been studied to identify its contribution to air particles. The analysis reveals the total amount of industrial emission of the iron containing components in the atmosphere. The presence of goethite, hematite, magnetic, pyrite, silicates, marine chloride and total absence of heavy metals could be confirmed in the Vitória city, E. S., Brazil.

The methodology of a qualitative monitoring of the air quality by nuclear techniques will be presented.

Fax: +55-27-335-2460, E-mail: souza@cce.ufes.br

P401 s.51 SAMPLE TREATMENT TECHNIQUES FOR THE DETERMINATION OF ENVIRONMENTAL RADIO-CARBON IN THE NUCLEAR POWER STATION AREA

H.J. Woo[1], S.Y. Cho[1], S.K. Chun[1], Y.S. Kim[1], D.W. Kang[2] and K.B. Sung[2]

[1]*Korea Institute of Geology, Mining and Materials, P.O. Box 111, Daedeok Science Town, Taejon, Korea, 305-350*
[2]*Korea Electric Power Research Institute, Munji-dong 103-16, Yusung-gu, Taejon, Korea, 305-380*

Summary: Sample treatment techniques are described for C-14 measurements in environmental samples such as drinking water, air and biota. A differential sampling method of CO_2 and non-CO_2 forms is also presented for stack gases.
Key words: environmental sample treatment, C-14, stack gas

With the growth of nuclear industry the environmental C-14 monitoring especially in CANDU power station area has become an important topic in our country. This report describes the environmental sample treatment techniques for C-14 measurement with liquid scintillation counter. The groundwater sample of maximum 100 liters is collected from well and inorganic carbon is removed by acidification and recirculated gas stripping through an absorber bottle containing 4 M NaOH of 600 ml with an extraction efficiency of more than 96 % within two hours. The biological samples are oven or freeze-dried and combusted to carbon dioxide in a high pressure combustion unit. A sampling system of stack effluents has been developed to determine ^{14}C activities in different chemical forms. The exhaust gas sample is passed through an assembly consisting of a bubbler containing 2 M NaOH of 200 ml for the absorption of $^{14}CO_2$, a tube furnace maintained at 500℃ with Pd/Al and Pt/Al catalysts, and another bubbler containing 2 M NaOH for absorbing the oxidized forms of ^{14}CO and hydrocarbons. The CO_2 collection efficiency is more than 99.5 % for a sampling time of two weeks at a flow rate of 400 ml/min. Passive samplers with 3 M NaOH of 400 ml in plastic trays are successfully used for atmospheric CO_2 sampling. $\Delta^{13}C$ measurements indicate that the measurement error of carbon-14 activity due to the isotopic fractionation is no more than 1.2 %. In most cases the CO_2 trapped in NaOH is precipitated as $BaCO_3$, and subsequently reconverted to CO_2 and transferred to Carbo-Sorb E and Permafluor V mixture for liquid scintillation counting. Considering the limitation of available amount of carbonate samples of non-CO_2 form, stack gas samples are measured by gel suspension counting method. In case higher precision is the deciding factor, benzene synthesis is employed with home-made benzene synthesis system.

Fax: +82-42-861-9727, E-mail: sycho@rock25t.kigam.re.kr

P402
s.51

ANOMALOUS ^{90}Sr DEPOSITION DURING FALL, 1995 AT MRI, TSUKUBA, JAPAN

Y. Igarashi[1] M. Aoyama[1], T. Miyao[1], K. Hirose[1] and M. Tomita[2]

[1] *Geochemical Research Department, Meteorological Research Institute*
1-1 Nagamine, Tsukuba, Ibaraki 305
[2] *Kansai Environmental Engineering Center*
2-3-39 Nakazakinishi, Kita-ku, Osaka 530

Summary: Although the level is fairly small, we observed excess ^{90}Sr deposition during the fall of 1995. The $^{137}Cs/^{90}Sr$ ratio was about 0.25, suggesting an accidental release of ^{90}Sr from nuclear battery used for satellite and remote site, etc.
Key words: excess ^{90}Sr deposition, $^{137}Cs/^{90}Sr$ ratio

Since the early 1990s, mean annual depositions of ^{90}Sr and ^{137}Cs have been ca. 150 and 300 mBq/m^2/y, respectively at MRI, Tsukuba. These levels seem almost the same as those observed in England since the late 1980s. A major source of recent radioactivity deposition has been postulated resuspension. We have proposed a hypothesis that the source of the resuspended radionuclides is not from within Japan but the aeolian dust from the Asian continent through the consideration on activity ratio of $^{137}Cs/^{90}Sr$ found in the deposited material and the surface soil in Japan. Although the level is fairly small, we observed the anomalously high deposition of ^{90}Sr during the fall of 1995; the deposition abruptly increased and reached 40 mBq/m^2/month in September. This corresponds almost a quarter of the so-far averaged annual ^{90}Sr deposition in the 1990s. The activity ratio of $^{137}Cs/^{90}Sr$ for this month was about 0.25, which is the lowest compared with those found during 1990-93; 0.9 to 4.7 which reflect the ratio in the surface soil. One potential source of the excess ^{90}Sr deposition is an accidental release of ^{90}Sr nuclear battery used for satellite and remote site, etc.

Fax: +81-298-53-8728, E-mail: yigarash@mri-jma.go.jp

P403

s.51

ATMOSPHERIC DEPOSITION OF S-35

S. Osaki[1], Y. Tagawa[2], T. Chijiiwa[2], S. Sugihara[1] and Y. Maeda[2]

[1] *Radioisotope Center, Kyushu University 16, Higashi-ku, Fukuoka, 812-81 Japan*

[2] *Faculty of Science, Kyushu University 33, Higashi-ku, Fukuoka, 812-81 Japan*

Summary : ^{35}S in aerosol, atmospheric depositions and rain water were determined about every 10 days for a year with ^{7}Be, ^{32}P, ^{210}Pb and ^{210}Po, and the transfer of ^{35}S existing as aerosol sulfate and gaseous SO_2 was discussed mainly from the ratios of $^{32}P/^{7}Be$, and $^{35}S/^{7}Be$.

Key words: sulfur-35, phosphorus-32, beryllium-7, aerosol, rain, deposition

The radionuclide of ^{35}S is produced in the atmosphere by the spallation reaction of argon atoms with cosmic rays. ^{35}S soon becomes sulfates, sulfur dioxide or organic sulfur compounds. Sulfur dioxide and the organic compounds are gradually oxidized to sulfates. Sulfates are attached to aerosol and deposit directly or with rain water. ^{35}S produced with cosmic rays labels sulfur-bearing compounds and has suitable half life of 87.5 days for studying the cycle of atmospheric species. Acid rain is formed in the atmosphere and strongly affected by sulfur dioxide and sulfates. The mechanisms of the deposition of ^{35}S elucidate the processes of the acid precipitation.

The atmospheric samples were collected on the rooftop(the height is 4m) of a small depository at Fukuoka (33.4°N, 130.2°E) with a high volume air sampler for aerosol, with a flat vessel containing water for atmospheric depositions, and with a flat vessel at rainy time for rain water. Sulfate species in samples were precipitated with barium ions and was purified by distillation with Sn(II)-strong phosphoric acid at 300°C. Dry powder of barium sulfate purified was dispersed with an oil gelling agent in liquid scintillator and measured with a low background liquid scintillation counter.

The average concentrations of ^{35}S were 0.078 $mBqm^{-3}$ for aerosol in surface air and 41 $Bqm^{-2}y^{-1}$ for atmospheric depositions and 0.045 Bql^{-1} for rain water. Assuming that ^{7}Be, ^{32}P and ^{35}S are produced at a same time and transported in same processes, the ratios of $^{32}P/^{7}Be$, and $^{35}S/^{7}Be$ can calculate the mean residence time of their nuclides. The ratios of $^{32}P/^{7}Be$ mostly show the reasonable values correspond to the residence times from 10 to 50 days, but those of $^{35}S/^{7}Be$ mostly show minus residence times (Fig.1). The differences between the cycles of ^{35}S and ^{32}P in the atmosphere are due to the difference of their chemical and physical forms. ^{32}P exists as phosphate species in aerosol, but ^{35}S exists as both sulfates in aerosol and sulfur dioxide of gaseous state. The higher concentration of ^{35}S suggests a large contribution of sulfur dioxide which can be easily transported. The abnormal ratios of $^{35}S/^{7}Be$ from aerosol, depositions and rain water give us some information on the cycle of gaseous sulfur dioxide.

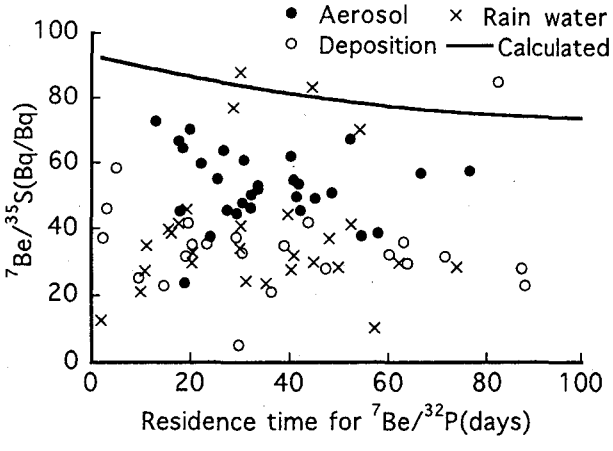

Fig. 1 $^{35}S/^{7}Be$ versus the residence time for $^{32}P/^{7}Be$

P404
s.51

CHARACTERISATION OF LOW LEVEL RADIOACTIVE SOLID WASTE INCINERATION PRODUCTS

V. Subramanian[1], D.S. Surya Narayana[1]*, P.M.Satyasai[2], A.R.Sundararajan[1] and Jaleel Ahmed[2]

[1]*Health and Safety Division, Indira Gandhi Centre for Atomic Research, Kalpakkam - 603102, INDIA*

[2]*Centralised Waste Management Facility, Bhabha Atomic Research Centre, Kalpakkam - 603102, INDIA*

Summary: Size distribution measurements and gamma spectrometry of the incineration products indicate that the particles of lower aerodynamic size should be considered more hazardous while assessing environmental impacts because they contain more quantities of toxic radionuclides.

Key words: Incineration products, Aerodynamic size, Gamma Spectrometry, Hazard Evaluation.

Abstract: Incineration as a method of treating low level radioactive solid wastes is attractive because of large volume reduction and low costs. However, the large volume reduction will result in high concentration of radionuclides in the resultant incineration products which are characterised by unequal distribution of radionuclides among the particles of different sizes. Hence, radioactivity distribution among the aerodynamically size separated incineration products has been determined and the results are reported in this paper. Separate runs have been carried out under identical experimental conditions with radioactive solid wastes of surface dose 20-50 μGy/hr (Type A wastes) and 150-200 μGy/hr (Type B wastes).

The size distribution measurements made on the particles collected before cyclone separator, bag-house and HEPA filters of the incinerator have shown that the maximum percentage of particulate mass lies in 4.7-3.3, 2.1-1.1 and 1.0-0.52 μm size ranges respectively. Gamma spectrometric analysis has shown the presence of Cs-137, Cs-134, Co-60 and Zn-65, during the incineration of Type A wastes in the particles collected by the air cleaning devices. In addition to the above radionuclides, Ru-106, Ag-110m and Sb-125 have been found in the incineration products of Type B wastes. In both cases, it is found that the specific activity of these radionuclides increases with the decrease in the aerodynamic size of the particles (see figure 1).

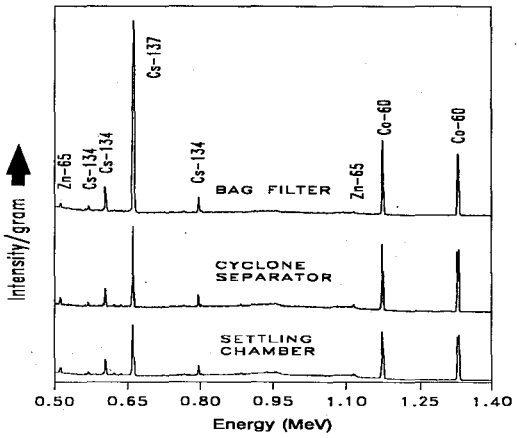

Figure 1: Gamma Spectrum of Incineration products of Type A wastes collected from the air cleaning devices of the incinerator

Present studies have shown that the collection efficiencies of the air cleaning devices are in accordance with the design criteria of the incinerator. The results also indicate that the particles of lower aerodynamic size should be considered more hazardous while assessing the inhalation risks associated with the handling of the incineration products during normal operations as well as during the release of aerosols into the working environment in case of accidental failure of air cleaning devices of the incinerator. The data is also useful as important input parameters for models predicting the radionuclide partition among the incineration products.

**fax: +91 4114 40235; email: dss@igcar.ernet.in*

P405
s.51

MACRO, MICRO NUTRIENTS AND TRACE METAL CONCENTRATIONS IN AYURVEDIC INDIAN MEDICINAL AND VEGETABLE LEAVES

Ramakrishna Naidu[1], Johannes Denschlag[2], Eric Mauerhofer[2], Nathali Porte[2] and Tatineni Balaji[1]

[1]Department of Chemistry, S.V.University, Tirupati - 517 502, India
[2]Institut fur Kernchemie, Johannes Guttenberg Universitat, D-55099, Mainz, Germany

Summary: Leafy samples often used as medicine in the Indian Ayurvedic system were analysed for 27 elements. Most of the leaves in the present study are found to be rich in Ca, Fe and Zn which are most essential for a healthy metabolism. Hence the use of these leaves in Ayurvedic medicinal preparation play an important role.

Keywords: Leafy samples, macro and micro nutrients, trace metals, Ayurvedic system.

Abstract: Leafy samples often used as medicine in the Indian Ayurvedic system were analysed for 27 elements by employing Instrumental Neutron Activation Analysis (INAA). Fresh samples of most herbs were collected from Sri Venkateswara University campus, Tirupati, A.P., India. Some samples were also collected from local market. Surface contaminants of the leaves were removed by washing with deionized water and then by washing with deionized double distilled water. Then the leaves were air dried in a clean drying chamber and then crushed to homogeneous fine powder of uniform particle size (<100 mesh) in an agate mortar. The samples were irradiated with thermal neutrons in a nuclear reactor and the induced activity was counted by gamma ray spectrometer using an efficiency calibrated high resolution High Purity Germanium (HPGe) detector.

The concentrations of macro nutrients viz, Ca, Fe, K etc. are in the range of 0.0309-366 mg/g. Among this, calcium is essential for healthy bones, teeth and blood and acts as a co-enzyme for normal growth and muscle function. The role of iron in the body is clearly associated with haemoglobin and the transfer of oxygen from lungs to the tissue cells and its deficiency results in anaemia.

The concentration of micronutrients viz., Co, Cr, Zn, etc. ranges from 0.0565 to 59.113 μg/g. Among this, the concentration of Zn is higher, whereas the concentration of Co is low. Zn deficiency is characterized by recurrent infections, lack of immunity and poor growth. The role of zinc is spermatogenesis may be correlated with high or low Zn content and its antifertility effect. The other micronutrients are found to be in low concentrations.

The concentrations of trace elements viz., As, Sb, La, Sm, Hg, Lu, Sn, Sc, etc. ranges from 0.0048 to 194.41 μg/g. Among this, the concentration of Lu is low and Sr is high. Neem leaves used for a variety of ailments such as diabetes, ulcers, eczema and lately as a contraceptive are rich in Rb, Sr, As and Sn. Cr is important in the potentiation of insulin as a constituent of glucose tolerance factor and the content of chromium is rich in Tulasi, Mandara, Molagaku, Menthaku and Gongura. Most of the leaves in the present study are found to be rich in Ca, Fe, Zn, which are most essential for a healthy metabolism. Hence the use of these leaves in Ayurvedic medicinal preparations play an important role.

P406
s.51

DISTRIBUTION AND MEAN RESIDENCE TIME OF NATURAL RADIONUCLIDES IN THE FOREST ECOSYSTEM

S. Sugihara, T. Baba[1], S. Osaki, Y. Maeda[1], Y. Inokura[2]

Radioisotope Center, Kyushu University, 6-10-1 Hakozaki, Higashi-ku, Fukuoka 812-81, JAPAN
[1]Department of Chemistry, Faculty of Science, Kyushu University, 6-10-1 Hakozaki, Higashi-ku, Fukuoka 812-81, JAPAN
[2]University Forests, Faculty of Agriculture, Kyushu University, sasaguri 811-24, JAPAN

Summary: Activity concentrations of natural radionuclides, ^{7}Be, ^{210}Pb and ^{210}Po, in precipitations, plant and soil were determined. The distributions and behavior of these radionuclides in the forest ecosystem were clarified.
Key Words: Natural Radionuclide, Forest, Mean Residence Time

Forests are important as a reservoir for radionuclides released to the atmosphere, since they occupy about 70% of land area in Japan. In recent years, the destruction of forests by acid depositions gives to worldwide discussion. So the behavior of environmental pollutants has been investigated in the forest ecosystem which lies between the atmosphere and the ground surface. We focused on natural radionuclides ^{7}Be, ^{210}Pb and ^{210}Po in the forest ecosystem and surveyed the migration behavior of these radionuclides to reach forest floor after they were trapped for forest canopy. This approach is important for the radiation protection because the forests will be the sources of radiation dose to human beings if nuclear power plant accident occurs.

Activity concentrations of these natural radionuclides in precipitations (rain, throughfall and stemflow), plant, and soil were determined by using gamma-ray spectrometry and alpha-ray spectrometry and the distributions of these radionuclides in the forest ecosystem were clarified. As a result, the ratios between output and input precipitations for the forest canopy are about 0.6 of ^{7}Be and ^{210}Pb and about 1.3 of ^{210}Po. We discussed the behavior and the mean residence time of the radionuclides estimated from the distribution. Moreover, we constructed a dynamic model of the transport and fate of radionuclides in the forest ecosystem. The model provides a methods of predicting the early effects from an instantaneous release of radionuclides and follows its cycling through the ecosystem for intermediate and long times. We could understand how pollutants interacted with the ecosystem and environmental contamination occurred by simulating the behavior of the radionuclides. Despite large variation and difficult interpretations, to simulate the behavior of radionuclides seems to have great potential as a tool for the study of both temporal and spatial dimensions of natural radionuclides distribution.

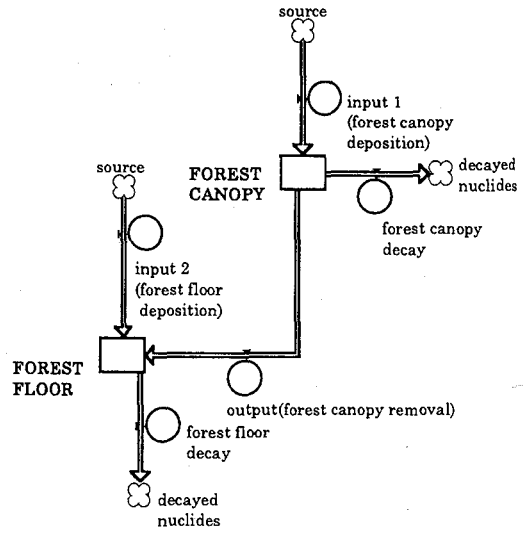

Fig. Conceptual representation of the migration behavior model for ^{7}Be.

Fax: +81-92-642-2706, E-mail: sugirad@mbox.nc.kyushu-u.ac.jp

P407
s.51

SORPTION AND DESORPTION OF RADIOACTIVE Cs, Sr, Zn, Se, AND I ON CALCAREOUS SOIL FROM GANSU PROVINCE

Z. Y. TAO, J. Z. DU, W. M. DONG, X. K. WANG, Z. J. GUO, L. Y. ZHENG

Department of Modern Physics, Lanzhou University, Lanzhou 730000, Gansu Province, P. R. China

Summary :
Key words:

In the recent years, the problems of soil contaminations by the radioactive pollutants has emerged as a crucial one. Although still incomplete, our knowledge of the phenomena governing the rate and transport of pollutants in the soils has improved significantly. One of the most important phenomena is sorption-desorption on soil particles. Because sorption-desorption is very much dependent on the type and the composition of soil, this paper only deals with the sorption and desorption of radioactive ^{134}Cs, $^{85+89}Sr$, ^{65}Zn, ^{79}Se and ^{125}I on the calcareous soils from Gansu province and focuses on the relationship between the sorption features of soils and their compositions. The effect of different solid soil components on the retention has been investigated by a batch technique and selective extraction method. The sorption and desorption isotherms have been determined and the average distribution coefficients (K_d) over the concentration ranges used here were calculated in an attempt to estimate the sorption-desorption hysteresis and the relative contribution of different solid soil components.

An irrigating warped soil sample and sierogem soil sample were respectively derived from the surface horizon (0-20cm) of cultivated lands of Jiuquan County and Yuzhong County. Calcareous soils are common in arid and semi-arid areas. The main conclusions obtained are as following:

The retention ability of Cs by calcareous soil is determined largely by oxides and silicate clays containing kaolinite and aluminium oxide predominately, the rediocesium "fixed" in the calcareous soil is a quite immobile nuclide in comparison with other nuclides because of the large K_d values and the sorption-desorption hyteresis, the clay is the significant trap for radiocesium.

The retention ability of Sr by calcareous soil is determined largely by oxides and silicate clays, the principle mechanism of Sr sorption on calcareous soil is ion exchange, the effect of interaction among soil solid components on the retention of Sr does not play significant role, the sorption-desorption hysteresis is negligible.

The carbonates in calcareous soil are the significant trap for zinc. The relative contribution of carbonates on the sorption of Zn on the whole soil is 70% roughly though the content of carbonates is only 10-12%. The high K_d value and the sorption-desorption hysteresis are the causes for the Zn unavailability in calcareous soil.

The oxides probably are the major trap of SeO_3 in the calcareous soil. The interaction effects among carbonates, organic matter and other solid components play an important role in the sorption of SeO_3 on the calcareous soil. The sorption-desorption hyteresis is attributed to clays and/or oxides.

The iodide has the highest mobility in the calcareous soil. The sorption of I^- on the inorganic components of this soil is rather low, and the organic matter acts as iodide trap. The sorption-desorption hysteresis can be attributed to organic matter and the carbonates are responsible for this hysteresis.

Fax: +81-931-888-1996

P408 s.51 GEOCHEMICAL ASSOCIATION OF CS-137 AND PU-239,240 IN THE OLIGO- AND MESOTROPHIC LAKE SEDIMENTS

S. Nagao, T. Matsunaga and S. Muraoka
Department of Environmental Safety Research, Japan Atomic Energy Research Institute,
2-4 Shirakata-Shirane, Tokai, Ibaraki 319-11, Japan.

Summary: Cs-137 and Pu-239,240 were mainly bound to organic matter-sulfides and aluminosilicate fractions in the oligo- and mesotrophic lake sediments from Japan.

Key words: Cs-137, Pu-239+240, lake sediments, geochemical association

Geochemical association of Cs-137 and Pu-239,240 in the oligo- and mesotrophic lake sediments were studied by sequential chemical extractions to understand the deposition processes of artificial radionuclides in lake. The lake sediments were collected by a gravity corer from Lake Towada (oligotrophic lake, silty clay sediment) in Aomori prefecture and from Lake Kizaki (mesotrophic lake, siliceous sediment composed mainly of shell of bacillariophyceae) in Nagano prefecture in Japan. The fractions separated and determined were exchangeable and bound to carbonate (leachable with 1M CH_3COOH), bound to oxides (leachable with 0.1M NH_2OH-HCl in 25% CH_3COOH), bound to organic matter-sulfides (leachable with 30% H_2O_2) and residual (digestion with HNO_3, HF and $HClO_4$). The radioactivities of Cs-137 and Pu-239,240 were determined by beta-spectrometry and alpha-spectrometry, respectively after the purification by ion exchange method. The Cs-137 and Pu-239,240 of the both sediments were mainly associated with the organic matter-sulfides and residual fractions but exhibited the different vertical profiles. In the Lake Towada sediments, the percentages of these radionuclides in the organic-sulfide fraction decreased with increasing depth in core from 38% to 18% (Cs-137) and from 54% to 5% (Pu-239,240) at the depth interval of 0-6 cm. On the other hand, about 30% of Cs-137 and 40-60% of Pu-239,240 in the Lake Kizaki sediments were associated with the organic matter-sulfide fraction and constant at 2-14 cm depth in core. The Pu/Cs-137 activity ratio of the organic matter-sulfide fraction was 0.007-0.023 for the Lake Towada sediments and 0.045-0.088 for the Lake Kizaki sediments, but of the residual fraction was 0.013-0.028 for the Lake Towada and 0.021-0.037 for the Lake Kizaki sediments. The differences in association patterns between Cs-137 and Pu at the both lakes may be controlled by the biological activity of surface water.

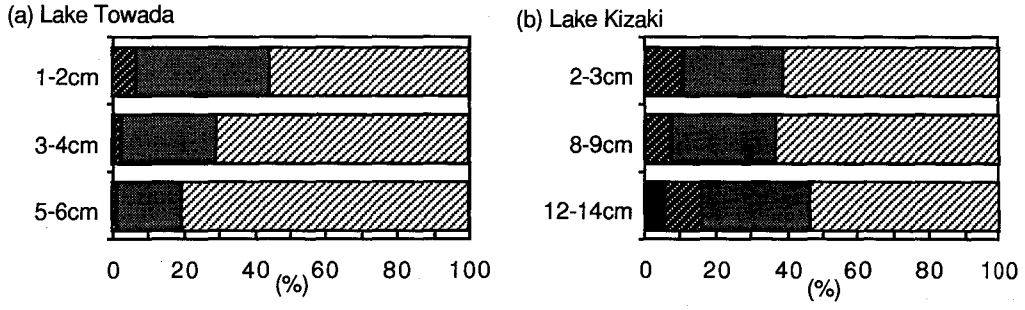

Fig.1 Percentages of Cs-137 in carbonate (■), oxides (▨), organic-sulfides (■) and aluminosilicate fractions (▨) in the oligotrophic lake sediments from Lake Towada and mesotrophic lake sediments from Lake Kizaki.

Fax and e-mail address: Fax. 81-29-282-5934, e-mail. nagao@sparclt.tokai.jaeri.go.jp

P409
s.51

A WET METHOD OF CARBON EXTRACTION FROM IRON ARTIFACTS FOR ^{14}C AGE MEASUREMENT WITH AMS

H. Oda, T.Nakamura and M.Furukawa[1]

Dating and Materials Research Center, Nagoya University, Furo-cho Chikusa Nagoya Aichi 464-01 Japan
[1]Faculty of Environmental and Information Sciences, Yokkaichi University, Yokkaichi Mie 512 Japan

Summary: We developed a wet method of carbon extraction from iron artifacts for AMS measurement. The method consists of dissolution of iron with Cu^{2+} solution and offers high extraction yield and low contamination by modern carbon.
Key words : iron artifact, radiocarbon dating, AMS, wet method

Japanese iron artifacts had been produced from iron-sand by reduction with charcoal and include a small amount of carbon. By means of AMS which requires about 1-mg carbon sample for ^{14}C dating, it is possible to measure ^{14}C age of the iron artifact. A dry method is commonly performed for carbon extraction from iron. The method consists of combustion of iron with O_2 and separation of CO_2 from O_2 in a vacuum line. The method, however, includes some problems. A sufficient carbon amount cannot be obtained by a single combustion procedure. A sequence of extraction requires a whole working day and a skillful preparation technique is needed to avoid contamination of modern carbon. For these problems, we have developed a wet method. An iron sample with a known carbon content was dissolved in 2M $CuCl_2$ solution and carbon was precipitated as aggregated colloid. Then, deposited metallic Cu was dissolved in 4M HCl. By filtration, carbon particles were collected on the quartz wool in a 6-mm ϕ glass tube. Collected carbon was converted to CO_2 with CuO at 850℃. The CO_2 was purified by vacuum distillation. The graphite target for AMS was prepared by reduction of CO_2 with H_2 and cat-Fe at 650℃. ^{14}C ages were measured with AMS at Nagoya University. The carbon content and the initial weight of treated iron sample are summarized in Table 1 and high extraction yield of carbon was indicated (80-90%). ^{14}C ages shown in Table 1 agree with known ages of corresponding samples treated by the dry method. It follows from this agreement that the wet method has negligible contamination by modern carbon. It should be noted that we can prepare a sufficient amount of CO_2 with the wet method from a low carbon content sample by treating it in a larger reactor.

Table 1. ^{14}C ages of iron standard samples prepared by the wet extraction method

No.	C-content [%]	weight of Fe [g]	yield [mgC]	([%])	^{14}C age [BP]	$\delta^{13}C$ [‰]
1	4.67	0.159	6.15	(83.0)	37150±330	-25.2±0.1
2	4.67	0.067	2.66	(84.8)	36290±330	-25.1±0.1
3	0.196	1.53	2.65	(88.4)	25980±270	-23.0±0.1
4	0.050	6.04	2.61	(86.4)	19330±140	-24.2±0.1

Fax: +81-52-789-3095, E-mail: oda@dmrc.eps.nagoya-u.ac.jp

P410
s.51

HOST PHASE OF PLUTONIUM-239,240 AND AMERICIUM-241 IN DEEP-SEA SEDIMENT

M.A. Haque[1] and T. Nakanishi[2]*
[1]*Graduate School of Natural Science and Technology*
[2]*Department of Chemistry, Faculty of Science*
Kanazawa University, Kakuma-machi, Kanazawa, Ishikawa 920-11, Japan

Summary : Fallout ^{239,240}Pu and ^{241}Am were determined in the sequentially extracted five phases of deep-sea sediment. Phase associations of these nuclides varied from sediment to sediment. These nuclides differ significantly in their associations with carbonate and residual phases of the sediments.
Key words: ^{239,240}Pu, ^{241}Am, deep-sea sediment, host phase

Host phase of fallout ^{239,240}Pu and ^{241}Am was studied in surface layers of deep-sea sediments from the Japan Trench and the Nankai Trough (Fig. 1). An analytical procedure involving sequential chemical extractions was employed for partitioning the host phases of ^{239,240}Pu and ^{241}Am in the sediment into five fractions: (1) exchangeable, (2) bound to carbonate, (3) bound to hydrous Fe-Mn oxides, (4) bound to organic matter and (5) bound to insoluble residue. Indicator elements (Ca, Fe, Mn and Si) were also analyzed in the individual extracted phases to check the efficiency of the phase separation.

From the analytical results of the indicator elements, the phase separation efficiency proved to be as satisfactory as intended.

Results of the host phase study are shown in Fig. 1. Both ^{239,240}Pu and ^{241}Am were not present in any particular phase in the studied sediments. From 15 to 56 % of total content of ^{239,240}Pu was found in hydrous Fe-Mn oxides phase, 19 to 49 % in organic matter and 14 to 49 % in residual phase. The proportion of plutonium in exchangeable and carbonate phases was less than 14 %. From 35 to 84 % of total content of ^{241}Am was found in hydrous Fe-Mn oxides phase, 8 to 43 % in organic phase and 7 to 38 % in carbonate phase. A few percent of total content of ^{241}Am was found in residual fraction, and ^{241}Am in exchangeable fraction was not detectable.

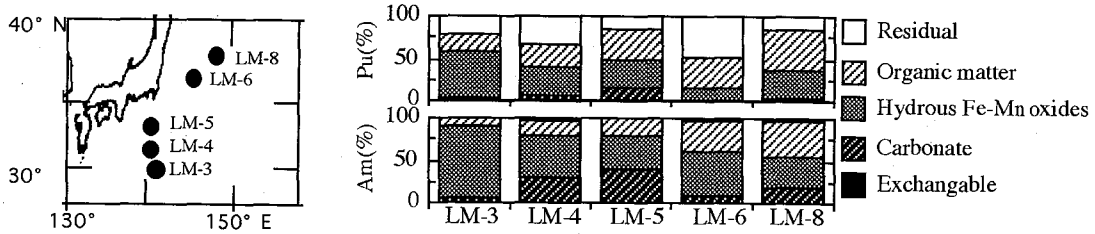

Fig.1 Distribution of ^{239,240}Pu and ^{241}Am among the phases in the deep-sea sediments.

^{241}Am/^{239,240}Pu activity ratios for the total content of ^{239,240}Pu and ^{241}Am in the surface layers of the sediments were in a range from 1.22 to 3.78, and these ratios are 4–12 times higher than that for integrated global fallout (*i.e.* about 0.3). This indicates that the removal of americium from the water column to sediment, largely by settling particles rich in hydrous Fe-Mn oxides, is rapid compared with that of plutonium. The wide range of the observed ^{241}Am/^{239,240}Pu activity ratios in the deep-sea sediments suggests that the distribution ratios of plutonium and americium between seawater and settling particles differ from sea area to sea area probably due to the difference in composition of settling particles, the difference being confirmed by the analytical results of indicator elements in the sediments. Much higher ^{241}Am/^{239,240}Pu ratios (*i.e.* from 2.67 to 11.6) were found in carbonate fraction. This may be resulted from preferential scavenging of ^{241}Am over ^{239,240}Pu by sinking carbonates and/or from preferential post-depositional (and/or upon sinking) dissolution of ^{239,240}Pu over ^{241}Am with the dissolution of carbonates in deep water. The dissolution of carbonates in deep seabed seems an important process of post-depositional diagenetic chemistry which leads to remobilization of plutonium from the solid to the aqueous phase.

Fax: +81-76-264-5742, E-mail: nakanisi@cacheibm.s.kanazawa-u.ac.jp

P411
s.51

REE GEOCHEMISTRY ON SEDIMENTARY ROCKS AND BASEMENT WEATHERED GRANITE AT TONO URANIUM DEPOSIT, CENTRAL JAPAN

H. SHIMIZU[1,2], N. SATO[1], T. KUNIMARU[2] and H. YOSHIDA[3]
1. Department of Environmental Science, Faculty of Science, Kumamoto University, Kumamoto 860, Japan; 2. Department of Environmental Science, Graduate School of Science and Technology, Kumamoto University, Kumamoto 860, Japan; 3. Tono Geoscience Center, Power Reactor and Nuclear Fuel Development Corporation, Toki 509-51, Japan.

Summary: REE patterns are reported for basement granitic rock and overlying sedimentary rocks from the Tono uranium deposit and REE migration processes during weathering and diagenesis are discussed.
Key words: REE, tetrad effect, uranium deposit, migration

Rare earth element (REE) abundances were determined on sedimentary rocks and weathered granitic rocks from the Tono uranium deposit, central Japan, in order to clarify migration process of these elements during weathering and diagenesis. At the Tono deposit, uranium ore-bodies are hosted in coarse- to medium grained sandstone and lignite-bearing tuffaceous sandstone of Miocene Mizunami Group which overlies the Cretaceous granitic rocks. The basement granitic rock at the deposit generally suffers from physical weathering and/or alteration, but from little chemical weathering. REE abundances in these sedimentary rocks hosting uranium deposit and basement weathered granitic rock were determined with ICP-MS.

Conjugate M- and W-type REE tetrad patterns are clearly observed for the natural pair of basement granitic rock and overlying sedimentary rocks. REE tetrad pattern ideally consists of four separate curves, La-Ce-Pr-Nd, Pm-Sm-Eu-Gd, Gd-Tb-Dy-Ho and Er-Tm-Yb-Lu; patterns consisting of upward convex and concave curves are called M- and W-type, respectively. REE tetrad patterns are considered to be associated with 4f electron filling. It has been reported that M-type tetrad pattern is observed for leucogranites and W-type tetrad pattern is observed for natural waters (Masuda et al., 1987), but conjugate M- and W-type tetrad patterns have not been reported for the natural pair.

Weathered granitic rock at the Tono site shows V-shaped REE pattern with steep inclination at light REE and gentle slope at heavy REE. Large negative Eu anomalies are observed for all REE patterns of the Tono weathered granitic rock. It should be noted that the REE patterns of the basement weathered granitic rock show M-type tetrad at heavy REE, *i.e.*, two upward convex curves, Gd-Tb-Dy-Ho and Er-Tm-Yb-Lu. The sedimentary rocks at the site show light REE enriched pattern with or without flat heavy REE span. Some sedimentary rock samples show W-type REE tetrad patterns at heavy REE, *i.e.*, two concave curves, Gd-Tb-Dy-Ho and Er-Tm-Yb-Lu.

These REE data might suggest that basement granitic rock at the Tono site suffered from weathering after deposition of overlying sedimentary rocks and that REE leached out from the basement granitic rock during the weathering were precipitated in or adsorbed on the overlying sedimentary rocks.

FAX:+81-96-342-3419
E-MAIL:hshimizu@sci.kumamoto-u.ac.jp

P412 s.51 MEASUREMENTS OF Ra-226 IN SCALE SAMPLES USING GAMMA-RAY SPECTROSCOPY

A. Aksoy, M. N. Al-Haddad and F. Z. Khiari

Energy Research Laboratory, King Fahd University of Petroleum and Minerals, Dhahran, 31261, Saudi Arabia

Summary: Natural radioactivity of scale samples from Ra-226 was measured. The setup was calibrated using three Ra-226 standards from IAEA. The concentrations of Ra-226 in seven scale samples from water wells were measured. Six samples had Ra-226 levels above the limit.

Key words: Natural radioactivity, scale samples, Ra-226, calibration, maximum permissible level.

Naturally occurring radioactive elements are present throughout the earth crust in trace concentrations. Due to the physical and chemical changes that happen in the formation water, oil, and gas processing, these trace elements tend to accumulate in the form of scale and sludge in the equipment where these changes take place. For instance, scale in the production pipes can be radioactive. This radioactivity is due to radium co-precipitating with barium and strontium sulfates in the scale formation. Scales may sometimes contain several thousand picocuries of radium per gram of scale. Radium is the second most toxic substance on earth next to plutonium, and is one of the long-lived (half-life of 1620 years) daughter isotopes of the natural uranium-238 series. When digested, radium concentrates in the bones. Radium-226 decays by alpha emission into a a radon nuclide, a noble gas. This radioactive gas can then escape from the parent mineral and migrate through the surrounding environment. The present study was undertaken to calibrate the high efficiency gamma-ray spectrometer to measure Ra-226 concentration levels in scale samples from local water in order to assess the magnitude of the low specific activity of scale waist. The study was carried out using a 5" x 5" NaI(Tl) detector with a PC-based data acquisition and analysis system to measure the activity of the 186 keV gamma-ray line from Ra-226. The setup was calibrated using three Ra-226 certified standards (IAEA-312, 313, and 314 with Ra-226 activities of 269, 343, and 732 Bq/kg, respectively) from IAEA, Vienna. The calibration curve is shown in the figure. Samples with masses between 90 - 200 g were crushed and placed in plastic containers of 3.5" diameter and 0.5" thickness and were measured for natural radioactivity for 24 h each. The MCA was calibrated in the 40 - 900 keV energy range using standard Na-22 and Cs-137 gamma-ray sources. The dead time of the electronics was less than 1%. The data was also corrected for room background which was also measured for 24 h using a pure sand sample (SiO_2) free from radioactivity. The lower limit of detection (LLD) for Ra-226 was 0.7 Bq/kg. As an application of the calibration, seven scale samples from various local water wells were studied for Ra-226 content.The results show that the radium content in the scale samples range from 369 - 1166 Bq/kg, corresponding to a range of 10 - 32 pCi/g. More results and details of the experiment with supporting drawings, figures and tables will be presented.

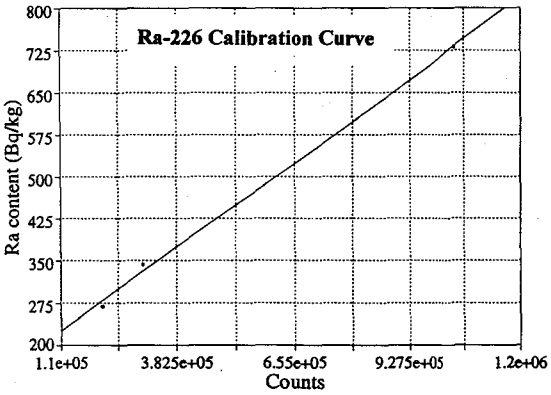

Fax: +00 966 3 860 42 81, E-mail: aksoy@dpc.kfupm.edu.sa

P413
s.52

A COMPARISON OF NAA ICP-MS FOR THE DETERMINATION OF TRACE ELEMENTS IN OMBROTROPHIC PEAT BOG

M. V. FRONTASYEVA[1] AND E. STEINNES[2]

[1] *Joint Institute for Nuclear Research, Frank Laboratory of Nuclear Physics, 141980 Dubna, Moscow Region, Russia*

[2] *Department of Chemistry, Norwegian University of Science and Technology, 7055 Trondheim, Norway*

Summary :

Key words:

Due to an increasing interest to retrospective studies on atmospheric deposition of chemical constituents from ancient times up to the present industrial era, peat bogs have been recognized as valuable environmental archives for this purpose. In particular ombrotrophic bogs are useful in this respect, because they receive all their supply of chemical substances from the air and the vertical migration of most elements is very slow. In the present work peat cores taken from two ombrotrophic bogs in Finnmark (Northern Norway) with strongly different pollution exposure were studied using epithermal NAA (IBR-2 pulsed fast reactor, Dubna), and the results were compared with data obtained by ICP-MS and ICP-ES (a few samples only). One core (Porsanger) was taken 80 km south of North Cape in a typical background area, the other one (Svanvik) close to the Russian border only 8 km west of the Nikel copper-nickel smelter. In total 42 elements (Na, Mg, Al, Cl, K, Ca, Sc, V, Cr, Mn, Fe, Co, Ni, Cu, Zn, As, Se, Br, Rb, Sr, Zr, Mo, Ag, Cd, Sb, I, Cs, Ba, La, Ce, Sm, Eu, Tb, Yb, Hf, Ta, W, Au, Hg, Pb, Th, U) were determined. Good agreement was observed for most elements determined by more than one analytical technique. Advantages and drawbacks of each technique for peat analysis are discussed, and recommendations on the method of choice for the various elements are given. (I am not sure if I understand your last sentence, but I suggest the following:) Most element show regular distributions along the peat profiles, and comparison of the two peat cores makes it possible to distinguish temporal trends associated with pollution from industries on the Kola peninsula.

Fax: 7(09612)65085, E-mail: marina@nf.jinr.ru

P414
s.52

ELEMENTAL CHARACTERIZATION OF INDUSTRIAL SLUDGES AND DOMESTIC WASTES FOR HEAVY METAL POLLUTANTS BY INAA

A.N. Garg * and V.V.S. Ramakrishna

Department of Chemistry, Nagpur University, Nagpur - 440 010, India
** Department of Chemistry, University of Roorkee, Roorkee - 247 667, (U.P.) India*

Summary : Industrial sludges from several industries and domestic waste from Bombay city have been analysed for 25 elements by INAA. Cr content was found higher in tannery, steel polishing and zinc plating industries. Ba, Cu, Cr, Sb and Mn were found higher in domestic waste.
Keywords : Industrial sludges, Heavy metal pollutants, Domestic waste, INAA

Industrial sludges are often used for the recovery of precious metals before dumping into low lying areas and agricultural fields. Also domestic waste from metropolitan cities is likely to contain many heavy metal pollutants in significant amounts. Industrial waste/sludge samples from chlor-alkali, tannery, zinc plating and steel polishing industries from different parts of India have been analyzed for upto 25 elements (As, Ba, Br, Co, Cr, Cu, Eu, Cs, Eu, Fe, Hg, Hf, K, La, Mg, Mn, Na, P, Rb, Sb, Se, Sr, Th, Zn and Zr) by employing thermal neutron irradiation followed by high resolution gamma ray spectrometry at different intervals. Three samples of domestic waste and a kitchen waste sample from Bombay city were also analyzed. Samples in dry powder form were procured from Solid Waste Division of the National Environmental Engineering Research Institute (NEERI), Nagpur. Several SRMs of environmental importance from NIST (USA), IAEA (Vienna) and NIES (Japan) were analyzed for quality assurance. Typical elemental contents in some samples are given in Table. It is observed that Cr content in sludges from tannery, steel polishing and zinc plating industries was higher. Similarly toxic pollutant Hg content in chlor-alkali waste was upto 2.18 $\mu g / g$ and Zn content in zinc plating sludge is also very high. Fe and Mn contents in all industrial sludges were high presumably due to intermixing with local soil. Several heavy metal pollutants such as Ba, Cu, Cr, Sb, Mn have been observed in significant amounts in domestic waste. Interestingly kitchen waste showed elevated levels of Ba and Zn. These elemental contents may be attributed to the use of coloured plastic products and other technological advancement thus causing addition of toxic heavy metals to the environment. It has been proposed that some toxic elements may be leached out from waste material and enter into our ecosystem causing serious health hazards.

Sludge/Waste Type, Place	Ba ($\mu g / g$)	Br ($\mu g / g$)	Cr ($\mu g / g$)	Cu ($\mu g / g$)	Hg ($\mu g / g$)	Sb ($\mu g / g$)	Zn ($\mu g / g$)
Chlor-Alkali, Alwar (n=3)	3540	39.8	18.8	209	0.95	0.61	21.9
Zn-Plating, Delhi	420	13.5	0.44%	0.24%	0.31	0.13	5.13%
Steel Polishing, Bombay	1520	10.7	1.05%	69.8	0.01	2.35	214
Domestic Waste, Bombay (n=3)	562	19.2	288	313	0.14	88.0	420
Kitchen Waste, Bombay	1080	14.6	341	159	0.12	55.8	786

Fax : +91-1332-73560, E-Mail : chemt@rurkiu.erent.in

P416
s.31

SOLVENT EXTRACTION BEHAVIOR OF HEXACHLOROTECHNETATE(IV) ION IN THE HCl-TBP SYSTEM

S. WATANABE*[1] and K. HASHIMOTO[2]

Department of Radioisotopes, Japan Atomic Energy Research Institute
[1]Takasaki-shi, Gunma-ken 370-12 , Japan
[2]Tokai-mura, Ibaraki-ken 319-11 , Japan

Summary : The solvent extraction behavior of $[TcCl_6]^{2-}$ has been studied in the HCl-TBP system. The chemical form extracted into TBP was assigned to $H_2[TcCl_6](TBP)_4$. The distribution coefficients of aqua complexes of $[TcCl_6]^{2-}$ were found to be in the order $[TcCl_4(H_2O)_2] < [TcCl_6]^{2-} < [TcCl_5(H_2O)]^-$.
Key words : hexachlorotechnetate(IV) ion, aqua complexes, solvent extraction, HCl, TBP

Hexachlorotechnetate(IV) ion, $[TcCl_6]^{2-}$, has been widely used as a starting material to synthesize technetium(IV) complexes. Only a limited number of studies, however, have been carried out on its chemical properties in contrast with TcO_4^-. The present paper describes experimental results on the solvent extraction behavior of $[^{99}TcCl_6]^{2-}$ in the HCl - TBP system together with that of its aqua complexes. The chemical form of the technetium extracted into TBP is also deduced.

Ammonium hexachlorotechnetate(IV) was prepared with a standard method of reducing TcO_4^- by conc. HCl. The distribution coefficient ($D_{Tc} = [Tc]_{organic} / [Tc]_{aqueous}$) of $[TcCl_6]^{2-}$ was determined as functions of HCl and TBP concentration under the conditions of a constant ionic strength. From the plots of D_{Tc} vs. HCl and TBP concentration on logarithmic scales, it was found that the chemical form extracted into TBP was $H_2[TcCl_6](TBP)_4$.

To investigate the solvent extraction behavior of aqua complexes of $[TcCl_6]^{2-}$, a $(NH_4)_2[TcCl_6]$ solution was irradiated by visible-light for a certain period of time. For the solution, the distribution ratio of technetium in the HCl-TBP system was measured and the species of aqua complexes were analyzed by paper chromatography; the contents of pentachloromonoaquatechnetate(IV) ion, $[TcCl_5(H_2O)]^-$, tetrachlorodiaquatechnetium(IV), $[TcCl_4(H_2O)_2]$ and the remaining $[TcCl_6]^{2-}$ were determined. The distribution ratio obtained was analyzed with the method of least-squares (Fig. 1), considering the reaction kinetics of each of the three components. The distribution coefficients of the three components were found to be in the order $[TcCl_4(H_2O)_2] < [TcCl_6]^{2-} < [TcCl_5(H_2O)]^-$.

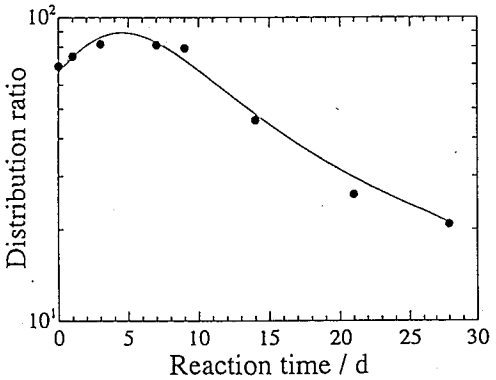

Fig. 1 Distribution ratio of technetium as a function of reaction time in the 2M HCl-TBP system.

FAX: +81-273-46-9690, E-mail: wata@popsvr.tokai.jaeri.go.jp

P417
s.31

STRUCTURES OF NITRIDOTECHNETIUM(V) AMINE OXIME COMPLEXES WITH DIFFERENT LENGTH OF CARBON CHAINS

Y. Kani, T. Takayama, T. Sekine, and H. Kudo

Department of Chemistry, Graduate School of Science, Tohoku University, Sendai 980-77, Japan

Summary: The intramolecular hydrogen bond distance in nitridotechnetium(V) amine oxime complexes was investigated by structural analysis. The O···O distance is in the order of PnAO > BnAO > PentAO, i.e. the shorter the carbon chains, the longer the O···O distance.

Key words: Nitridotechnetium complex, Amine oxime ligand, Intramolecular hydrogen bond

Nitridotechnetium complexes have attracted increasing interest in coordination chemistry. The powerful π electron donation of the nitrido ligand influence on the structural configuration of nitridotechnetium complexes. We have synthesized nitridotechnetium(V) complexes of amine oximes with various carbon chains such as ethylene amine oxime (EnAO), propylene amine oxime (PnAO), butylene amine oxime (BnAO), and pentylene amine oxime (PentAO). Structures of the TcN-PnAO and TcN-BnAO complexes were determined by X-ray crystallography. The structures of both the complexes are distorted octahedral. The Tc atom shifts outward from a basal plane defined by the four nitrogen atoms of amine oxime ligand. This distortion should be caused by the π donation of the nitrido ligand. The amine oxime ligand is coordinated in the equatorial plane. The nitrido and H_2O ligands are at apical positions of the complexes.

The TcN-PnAO, TcN-BnAO, and TcN-PentAO complexes have an intramolecular hydrogen bond between two oxime groups. The distance between oxime oxygens (O···O) in the TcN-PnAO and TcN-BnAO complexes is 2.720 and 2.512 Å, respectively. The O···O distance is in the order of PnAO > BnAO > PentAO, depending on the length of carbon chains in the amine oxime ligands. The shorter the carbon chains, the longer the O···O distance. The TcN-EnAO complex with the shortest carbon chains has no intramolecular hydrogen bond.

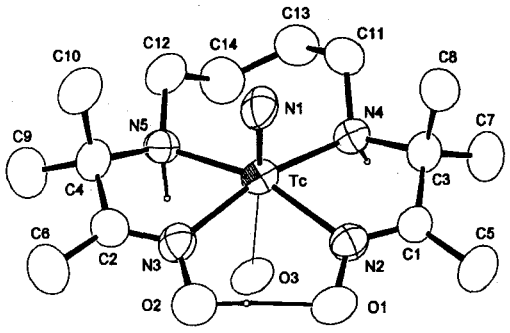

Figure 1. ORTEP drawing of the complex cation $[TcN(bnao)(H_2O)]^+$

Fax: 81-22-217-6597, e-mail: kani@mail.cc.tohoku.ac.jp

P418
s31

SELECTIVE FORMATION OF *CIS* ISOMER OF NITRIDOTECHNETIUM(V) COMPLEX WITH 2,2′:6′,2″-TERPYRIDINE

T. Takayama, S. Oshikiri, T. Sekine, and H. Kudo
Department of Chemistry, Graduate School of Science, Tohoku University, Sendai, 980-77, Japan

Summary: In the reaction of *trans*-[$TcNCl_2(PPh_3)_2$] with terpy, *cis*-[$TcNCl_2$(terpy)] was selectively formed. The formation process as well as the reactivity of this complex is discussed with the aid of theoretical calculation.
Key words: Nitridotechnetium complex, Terpyridine ligand, *Cis* isomer

Technetium complexes with a metal-nitrido triple bond (Tc≡N) has attracted current interest in coordination chemistry as well as in nuclear medicine. A strong *trans* influence of the nitrido ligand would play important roles in determining chemical and structural properties of these complexes.

We have studied the formation of the nitridotechnetium complex with a tridentate ligand, 2,2′:6′,2″-terpyridine (terpy). The reaction of *trans*-[$TcNCl_2(PPh_3)_2$] with the terpy in benzene solution gave only *cis*-[$TcNCl_2$(terpy)]. The ^1H NMR spectrum of the magnetically equivalent ortho protons (6,6″) of the terpy ligand of this complex appeared at 9.3 ppm in CD_3OD solution, shifting largely downfield compared with the free terpy. This is ascribed to the deshielding against ortho protons in the terpy ligand coordinated to the equatorial position by the π bond between technetium and nitrogen. The *cis* isomer is likely more stable than the *trans* isomer toward the *trans* influence of the nitrido ligand.

Addition of excess LiCl to the methanol solution of *cis*-[$TcNCl_2$(terpy)] gave no changes in UV-vis and ^1H NMR spectra. The fact reveals that the *cis-trans* isomerization does not occur in polar solvents like water, methanol, and acetonitrile. When NH_4PF_6 was added to acetonitrile solution of *cis*-[$TcNCl_2$(terpy)], [TcNCl(MeCN)(terpy)][PF_6] was obtained as a purple precipitate. Cationic solvates might be formed in polar solvents, the chloro ligand at *trans* position of the nitrido ligand was replaced for a solvent molecule.

The geometry of *cis*-[$TcNCl_2$(terpy)] was optimized using a density functional method. The technetium-chlorine bond length (2.76Å) at the *trans* position (Tc-Cl_{trans}) of the nitrido ligand is longer than that at the *cis* position (2.44 Å). The longer Tc-Cl_{trans} bond length reflects a significant *trans* influence of the nitrido ligand and lead to experimental evidence that the Cl_{trans} ligand was labile in the substitution reaction.

Fax: 81-22-217-6597, e-mail: takayama@mail.cc.tohoku.ac.jp

P419
s32

ANIMAL EXPERIMENTS ON ^{111}In-DTPA-D-Phe^{1}-Octreotide

F. Chen[1], F. Wang[2], F. Li[1], L. Xiao[2], C. Chou[1] and S.C. Wang[1]
1. Dept. of Nuclear Medicine, PUMC and CAMS, Beijing 100730, P. R. China
2. China Institute of Atomic Energy, P. O. Box 275(58), Beijing 102413, P. R. China

Summary: The ligand DTPA-D-Phe^{1}-octreotide was labelled with ^{111}In via a single-step procedure. The stability in blood and in urine was investigated. The imaging of nude mice bearing pancreatic tumor demonstrated that best localization appeared at 8hr postinjection.
Keywords: ^{111}In-DTPA-D-Phe^{1}-octreotide, receptor imaging, animal experiment

For the investigation of the biological properties of ^{111}In-DTPA-D-Phe^{1}-octreotide, this somatostatin receptor-positive tumor imaging agent was prepared by ourselves. The ligand DTPA-D-Phe^{1}-octreotide was labelled with ^{111}In via a single-step procedure to obtain ^{111}In-DTPA-D-Phe^{1}-octreotide with a labelling yield of >99%. HPLC was used to determine the labelling yield, as well as the percentage of decomposed components from ^{111}In-DTPA-D-Phe^{1}-octreotide in blood and urine (in vivo). The radiocomponent of ^{111}In-DTPA, derived from ^{111}In-DTPA-D-Phe^{1}-octreotide decomposition, showed 50% of radioactivity in blood and 40% in urine at 3hr postinjection, see table 1. Biological properties were evaluated by biodistribution in normal mice, as well as dynamic and static images of nude mice bearing pancreatic carcinomas. Rapid blood and urine clearance, high adrenal uptake and good T/B ratio (7.29, 24hr postinjection) were observed. Images of tumors could be obtained from 0.5 up to 48hr after administration of this agent but the best localization appeared at 8hr when 20μg of DTPA-D-Phe^{1}-octreotide labelled with 37MBq of ^{111}In were used. Our results show that ^{111}In-DTPA-D-Phe^{1}-octreotide is suitable for clinical trials.

Table 1 Percent Radioactive Content of ^{111}In-DTPA Decomposed in Blood and Urine

	30 min	*3 hr*	*24 hr*
Blood (in vitro)	< 1 %	< 1 %	< 5 %
Blood (in vivo)	< 5 %	50 %	> 50 %
Urine	5 %	40 %	> 95 %

Fax: +86-10-65124875, E-mail: chenfang@cdm.imicams.ac.cn

P421 s.33/14 Simultaneous biobehavior of Sc, Mn, Fe, Co, Zn, Se, Rb and Zr trace elements in C57BL/6N mice.

Shigeo Oishi [1], Ryohei Amano [1], Atsushi Ando [1], Shuichi Enomoto [2] and Fumitoshi Ambe [2]

1). School of Health Sciences, Faculty of Medicine, Kanazawa University
2). The Institute of Physical and Chemical Research (RIKEN)

Summary: The radioactive multitracer technique was applied to the study of biobehavior of trace elements in normal C57BL/6N mice. Comparative biobehavior of Mn, Co, Zn, Se, Rb and Zr tracers in brain was discussed at 6, 12, 24 and 48 h after intraperitoneal injection.
Key words: multitracer, C57BL/6N mice, bio-trace elements, metal homeostasis

Multitracer is found a toxicologically and pharmacologically useful radioactive tracer in assessing biological systems for maintenance of homeostasis of bio-trace elements. It enables simultaneous tracing of various elements in the identical system and a strict and accurate comparison of their behavior, to minimize the undesirable effects of both peculiarities of samples and variation in experimental conditions. In this work, we applied it to the study of biobehavior of Sc, Mn, Fe, Co, Zn, Se, Rb and Zr trace elements in normal C57BL/6N mice. The tissue distribution of the 8 elements was examined among 11 organs (brain, cardiac muscle, lung, liver, spleen, pancreas, kidney, bone, thighbone muscle, eyeballs and testes) and blood, and evaluated in terms of "tissue uptake rate (the percentage of injected dose per gram of tissue, %dose/g)".

Male C57BL/6N mice were purchased from Charles River Japan Inc., and fed a standard laboratory diet and had free access to drinking water in plastic and steel cages during 1 week prior to administration. A no-carrier-added radioactive multitracer solution was obtained from the Ag(purity: more than 99.99%) target irradiated with 135MeV/nucleon N-14 beam accelerated in RIKEN Ring Cyclotron. The preparation for a multitracer solution from Ag target was carried out in Radioisotope Center, Kanazawa University. After evaporation of the no-carrier-added multitracer solution containing hydrochloric acid, a physiological saline solution was added to prepare the radioactive multitracer solution for injection. In general, more than 35 radioisotopes of 19 elements (Be, Na, Sc, V, Mn, Fe, Co, Zn, Ga, As, Se, Rb, Sr, Y, Zr, Tc, Ru, Rh and Pd) can be observed in the solution for injection. Among these radioisotopes, the above 8 elements (Sc, Mn, Fe, Co, Zn, Se, Rb and Zr) could be used and evaluated in this experiments. At 6, 12, 24 and 48 hr after intraperitoneal injection (0.2ml) to 20 mice, the mice were sacrificed under ether anesthesia and about 0.2ml of blood was collected, and then the above 11 organs were excised. These tissues were weighed immediately and freeze-dried. The dried samples were subjected to gamma-ray spectrometry with pure Ge detectors against an appropriate standard to obtain the tissue uptake rate.

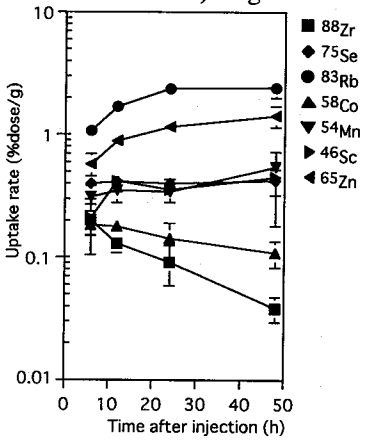

Fig1. Tissue uptake by brain in C57BL/6N mice.

All 8 radioisotopes were observed in all tissues except brain, bone and eyeballs. Uptake behavior of the 8 trace elements was reflected by their homeostasis. In this symposium, we discuss some results concerning essential trace elements focusing on their uptake by brain. In brain, Mn, Co, Zn, Se, Rb and Zr tracers were observed at 6, 12, 24 and 48 h after injection (Fig. 1). The uptake rate of Se tracer showed no significant time-dependent changes. However, the uptake rates of Rb, Mn and Zn tracers were increasing with time, and on the other hand those of Co and Zr tracers were decreasing with time. The high Se, Rb, Mn and Zn retention in brain suggests involvement of the elements in the brain function.

PHONE: +81-76-265-2534
FAX : +81-76-234-4351
E-mail : oishi@kenroku.ipc.kanazawa-u.ac.jp

P422
s.33

PRODUCTION OF POSITRON EMITTERS AND APPLICATION OF THEIR LABELED COMPOUNDS TO STUDIES ON PLANTS.

N. S. ISHIOKA,[1]* H. MATSUOKA[1], S. WATANABE[1], A. OSA[2], M. KOIZUMI[2], S. MATSUHASHI[3], T. KUME[3], A. TSUJI[4], H. UCHIDA[4] AND T. SEKINE[2].

[1] *Department of Radioisotopes, Japan Atomic Energy Research Institute (JAERI), Takasaki, Gunma 370-12, Japan*
[2] *Department of Chemistry and Fuel Research, JAERI, Takasaki, Gunma 370-12, Japan*
[3] *Department of Radiation Research for Environment and Resources, JAERI, Takasaki, Gunma 370-12, Japan*
[4] *Central Research Lab., Hamamatsu Photonics Co., Hamakita, Shizuoka 434, Japan*

Summary: The positron emitters ^{11}C, ^{13}N, ^{18}F and ^{48}V and their labeled compounds have been produced for studies on plants. Using a positron-emitter two-dimensional imaging system, we can trace dynamically the positron emitter in a plant to elucidate the physiological function of plants *in vivo*.
Key words: Positron emitters, radionuclides, labelled compounds, plant physiology, annihilation γ-rays

Radionuclides to be used mainly in biomedicine have been produced with an AVF cyclotron in the TIARA facility of JAERI at Takasaki. Recently, the TIARA has provided new possibilities of studying dynamically the physiological function of plants *in vivo* with positron emitters: a positron-emitter two-dimensional imaging system has been developed together with production methods of positron emitters. The present paper describes some experience on the production of positron emitters and their labeled compounds and on the plant physiological experiments of plants using them.

The positron-emitter two-dimensional imaging system consists of two planer detectors, each of which is a $Bi_4Ge_3O_{12}$-scintillators array coupled to a position-sensitive photomultiplier tube. The two detectors are placed facing each other with a sample plant between and detect annihilation γ-rays from the sample. Although the detection area is limited to 6 cm x 5 cm and the resolution in space is as large as 2 mm, the great advantage of the system is that the sample plant can be fed and watered, receiving light, as it is alive.

Table 1 shows the positron emitters produced so far. We have developed the irradiation system of a water target to keep the purity of the target for producing ^{13}N and ^{18}F in water. Instead of transporting through a tube, a small amount of water in a Ti vial is transferred by a small truck between the irradiation port and the hot cell. In addition, to avoid the increase of temperature during irradiation, the target water can be frozen before irradiation. With this system, we obtained a sufficient amount of radioactivity for experiments on plants. Production of other positron emitters will be also discussed in the symposium.

Using the positron-emitter two-dimensional imaging system, we have observed, for instance, the aqueous $^{18}F^-$ in rose to examine the uptake of water by the rose with and without γ–ray irradiation.

Table 1 Production and use of positron emitters in TIARA

Nuclide	Half-Life	Reaction	Target material	Tracer for experiments on plants
^{11}C	20 min	$^{14}N(p,\alpha)^{11}C$	N_2 gas	$^{11}CO_2$, ^{11}C-Methionine
^{13}N	10 min	$^{16}O(p,\alpha)^{13}N$	$H_2{}^{16}O$ ice	$^{13}NO_2^-$, $^{13}NO_3^-$
^{18}F	110 min	$^{16}O(\alpha,pn)^{18}F$	$H_2{}^{16}O$ ice	Aqueous $^{18}F^-$
		$^{18}O(p,n)^{18}F$	$H_2{}^{18}O$ ice	^{18}F-FDG
^{48}V	16 day	$^{45}Sc(\alpha,p)^{48}V$	Sc foil	Aqueous ^{48}V

Fax:+81-273-46-9690, E-mail:ishioka@taka.jaeri.go.jp

P423 s.33 STUDY OF OPTIMUM CONDITION FOR SYNTHESIS OF [γ-^{32}P]ATP WITH HIGH SPECIFIC RADIOACTIVITY

F. SAKAMOTO[1,2], M. IZUMO[1], K. HASHIMOTO[1] and Y. FUJII[2]
[1] *Department of Radioisotopes, Japan Atomic Energy Research Institute, Tokai-mura 319-11, Japan*
[2] *Graduate School of Science and Engineering, Ibaraki University, Mito-shi 310, Japan*

Summary: The optimum condition for synthesis of [γ-^{32}P]ATP with high specific radioactivity has been reported. Taking into account the maximum radioactivity of $H_3{}^{32}PO_4$, we can obtain about 230 TBq/mmol of specific radioactivity.
Key words: [γ-^{32}P]ATP, specific radioactivity, luciferase-luminescence assay

[γ-^{32}P]ATP has been widely used in many fields of the genetic engineering. Many preparation methods of [γ-^{32}P]ATP have been reported, but studies on the optimum condition for high specific radioactivity of [γ-^{32}P]ATP have so far been limited. We report the optimum condition to synthesize [γ-^{32}P]ATP with high specific radioactivity by the enzymatic method in this study.

According to the methods reported, a part of glycolytic pathway has been utilized to synthesize [γ-^{32}P]ATP. And the synthetic method consists of 4 reaction steps starting from glycerol 3-phosphate. But we utilized more convenient method which consists of 3 reaction steps starting from fructose 1,6-diphosphate. The impurities of phosphorus (ATP and other P) in the chemicals reduce specific radioactivity of synthesized [γ-^{32}P]ATP. Therefore we measured the chemical quantity of ATP and other P in all chemicals by means of luciferase-luminescence assay (Table 1). As a result, we found that there were much phosphorus in lactate dehydrogenase. We reexamined the necessity of the enzyme. It was found that no use of lactate dehydrogenase increased the specific radioactivity of [γ-^{32}P]ATP with no serious decrease of the chemical yield. Finally we examined the dependence of the chemical yield on the chemical quantity of H_3PO_4 (Figure 1). The maximum quantity of H_3PO_4 is 4.4×10^{-9} mol with no decrease of the yield. The value is equal to the chemical quantity of about 1.5 GBq of carrier-free $H_3{}^{32}PO_4$. In our estimate for the specific radioactivity from the chemical quantity of all ATP and the radioactivity of [γ-^{32}P]ATP, we will able to obtain about 230 TBq/mmol of specific radioactivity using 1.5 GBq of $H_3{}^{32}PO_4$.

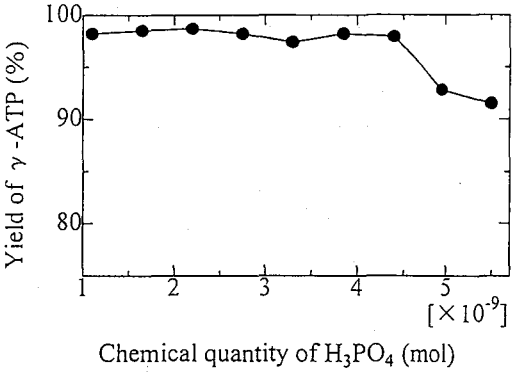

Figure 1 Dependence of chemical yield of γ-ATP on chemical quantity of H_3PO_4

Table 1 Impurities of phosphorus in the chemicals used for one synthesis

Chemicals	Chemical quantities (mol)	
	ATP	other P
Adenosine 5'-diphosphate	1.8×10^{-11}	4.7×10^{-10}
Fructose 1,6-diphosphate	$<10^{-12}$	3.8×10^{-10}
β-Nicotinamide adenine dinucleotide	$<10^{-12}$	2.3×10^{-11}
Sodium pyruvate	$<10^{-12}$	1.5×10^{-10}
Dithiothreitol	$<10^{-12}$	1.2×10^{-10}
Aldolase	$<10^{-12}$	$<10^{-12}$
Glyceraldehyde 3-phosphate dehydrogenase	$<10^{-12}$	$<10^{-12}$
Lactate dehydrogrnase	$<10^{-12}$	2.1×10^{-9}
3-Phosphoglycerate kinase	$<10^{-12}$	7.0×10^{-10}
Solvent	$<10^{-12}$	3.8×10^{-10}

FAX: +81-29-282-5963, E-mail: buntoku@popsvr.tokai.jaeri.go.jp

P424
s.33

INSTRUMENTAL NEUTRON ACTIVATION ANALYSIS (INAA) OF TRACE ELEMENTS IN ORGANS AND TISSUES OF MICE - EFFECTS OF ZINC-DEFICIENT DIET

M. IWAMA, K. TAKIGUCHI, K. SHINOTSUKA,
M. YANAGA, M. NOGUCHI and T. OMORI
Faculty of Science, Shizuoka University, 836 Ohya Shizuoka-shi 422, Japan

SUMMARY : Several organs of Zn-def. mice and control mice were analyzed by INAA. Zinc concentrations of Zn-def. mice were not lower than those of control mice except for bone and pancreas. However, Co content increased significantly in all organs of Zn-def. mice compared with control mice.
KEY WORDS : INAA, Trace Element, Zinc Deficiency in Mice, Organs and Tissues

INAA method was applied to investigate the physiological effect of zinc deficiency upon the concentration of the other elements in mice. Eight-weeks-old male mice of the ICR / Jcl strain were divided into two groups ; one fed with zinc-deficient diet and distilled water (Zn-def. mice) and the other with control diet and distilled water (control mice) *ad libitum* for 3 weeks. Ten organs and tissues were removed (some of them were fixed for histological observation), weighed separately, and freeze-dried.

Each sample (20-100 mg), which was doubly wrapped in polyethylene film, was irradiated in the TRIGA MARK II Reactor of the Institute for Atomic Energy, Rikkyo (St. Paul's) University with thermal neutron fluxes of 1.4×10^{12} $cm^{-2}s^{-1}$ for 10 h and 4.1×10^{11} $cm^{-2}s^{-1}$ for 5 min, respectively. The γ-ray spectroscopic measurements were done with HPGe detectors.

Concentrations of twelve elements, Na, Mg, Al, Cl, K, Cr, Mn, Fe, Co, Zn, Se and Rb, were determined. Contrary to our expectation, zinc concentrations in the organs and tissues of Zn-def. mice were not lower than those of control mice, except for bone and pancreas. No typical symptoms of zinc deficiency disease, which are skin injury and retarded sexual maturation etc., were observed even for Zn-def. mice. However, Zn concentrations in bone and pancreas of Zn-def. mice were much lower than those of control mice. It is considered that Zn, which had been accumulated in bone and/or pancreas, was supplied to other organs and tissues of Zn-def. mice. On the other hand, Co content in all organs of Zn-def. mice were higher than those of control mice, as shown in Fig.1. The distinct behavior of Co may plausibly be explained by the partial substitution of Co with Zn in metal proteins for the zinc-deficient diet.

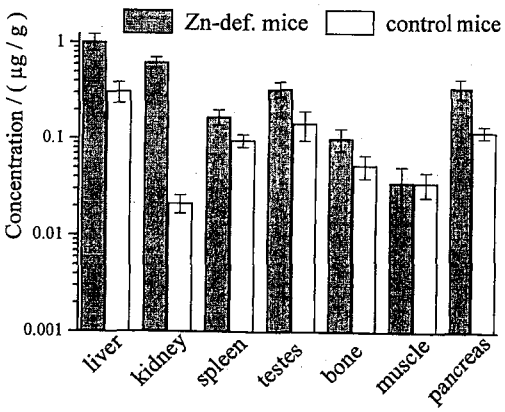

Fig.1. Concentration (μg / g) of Co in various tissues in the Zn-deficient and control mice. Each datum in the figure represents the mean value ± S.D.

054-238-3989 (FAX) srgmi1@sci.shizuoka.ac.jp

P425
s.32

CELL-KILLING EFFICIENCY AND NUMBER OF PLATINUM ATOMS BINDING TO DNA, RNA AND PROTEIN MOLECULES OF HeLa CELLS TREATED WITH COMBINATIONS OF HYPERTHERMIA AND CARBOPLATIN

M. Akaboshi, K. Kawai, Y. Tanaka, J. Takada and T. Sumino

Research Reactor Institute, Kyoto University, Kumatori-cho, Sennan-gun, Osaka, 590-04, JAPAN

Summary: HeLa S-3 cells were treated with ^{195m}Pt-carboplatin for 60 minutes at various temperatures and the relationship between the lethal effect and the number of Pt atoms binding to DNA, RNA and proteins was examined. From 0 °C to 44 °C, the cell-killing efficiency of Pt atoms increased by a factors of 11.9.

Key words: ^{195m}Pt, ^{195m}Pt-carboplatin, HeLa cell, Hyperthermia, Cell killing efficiency

Effect of hyperthermia on the cell killing efficiency of Pt atoms binding to DNA, RNA and protein molecules of HeLa cells treated with ^{195m}Pt-radiolabeled *cis*-diamine(1,1-cycrobutane-dicarboxylato)platinum(II) (carboplatin) was examined. HeLa S-3 cells were treated with ^{195m}Pt-carboplatin for 60 minutes at various temperatures and the relationship between the lethal effect and the number of Pt atoms binding to DNA, RNA and proteins was examined. The mean lethal concentrations (D_0) of carboplatin for 60 min-treatment at 0, 25, 37, 40, 42 and 44 °C were 671.2, 201.5, 67.3, 33.4, 20.2 and 15.6 μM, respectively. By using identically treated cells, the number of Pt-atoms combined with DNA, RNA and protein molecules was determined in the subcellular fractions. Thus, the D_0's given as the drug concentrations were replaced with the number of Pt-atoms combined in each fraction. Then the efficiency of the Pt atom to kill the cells was expressed as the reciprocal of the number of Pt-atoms combined and was calculated for each molecule. The cell-killing efficiency for DNA molecule was 0.699, 1.42, 2.65, 4.84, 7.74 and 8.28x10^4 nucleotides, respectively, for the conditions described above. (Fig.) From 0 °C to 44 °C, the cell-killing efficiency of Pt atoms increased by a factors of 11.9.

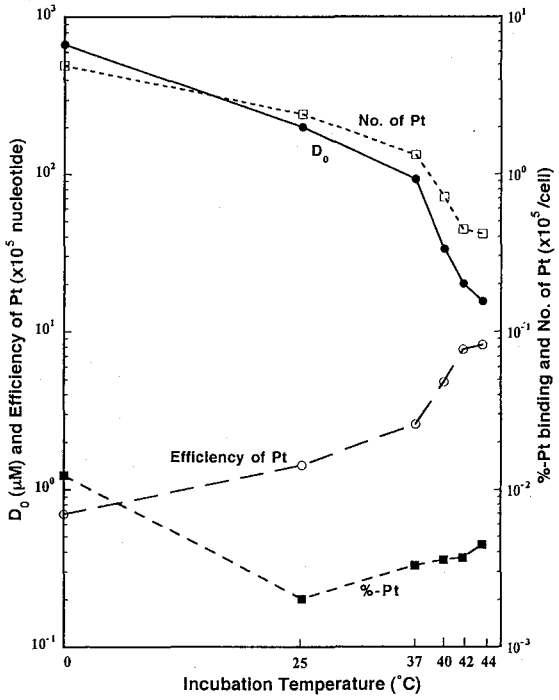

Fig. The variations in D_0, %-Pt, number of Pt-atoms binding to DNA, and cell-killing efficiency of Pt-atoms with incubation temperture.

P426
s.33

DYNAMICS OF TRACE ELEMENTS IN LIVER DISEASE RAT AND MICE

S. Enomoto, R. Hirunuma, S. Ambe, and F. Ambe
The Institute of Physical and Chemical Research(RIKEN), Wako, Saitama 351-01, Japan

Summary: We discuss dysbolism and accumulation of trace elements using LEC rats as a model animal of liver cancer that derives from Wilson disease by using the multitracer technique. We observed the hepatopathy and the storage of bone seeker in the liver have a close relation to the fiberization of the liver.
Key words: multitracer, liver disease, bio-trace elements

The LEC rats genetically contract the jaundice at 4～5 months which causes acute hepatitis, and approximately the half of them die for that. Survived rats passe through chronic hepatitis, liver cirrhosis, and contracts the liver cancer. Critical causes of the hepatitis were examined in detail. In this paper, we discuss dysbolism and accumulation of trace elements using LEC rats as a model animal of liver cancer that derives from Wilson disease.

As the liver-cancer bearing rats was used an 80-week-old LEC strain and as normal rats was used a 12-week-old Wistar strain. A tenth ml of a multitracer solution in the physiological saline was injected to each rat intravenously. After 24 hrs from the administration, the rats were sacrificed and liver, kidney, spleen, and brain were collected. The gamma-rays were measured by a Ge semiconductor detector.

The uptake of Sc, V, Mn, Zn, Rb, As, and Zr in the liver of LEC rats was larger compared with that of normal ones. The uptake of Sc, V, Zn, and As by LEC rats was two times, that of Mn 1.5 times, that of Ga 3 times, and that of Zr 4 times that of normal ones. On the other hand, the uptake of Se and Y decreased by cancer bearing. In the kidney, the uptake of Sc, Ga, As, and Zr increased compared with that of normal rats. The uptake of As and Zr was 3 times that of the normal ones. The uptake of Mn, Zn, Se, Rb, Ru, and Rh decreased. There was no change for V, Cr, and Co. The liver of LEC rat cancerated, and liver tissue grew a large number of false bile ducts in the marginal zone of leaflets, and fibrous disease of hepatic duct surrounded by the fibroblast was recognized frequently. Because Ga has a tumor seeking property, the uptake of Ga by LEC rat increased. In the liver, As is methylated by S-adenosyl methionine, and becomes monomethyl arsonic acid and dimethylarsinic acid, and it is excreted from the kidney. In LEC rats are caused various enzymatic abnormalities by the Cu dysbolism; especially, in our result, there were remarkable decrease in ceruloplasmin and increase in copper and metallothionein in liver. In LEC rats, the lowering of the concentration of glutathione peroxidase and cytochrome P-450 is reported. It is considered that As may increase in liver and kidney; because of an enzymopathy and a dysbolism, the methylation does not work completely. In the liver of LEC rats, the uptake of the essential elements such as Mn, Co, and Zn increased, since the essential elements are closely related to enzymes. In the organs such as kidney, spleen, and brain, there was also a change in the uptake of Mn, Co, and Zn. In these organs, this tendency seems to originate the enzymatic abnormalities as well as to result in the liver cancer. The uptake of essential elements is remarkably different between our data of acute alcoholic hepatopathy mice and LEC rats. In case of mice which contracted an acute alcoholic hepatopathy, the initial state of the hepatic disorder, the abnormalities of enzymatic system and other proteins are not directly connected with the dysbolism of the essential elements. However, in the LEC rats of the last stage of cancer, our result suggested that the uptake of the essential elements was increased, since the homeostasis maintenance mechanism of the trace elements in the whole body is collapsed by a remarkable liver injury. Uptake of the bone seeking elements such as Sc and Zr increased. These results suggests that the hepatopathy and the storage of bone seeker in the liver have a close relation to the fiberization of the liver.

Fax: +81-48-467-9423, E.mail: semo@postman.riken.go.jp

P427 s.14 PRODUCTION OF CARRIER-FREE MULTITRACERS CONTAINING MG-28 AND CA-47 BY HIGH-ENERGY HEAVY-ION IRRADATION

S. Ambe, T. Ozaki, R. G. Weginwar, S. Enomoto, and F. Ambe

The Institute of Physical and Chemical Research (RIKEN), Wako, Saitama, 351-01, JAPAN

Summary: With the aim of preparing carrier-free ^{28}Mg and ^{47}Ca simultaneously, V, Ti, and Fe targets were examined by irradiating with high-energy heavy ions (^{12}C, ^{14}N, and ^{16}O) accelerated by the RIKEN Ring Cyclotron and chemical separation procedures for the tracers have been established.
Key words: Mg-28, Ca-47, multitracer, V target, Ti target, Fe target, high-energy ions

Radiotracers of Mg and Ca are indispensable for studies of minerals in plants and animals. ^{28}Mg is only one useful tracer of Mg, but it is not commercially available. ^{47}Ca is advantageous over commercially available ^{45}Ca, which is not carrier-free and requires β-counting. With the aim of preparing carrier-free ^{28}Mg and ^{47}Ca simultaneously, V, Ti, and Fe targets were examined by irradiating with high-energy heavy ions of ^{12}C, ^{14}N, and ^{16}O accelerated by the RIKEN Ring Cyclotron. Firstly, the yields of ^{28}Mg and ^{47}Ca were determined. Secondly, chemical separation procedures of the tracers from the Ti and V targets have been established.

Stacks of discs (100μm x 23mmφ) of Ti, V, and Fe were irradiated with a 135MeV/u beam of ^{12}C, ^{14}N, or ^{16}O for one hour. They were subjected to γ-ray measurement with HPGe detectors for determination of the yields. Among the three targets examined, V gave the highest yield of ^{28}Mg irrespective of the kind of beams. Iron showed the lowest yield. The yield for ^{28}Mg increased in the order of $^{12}C < {}^{16}O < {}^{14}N$. On the other hand, little difference in the yields for ^{47}Ca was observed among the beams. Among the three targets, V gave the highest yield for ^{47}Ca. Iron showed the lowest yield.

Titanium and V targets irradiated for 2 days were used for the study of chemical separation. A disc of Ti (300μm x 23mmφ) was dissolved in a diluted HF solution (4 cm^3 of c. HF+10 cm^3 of H_2O). After addition of one cm^3 of 30% of H_2O_2 to the solution and dilution to about 30 cm^3 with water, the solution was passed through a cation exchange resin column (8 cm^3, H-form). Titanium was washed out with 10 cm^3 of 0.5 mol dm^{-3} HF and then 10 cm^3 of water. ^{47}Ca was eluted with 80 cm^3 of 2 mol dm^{-3} HNO_3. About 50 μg of Ti was found in the ^{47}Ca fraction. The cation exchange procedure was repeated to purify the tracer. The resulting solution contained 95% of ^{47}Ca, 50% of ^{22}Na, and 4% of ^{48}V.

A disc of V (100μm x 23mmφ) was dissolved in 4 cm^3 of 6.5 mol dm^{-3} HNO_3. After addition of one cm^3 of 30% of H_2O_2 to the solution and dilution to about 50 cm^3 with water, it was passed through a cation exchange resin column (7 cm^3, H-form). Vanadium was washed out with 140 cm^3 of 0.1mol dm^{-3} HNO_3 + 1% H_2O_2. ^{47}Ca was eluted with 100 cm^3 of 2 mol dm^{-3} HNO_3. The decontamination factor of V was 10^{-4}. The cation exchange procedure was repeated to purify the tracer. The resulting solution contained 95% of ^{47}Ca, 100% of ^{7}Be, 20% of ^{51}Cr, 10% of ^{22}Na, and 10% of ^{46}Sc. No peaks due to ^{48}V were detected in the solution. The decontamination factor of V was less than 10^{-6}.

Fax: 048-462-4661 E-mail: shizambe@postman.riken.go.jp

P428
S.14

METABOLISM OF TRACE ELEMENTS IN MARINE EUGLENA: A STUDY USING THE MULTITRACER

R.G.Weginwar*[1], M. Katayama[2], S.Ambe[1], S.Enomoto[1], T.Ozaki[1], F.Ambe[1]

1.The Institute of Physical and Chemical Research (RIKEN), Wako, Saitama 351-01, Japan.

2.Osaka Prefecture University, Osaka, Japan.

Summary: The behavior of various trace elements in marine euglena is being studied by the multitracer technique. As the first step, the relative amounts of elements incorporated and excreted in the two kinds of euglena is determined.

Key words; Multitracer, trace elements, green euglena, yellow euglena

In recent years, pollution in marine environment has become a serious problem for human lives and it is mainly due to industrial waste as well as human life. Another problem is the radioisotopes emitted from nuclear testings and accidentally leaked from nuclear plants into the ocean. The waste may influence human bodies possibly through food chains. Therefore, the mechanism of the incorporation of trace elements from sea water into plants and animals is important for our own health.

In this study, the incorporation and excretion of various trace elements in the two kinds of marine euglena (green euglena containing chlorophyll, thus plant metabolism and yellow euglena without chlorophyll, thus animal metabolism) is experimentally investigated using a radioactive multitracer technique. From Fig. 1 and 2, it is evident that the rate of incorporation of Be, Sr, Rb and Zn is quite different in both euglena. Similarly it is observed that the rate of excretion is different in both euglena for most of the elements. A further work is being carried out on incorporation as well as excretion of trace elements in marine euglena in order to understand the detailed mechanism.

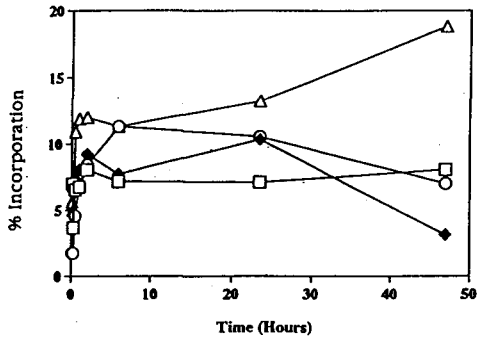

Fig.1 Percentage incorporation of Be, Sr, Rb and Zn in green euglena at different time.

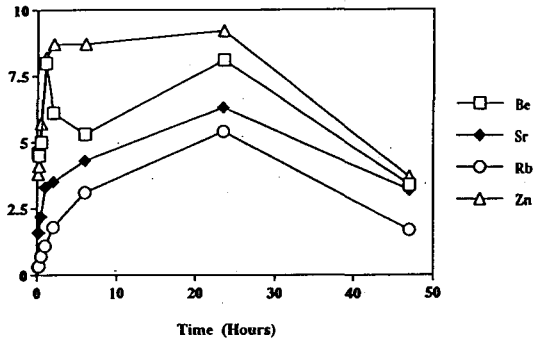

Fig.2 Percentage incorporation of Be, Sr, Rb and Zn in yellow euglena at different time

Fax:+81-48-462-4662/ email: rajiv@postman.riken.go.jp

P429
s14

APPLICATION OF THE MULTITRACER TECHNIQUE: TIME DEPENDENCE OF DISTRIBUTION OF TRACE ELEMENTS IN SE-DEFICIENT RATS

R. Hirunuma*, N. Sotogaku[1], K. Endo[1], S. Enomoto, S. Ambe, and F. Ambe

The Institute of Physical and Chemical Research(RIKEN), Wako, Saitama 351-01, Japan
[1]Showa College of Pharmaceutical Sciences, Machida,Tokyo 194, Japan

Summary: The distribution of trace elements in Se-deficient rats were examined by the multitracer technique. The observed decrease of the uptake of Fe and As by the spleen in Se-deficiency suggests that the deficiency causes hemopoietic hypofunction of this organ.
Key words: Se-deficient rats, multitracer, trace elements, heavy-ion beam

Selenium is one of the essential trace elements and is known as the central ion in glutathione peroxidase. It is well known that fishes with high concentration of mercury in their body have also high concentration of Se, and that mercury poisoning is inactivated by action of Se. It is also reported that Se is in a competitive or synergetic relationship with several metals such as Mn, Fe, Co, Zn, and As. Therefore, it is very interesting and important to clarify the distribution of trace elements in various organs of Se-deficient rats. However, no systematic study has been reported on the behavior of trace elements in Se-deficient rats. In the present study, the distribution of trace elements in Se-deficient rats were examined by the multitracer technique, which can be used to evaluate the behavior of many elements under a same experimental condition.

A multitracer solution containing radioisotopes of 20 elements was prepared from a silver target irradiated by a heavy-ion beam of 135 MeV/nucleon from RIKEN Ring Cyclotron. After chemical separation, this multitracer was dissolved in saline. Se-deficient rats were fed with Se-deficient diet (produced by Oriental Yeast Co., LTD.) until the age of 12 weeks. As a reference, 12-week-old Wistar rats were used. A tenth ml of saline containing the multitracer was injected intravenously into each rat. The Se-deficient and normal rats were sacrificed at 3, 12, 24 and 72 hours after injection, and the radioactivities of their organs, tissues and blood were determined by γ-ray spectrometry. The observed γ-rays were assigned on the basis of their energies and half-lives.

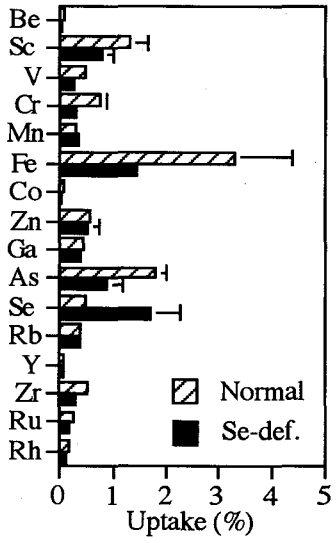

Fig. 1. Uptake (%) of various elements in normal and Se-deficient rats.

The behavior of Be, Na, Ca, Sc, V, Cr, Mn, Fe, Co, Zn, Ga, As, Se, Rb, Sr, Y, Zr, Tc, Ru, and Rh was examined. There were little individual differences in each group of rats. At 72 hours after injection, the uptake of Se was larger in the brain, intestine, spleen, and testicles of the Se-deficient rats than in those of the normal ones, contrary that was smaller in the liver.

The elements, Se, Fe, and As, are closely related to hemoglobin. Arsenic is bound to a globin part of hemoglobin in erythrocytes, and Fe is a constituent of hemoglobin. Glutathione peroxidase has a greater affinity for hemoglobin. The observed decrease of the uptake of Fe and As by the spleen in Se-deficiency suggests that the deficiency causes hemopoietic hypofunction of this organ.

Fax: +81-48-467-9423, E-mail: rhiru@postman.riken.go.jp

P430
s.12

ISOTOPIC MOLECULAR EXCHANGE STUDY OF CARBONS FROM DIFFERENT POLYMER PRECURSORS

K. László, A. Bóta, M. Takács, L. G. Nagy

Department of Physical Chemistry, Technical University Budapest
Budapest, Budafoki út 8. H-1111 Hungary

Summary: Carbonaceous materials were prepared from different natural and synthetic polymer precursors, such as cellulose, polyethyleneterephthalate or polyacrylonitrile. It has been concluded that polymers can be converted to carbonaceous final products with special properties.

Keywords: isotopic molecular exchange, Activated carbon, Polymer precursor

Carbonaceous materials were prepared from different natural and synthetic polymer precursors, such as cellulose, polyethyleneterephthalate or polyacrylonitrile (CEL, PET, PAN, respectively). The adsorption capacity of the products was enhanced by steam activation until a 50 % burn-off was reached. Microscopic, X-ray scattering, gas adsorption and isotopic molecular exchange methods were used to describe the matrix and pore structures of the carbons. The effect of the precursor polymer and the nature of the heat treatment were studied. The average pore sizes were calculated from both small angle X-ray scattering (SAXS) and low temperature nitrogen adsorption data. Isotopic molecular exchange was performed by toluene labelled with ^{14}C. From the slope of the exchange curves the half-time of the exchange process was derived. Using a simple diffusion model the pore length was calculated from this modell as well. Fractal approach was also used to understand the development of the structure. Mass and surface fractal dimensions, D_m and D_s values were calculated from X-ray and nitrogen adsorption data. The development of the pore structure was followed by the comparison of all these characteristic parameters before and after activation.

It has been concluded that polymers can be converted to carbonaceous final products with special properties. Their adsorption properties and pore size distribution are determined by the structure of the starting material. Some of them shows very favourable adsorption properties as a consequence of the matrix structure. Varying the conversion the pore structure can be shifted from the mainly microporous size toward the larger transient pores.

Acknowledgement
The authors wish to express their appreciation for the financial support provided by the OTKA Fund (Budapest, Hungary), Project Nos. T 017019 and T 017039 and to Ms. Emese Fülöp and Mr. György Bosznai for their experimental work.

Fax: 36-1-463-2909, E-mail: KLASZLO@CH.BME.HU

P431
s.14

MULTITRACER STUDY ON COORDINATING OF THE RARE EARTH ELEMENT WITH METALLOTHIONEIN

J. Chou, S. Enomoto, S. Ambe, F. Ambe
The Institute of Physical and Chemical Research (RIKEN),
Wako, Saitama 351-01, Japan

Summary: The multitracer technique was applied to study interactions between metallothionein and various rare earth elements (REE) simultaneously in vitro. The binding percentages of the REE to metallothionein changes with their ionic radii and is dependent on the pH in the solution.

Key words: Multitracer, metallothionein, rare earth element

Metallothioneins are low-molecular-weight, cysteine-rich proteins normally found in association with Zn^{2+} and Cu^{2+}. It has been shown to bind various metals including toxic species, such as Cd and Hg, as well as the essential trace elements Zn and Cu. Holt et al. have ranked the affinities of selected divalent cations for MT as: Hg>Cu>Cd>Zn. Ni and Co appear to bind to MT only sparingly. The REE has been shown to be involved in many important biological function and is considered to be harmful, interrupting physiological functions. But so far, there is no report about the coordination with MT. Multitracer was used to study the interaction between MT and REE simultaneously.

The interactions between MT and REE in vitro in the neutral solution were determined using multitracer technique. The binding percentage is shown in figure 1. The results indicated that MT can coordinate with some REE. Among the tested REE, Eu has the highest binding percentage to MT and Lu has the lowest percentage. For Ln^{3+}, from Ce to Lu, the number of atom increases gradually, but ionic radius progressively decreases. From Ce to Lu, the binding percentage increases first and then decreases with decreasing ionic radii. The metallothionein has an unique distribution of cysteinyl residues in the amino acids sequence to accommodate the formation of metal-thiolate clusters by which the metal ions are bound to MT. But in generally, Lanthanides coordinate with the unprotonated carboxyl group of amino acids in the protein. Thus, for REE, they are not similar to transition elements which bind to cystines in the metallothionein. The major ligand for REE ions on metallothioneins is the carboxyl group, not the thiolate ligand of the cystine.

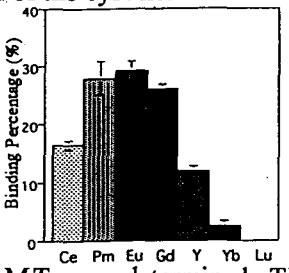

Figure 1. The binding percentage of REE coordinated with metallothionein at pH of 7.4. Each datum in the figure represents the mean values ±S.D. obtained from three preparations.

The pH dependence of binding percentage of REE to MT was determined. The binding percentage is dependent on the pH solution. For REE, in the basic solution, the binding percentage is higher than that in the acid solution. At pH of 3, for all the tested REE, the binding percentage decrease to zero.

email address: chouju@postman.riken.go.jp

P432
s.13

RARE EARTH BROMATES : RETENTION STUDIES FOLLOWING (n,γ) ACTIVATION

V.G. Dedgaonkar, R.G. Apte and D.A. Bhagwat
University Department of Chemistry, University of Pune, Pune 411 007 (India)

Summary : The initial retentions (at ~20°C) of (n,γ) activated rare earth bromates with respect to ^{80}Br, ^{80m}Br and ^{82}Br, lie over the ranges 19-23, 21-23 and 28-32% respectively. Cation effect on retention isdiscussed in the light of various parameters like lanthanide contraction, lattice energ etc

Key works : Retention, annealing , cation effect, dehydration.

Microcrystalline rare earth bromates were subjected to neutron activation for 24 h using a ^{252}Cf source (flux : 10^9 n s^{-1}, nominal). Separation of activities in the Br^- and BrO_3^- forms was carried out using solvent extraction procedure. Retention studies on bromates were supplemented by dehydration data obtained under isothermal conditions. The initial retention values obtained at room temperature for La, Pr, Nd, Sm, Gd, Dy and Er bromates with respect to ^{80}Br, ^{80m}Br and ^{82}Br were in the ranges of 19-23, 21-23 and 28-32 % respectively. The values do not differ much indicating only a limited role of cations in determining the initial retention. Thus structural differences that arise due to changed co-ordination number do not result in different retention values in these bromates. Similarly, periodic properties like lanthanide contraction and variable oxidation states are known to affect phenomenon like hydration energy and the dehydration process and yet the retention remains negligibly influenced. Extent of bond rupture in these bromates is independent of the cation effect. Identical values of lattice energy obtained for these salts using the Kapustinskii equation indicate that identical crystal free space is responsible for the identical initial retention values.

When subjected to isothermal heating over a temperature range of 70-140°C, the retention increased progressively with time. At 100°C it reached almost 100% in the case of $Sm(BrO_3)_3.9H_2O$ while other systems showed only ~80% . The compound that showed higher water loss also had higher recovery. Structural rearrangement occurring may increase lattice mobility and create additional vacancies that yield increased recombination. Besides, profusely hydrated salts have significant hydrogen bonding between BrO_3^- and H_2O and thus have greater number of modes of vibration that can reduce the recoil separation and thus facilitate the recombination. Since there is a change in oxidation state of recoil species during annealing, which is concurrent with the process of dehydration, it is likely that rare earth cations like Sm^{+3} and Nd^{+3} can undergo redox reactions during dehydration. Thus, cation effect that was non-located significantly in the initial retention becomes vivid upon the heat treatment. Further on heating, oxygen from the lattice water coordinated to Al^{+3} is used to form an oxide and the BrO_3^- remains undisturbed. Damage to BrO_3^- ion in this lattice is minimum as compared to the rare earth salts and therefore, $Al(BrO_3)_3.9H_2O$ shows higher retention (and also recovery) even at lower temperature. The effect of water moleculars is thus cation dependent and leads to different annealing and retention behaviour. Chemical transformation following (n,γ) activation and the mode of thermal decomposition of a salt are therefore governed by similar periodic properties of cations and anions in that salt.

P433
s.13/61

DIRECT PREPARATION OF RADIOACTIVE CARBON LABELED FULLERENES USING NUCLEAR REACTION

K. Masumoto, T. Ohtsuki[1]*, K. Sueki[2]*, K. Kikuchi[2]*

Radiation Science Center,High Energy Accelerator Research Organization, Tanashi, Tokyo 188

[1] *Laboratory of Nuclear Science, Faculty of science, Tohoku University, Sendai, Miyagi 982*

[2] *Faculty of Science, Tokyo Metropolitan University, Hachioji, Tokyo 192-03*

Summary: The ^{11}C and ^{14}C labeled fullerens were obtained by chraged-particle irradiation and neutron irradiation, respectively. It was found that recoiled atoms can be easily substitute with a carbon atom of fullerene after nucear reactions. HPLC method is effective to separate labelled fullerens for tracer use.

Key words: Fullerenes, C_{60}, C_{70},Labeling, ^{11}C, ^{14}C, Charged particle reaction, Neutron reaction

Recently fullerenes attract many scientists of various fields, because of their interesting chemical and physical properties. The production of labeled fullerens is important for studying the chemical or physiological behavior of trace amount of fullerenes. Applying the usual chemical systhesis to the production of radioactive fullerene involves the handling of intense radoactivity and the time-consuming process. In order to open a new labeling method and study their mechanism, the direct introduction of radioactive carbon into fullerene has been tried by proton and neutron irradiation.

Proton irradiation was performed by using AVF cyclotron at Cyclotron Radioisotope Center, Tohoku University. Samples were irradiated by 12 MeV proton for 20 min at the average current of 1 μA. Neutron irradiation were performed for two days by JMTR at Oarai Research Establishment of JAERI. In case of chraged-particle and neutron irradiation, ^{11}C and ^{14}C was produced by using $^{11}B(p,n)^{11}C$, $^{14}N(p,\alpha)^{11}C$ reactions and$^{14}N(n,p)^{14}C$ reaction, respectively. Fullerenes (C_{60}, C_{70} and their mixture) were mixed homogeneously with boron or nitrogen compound. Irradiated samples were dissolved into CS_2 and filtrated by milipore filter to remove boron and insoluble byproducts. After CS_2 was evaporated, CS_2 soluble fraction was dissolved into toluene-hexane mixture (7:3) and injected into HPLC column (Buckyclutcher, 250mm × 10 mm id). Flow rate was adjusted at 3ml/min. After separation, the absorbance of eluate were measured by UV-detector at 290 nm. To detect ^{11}C labeled compounds, a elution tube was coiled and sandwiched between a pair of BGO-scintillation detectors coupled with coincidence counting circuit to detect 511keV anihilation γ-ray. To detect ^{14}C radioactivity, eluate was collected by the fraction collector every 1 min and checked with the liquid scintillation counter.

From the radiochromatogram after proton irradiation of the C_{60} and boron mixture, three major peaks were obsedved as shown in Fig.1.. The first peak appeared at the retention of 6 min was attributed as C_{60} molecule labelled with ^{11}C, such as $^{11}CC_{59}$. The second large peak appeared at 10 min seems to be a C_{60}-dimer. The third broad peak, which may be a C_{60}-trimer was observed around 20 min after injection. The activity ratio of above three peaks was 1:5:1. The same chromatograph was also obtained in the case of the C_{60} mixture with Si_3N_4 and CH_2N_4. In case of the C_{70} and boron mixture, the first and second large peaks are assigned as C_{70} monomer and dimer. The second peak was broader than that of single component. It seems to be the compound peak of three types of geometrical isomer of C_{70} dimer. Almost similar results were obtained by neutron irradiation.

Obtained results were same as the case of photon activation. In this case, ^{11}C is produced from carbon of fullerens by $^{12}C(\gamma,n)^{11}C$ reaction. Therefore it was not clear whether ^{11}C remained in its fullerene molecule after photonuclear reaction or attacked a neighboring fullerene molecule. It was found that the ^{11}C or ^{14}C labeling induced by nuclear reactions is mainly caused by the substitution reaction between a carbon atom in fullerene and ^{11}C or ^{14}C. When fullerene network is opened by the attack of ^{11}C, the open end of carbon network can easily coalesce with neighboring fullerene molecules. It is important that these higher order fullerenes were chemically stable in liquid phase and carrier-free.

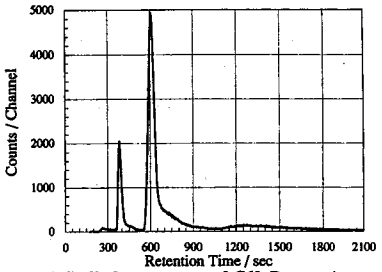

Fig 1. Radiochromatogram of C60+Boron mixture irradiated with proton.

Fax:+81-424-69-2145, E-mail: masumoto@tanashi.kek.jp

P434
s.13

FACTORS DETERMINING THE DAMAGE COEFFICIENTS AND THE LOW-FREQUENCY NOISE IN MeV PROTON IRRADIATED SILICON DIODES (ABSTRACTS OF THE APSORC '97)

E. Simoen*, C. Claeys, H. Ohyama[1], Y. Takami[2] and H. Sunaga[3]
IMEC, Kapeldreef 75, B-3001 Leuven, Belgium
[1]*KNCT, 2659-2 Nishigoshi Kumamoto, 861-11 Japan*
[2]*Rikkyo University, 2-5-1 Nagasaka Yokusaka Kanagawa, 240-01 Japan*
[3]*Takasaki JAERI, 1233 Watanuki Takasaki Gunma, 370-12, Japan*

Summary : The impact of several factors, related to the doping density, the substrate type and the thermal pretreatment on the proton radiation damage coefficients of Si diodes is discussed and verified experimentally. The obtained coefficients are compared with theoretical NIEL predictions.
Key words: Silicon diodes, high energy proton irradiations, damage coefficients, NIEL

Nowadays, there exists a thorough understanding of the microscopic damage mechanisms, occurring when a semiconductor device is subjected to high energy particle irradiation.Two questions are addressed in this paper: what are pertinent factors determining the leakage current damage coefficient in proton irradiated Si diodes and, secondly, can we extend the NIEL concept for the low-frequency (LF) noise spectral density? Detailed description of the diode processing, lay-out and current-voltage (I-V) and noise characterisation has been given in previous publications [1,2]. Proton irradiations have been performed in different facilities at room temperature and on un-biased devices mainly. The reverse current at -6 V and 296 °C has been measured on diodes with different geometry, to separate the bulk generation current density J_A from the surface generation current. The corresponding damage coefficient K_A is calculated as $\partial J_A/\partial\Phi$, with Φ the proton fluence at a given energy.
Data will be presented of K_A versus the proton energy in the range from 10 to 100 MeV (Fig. 1). A reasonable agreement with the microscopic damage parameter NIEL is obtained. It will be shown, however, that several factors have to be taken into account in order to relate both parameters. The degradation of an irradiated Si diode depends amongst others on the substrate type and doping density of the starting material. Another factor is the time elapsed after the irradiation.
The situation with respect of the LF noise spectral density is even more complex. A clear increase of S_I after proton irradiation is observed for the Float-Zone (FZ) Si diode, whereby the nature of the characteristic changes significantly (Fig. 2). It is shown that the excess 1/f noise is significantly larger than the shot noise limit $2qI_F$, with q the electron charge and I_F the diode forward current. This result will be discussed in view of the existing models for the 1/f noise in Si diodes. One can conclude that as to the noise, no simple relationship with the microscopic damage (NIEL) can be found.

[1] J. Vanhellemont et al., IEEE Trans. Nucl. Sci **NS41**, 1924 (1994).
[2] H. Ohyama et al., Phys. Stat. Sol. (a) **156**, 215 (1996).

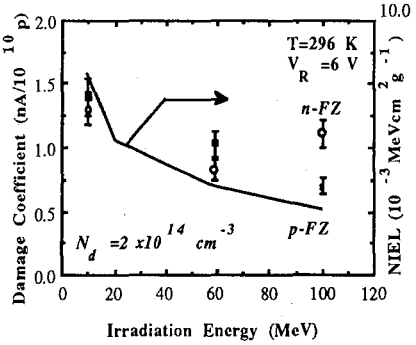

Fig. 1. K_A versus proton energy for Si n^+p and p^+n diodes.

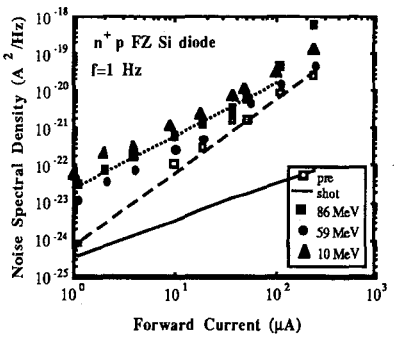

Fig. 2. S_I vs forward current at f=1 Hz and at different proton energies for n^+p Si diodes.

Fax: +32-16 281 214, E-mail: simoen@imec.be